Antenna designs for MIMO systems

1 ANTENNA DESIGNS FOR MIMO SYSTEMS

1.1 Introduction

This chapter describes the development and testing of antenna elements for use in a Multiple-input-multiple-output (MIMO) application. MIMO wireless systems have antenna arrays at both the transmitter and receiver terminals.

This project focuses on the terminal MIMO antenna array design. The requirements of the antenna element at the terminal are as yet not well-defined but will include (for commercial reasons) low antenna profile, low volume, light weight and low cost while maintaining good electrical properties such as return loss and isolation (-20dB). The pattern coverage for a terminal should be as omni-directional as possible since the location of the base station is often unknown. However, the patterns need to direct energy away from the circuit board of the device, i.e. laptops, PDAs and handsets, so that electromagnetic interference (EMI) is reduced.

1.1.1 The need for multiple antennas

The radio environment on electrically small platforms is changing rapidly. Until recently one radio was used in isolation and was usually connected to only one antenna. The situation today is very different: there is usually more than one radio used at once for example a handset may have 4 cellular bands, GPS and Bluetooth™. Sometimes WLAN radios are also present. This means that more RF filtering of signals is necessary. It is also becoming common for each radio to use more than one antenna in order to create diversity or for MIMO applications. The changing situation is described in Figure 1.1.

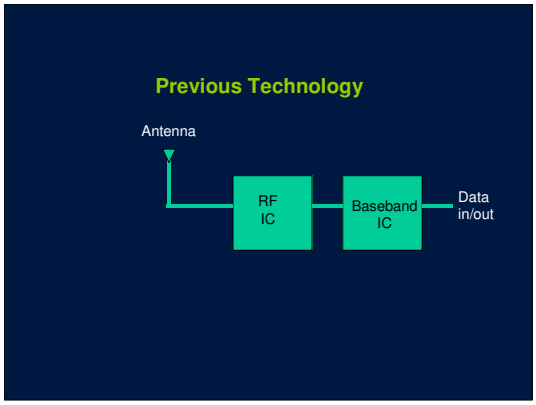

Figure 1.1a. In the past, one antenna would typically be used with each radio.

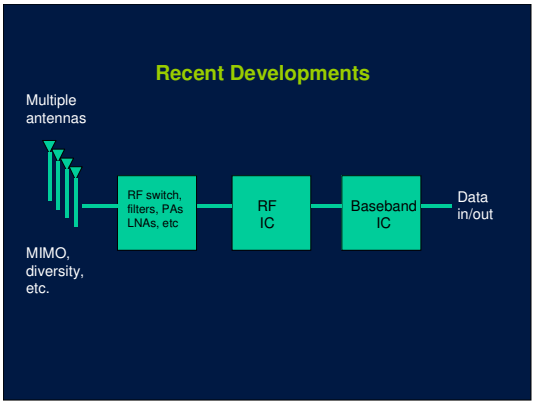

Figure 1.1b. Now several antennas are often used with each radio and several radios are sometimes used

Antenna diversity is already used with WLAN radio in order to counter multipath, reduce outages and improve the quality and reliability of the communications link. Generally three types of diversity are used, two antennas can be deployed as far apart as possible to create some spatial diversity, they can be oriented orthogonally to give polarisation diversity or they can have different beams patterns. Diversity in current WLAN systems is usually restricted to two antennas for each radio as this is enough to ensure that if one antenna is in an RF null, the other is generally not, thereby providing better performance in multipath environments. Only one radio is present and so the receiver listens to one antenna at a time and a RF switch is used to select the antenna giving the best signal.

Whilst simple diversity switching seeks to minimise the effects of multipath, MIMO makes use of multipath in order to improve the signal quality and reliability. A MIMO system generally uses more than two antennas, typically four, and is a more powerful technique than diversity switching for improving a communications link. The technique is powerful and can be improved further by employing a larger number of antennas than those actually used and then using an optimal subset selected on the basis of the quality of the channel.

MIMO systems are more complex than diversity switching systems, but the benefits are widely perceived as being worth the additional expense. In a speech on 18 Sept 2003 about Radio Renaissance for the future, Intel CTO Pat Gelsinger, announced that in future all Intel platforms will carry MIMO. In his words "The ultimate vision that Intel has is that we want to make wireless *the* access technology," he told Intel Developer Forum attendees. "Simply put, [that means] no more copper." There are quite instructive press releases from Intel on MIMO that can be found at:

http://www.intel.com/pressroom/archive/speeches/gelsinger20030918.htm

http://www.intel.com/technology/itj/2003/volume07issue03/art05_air/p04_mimo.htm

A MIMO-friendly chipset has now been launched by WLAN chip vendor Airgo Networks. One of the key remaining problems is to create the multiple antennas required by MIMO systems in an ever-decreasing space.

1.1.2 The need for antenna integration

In general, the space available for multiple antennas is no greater than that available before for a single antenna. Indeed, there is great pressure for space inside handsets and the space available for the antenna is shrinking all the time. Similarly with WLAN antennas - such as those fitted inside the lids of laptop computers - the size requirements placed on the antenna (especially the width) are continually being reduced. Furthermore, there is increasing

pressure from both OEMs and tier1 equipment manufacturers for further integration of components, including the antenna.

When multiple bands are used there is a need for filtering to separate the bands and further filtering is necessary to separate the signals when more than one radio is used. Antenna switching and diplexing is also usually necessary. All of these components are usually collected together into a FEM (Front End Module). FEMs introduce losses and take up further real estate on the PCB. On a typical handset the FEM introduces nearly 3 dB of loss and takes up about 100 mm^2 on the PCB. The total radio solution for a handset usually consists of three components, the RFIC, a power amplifier and the FEM; the total real estate amounts to somewhere in the region 250-400 mm^2. This is a very large area, but not as big as the antenna, which is often around 700 mm^2 for cellular radio. Similar real estate problems exist on WLAN platforms.

The key to reducing the PCB area occupied by radio systems, and to putting several antennas where there was once only one, is to integrate the antennas and radio systems into a single module. This will perhaps be most easily accomplished using LTCC or HTCC technology (Low or High Temperature Co-fired Ceramics). These are both mature technologies where multiple metallised ceramic layers are stacked and fired to produce a RF module having considerable functionality but with low losses. At present there are many examples of radio modules on LTCC substrates and chip antennas fabricated using LTCCs but they are not used together because the radio works only with a groundplane and the chip antennas work only without. Antenova has developed an antenna technology that is both small, ceramic based and works with a full groundplane and so is suitable for developing into a combined LTCC antenna/RF module.

1.1.3 Antenna design factors affecting MIMO performance

For MIMO, diversity systems and similar multi-antenna techniques to work effectively there must be more than one radio receiver output (for the receiving case) and the outputs must be significantly different, i.e. the signals are uncorrelated and vary independently. Similar arguments apply to the transmission case. In turn, this implies two conditions that must be fulfilled:

1. There must be diverse copies of the signal arriving at the antenna system (essentially, multipath must be present on the link).
2. The antenna system must be capable of receiving these signals in such a way that the diversity between them is not significantly down-graded.

In this section we consider what antenna properties are desirable for good diversity antennas.

Diversity systems

The use of diversity reception in mobile radio systems relies on the realisation of two or more receive signal paths in which the variation of signal level with time is to some extent uncorrelated[1]. Diversity itself is a difficult concept to define and even harder to measure directly. However, it is clear that a pair of antennas with good diversity performance will have radiation patterns that have a low 3-D cross-correlation. Good antenna diversity performance can only be achieved in 3 ways in an electrically small system:

1. **Spatial diversity** The antennas are far enough apart to sample signals that are significantly de-correlated. In electrically small devices such as handsets and PDAs there is very little spatial diversity available as the devices are often only of the order of, or less than, a wavelength in size. In the case of spatial diversity, the antennas do not necessarily need to have low 3-D cross-correlations.
2. **Beam diversity** In any given direction antennas have different gains. This results in a different weighting of multipath components of the desired signal being delivered by each antenna. Electrically small antennas are low directivity devices so beam diversity is a weak effect contributing to diversity reception.
3. **Polarisation diversity** This is the simplest form of diversity to achieve with a small antenna system and forms the basis many current diversity receive systems. In this case, two antennas may have the same gain in a given direction, but they respond to orthogonal polarisations.

In practice all antenna pairs exhibit all three types of diversity and no antenna offers a perfect diversity solution. It is usually a combination of these different types of diversity that must be considered, even if the polarisation effect is generally the strongest. The optimum choice of diversity system is a function of the nature of the propagation path between the transmitter and receiver, particularly the amount of polarisation scattering and the angular power spread of the components of the received signal.

In the MIMO environment, propagation is characterised by a wide angular spread between received signal components, so pattern diversity is particularly effective. Some polarisation scattering is also typical, so polarisation diversity can also contribute to the channel performance. In any case, the choice between these two approaches generally only exists when 2 antennas are used. When 4 or more antennas are used for a MIMO system, there is little option but to optimise all three types of diversity.

Design factors

Good diversity performance between two antennas depends on several factors:

1. The antennas must have some degree of directivity that can be controlled;
2. The antennas must have some level of cross-polar discrimination;
3. The antenna should have differently-directed spatial radiation patterns;
4. Coupling between the antennas must be minimised;
5. The multiple antenna system must be as efficient as a single antenna, or the diversity gain of the system will be squandered;
6. The antennas must be electrically small to minimise interaction between them.
7. The antennas must have properly matched terminations[4]

It is clear that imperfect cross-polar discrimination at the receiving antennas forms a mechanism that couples the polarisation components and increases the correlation between the two branches of the diversity system. This imperfection will reduce the achieved diversity gain and the degree of this effect has been recently investigated, see figure 1.2[1].

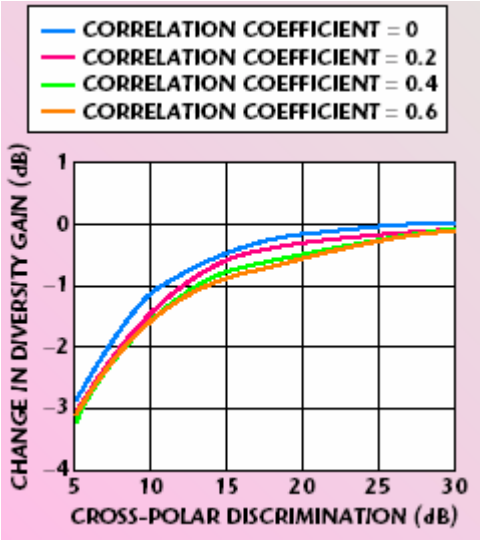

Figure 1.2: The reduction in diversity gain as a function of antenna cross-polar discrimination and the correlation of the incoming orthogonal signal components[1].

Figure 1.2 shows that the extent of lost diversity gain in a 2-branch system is only weakly dependent on the correlation of the incoming signal. As the signal correlation increases from 0 (ideal antenna pair) to 0.6, the effect of finite cross-polar discrimination typically reduces the available diversity gain by approximately 0.3 dB. This is not a big loss in diversity gain and shows that high cross-polar performance is not a primary requirement for diversity antennas. It is also shown that the extent of lost diversity gain is only weakly dependent on the correlation of the incoming signal[2].

Coupling between the antennas is also an important fact as it has been identified that the MIMO channel capacity with antenna coupling is influenced by two effects if spatial correlation is not considered[3]: In certain cases it is suggested that some increase in coupling can have beneficial effects.

It should be noted that low coupling between antennas does not automatically mean they will produce signals having low correlation. A pair of collinear dipoles can have a low coupling coefficient (they do not radiate into each other) but they have a high correlation as they both have the same beam and polarisation characteristics.

If antenna coupling is to be minimised for antennas mounted on a small device such as a PDA or handset, the following factors need to be considered:

1. *Currents induced in the common groundplane:* These are likely to couple antennas together. The best approaches are probably to use a balanced (differential) antenna design that drives against itself rather than the groundplane (the QMUL dielectric loaded double folded dipole is an example of this) or a DRA design where the high current region is essentially contained within the dielectric material (as in the case of the Antenova solution).
2. *Direct radiation between the two antennas:* This can be minimized by choosing resonant modes of the antenna that create nulls in the field patterns in the direction of the other antenna. This is not easily achieved when the antennas lie in each other's near field.
3. *Scattering from nearby objects:* The presence of scattering materials (radomes, PCBs, etc.) near to antenna can be a significant cause of coupling that can be minimized by careful design of the whole device.

In conclusion, the realisation of multiple radio signals having low correlation depends on the development of electrically small and efficient antennas having a reasonable, but not necessarily outstanding, cross-polar and radiation pattern performance and a degree of coupling between them that can be controlled to suit the application.

References

[1] B.S. Collins, "The effect of imperfect antenna cross-polar performance on the diversity gain of a dual-polarised receiving system" *Microwave Journal*, Volume 43, No. 4, pp 84 – 94, April 2000.

[2] A.M.D. Turkmani, A.A. Arowojolu, P.A. Jefford and C.J. Kellett, "An experimental Evaluation of the Performance of Two Branch Space Diversity Schemes at 1800 MHz," *IEEE Transactions Veh. Tech.*, Vol. VT-44, No. 2, May 1995, pp. 318–326.

[3] H. Mbonjo, J. Hansen, V. Hansen, "MIMO Capacity and Antenna Array Design", submitted to Globecom 2004. See also:

http://www.stanford.edu/~jchansen/MCA.pdf

[4] J W Wallace, M A Jensen, "Terminal-Dependent Diversity Performance of Coupled Antennas: Network Theory Analysis", IEEE trans. Antennas Propagat., vol 52, pp. 98-105, January, 2004.

1.1.4 Diversity

Polarisation Diversity

On a terminal, two or more antennas can be used that are oriented and polarised so as to have substantially different gains in the direction of an incoming signal. The signals received on the two antennas can then be combined optimally in the DSP to enhance the received C/I.

Similarly, it may be possible to use the antennas for the transmission of radiation on one polarisation or a combination of polarisations in order to optimise the reception of the terminal transmission at the base station unit.

Spatial Diversity

Multiple antennas on a terminal can be located in different positions around the handset so as to experience a different fading pattern in the radio environment. The radiation received can then be combined optimally in the DSP to enhance the received C/I. There could be similar benefits in transmission.

PCBs for the required applications are electrically small so the antennas would need to be as far apart as possible, i.e. in the corners. The theoretical optimum performance is obtained for a distance between the antennas of approximately 38% of a wavelength.

Pattern (Directional) Diversity

Multiple antennas can be used that are directional and oriented so as to receive substantially different signals according to the angle of arrival of the incoming radiation. The radiation received can then be combined optimally in the DSP to enhance the received C/I. Again; there could be similar transmission benefits. In this case, the distance between the two antennas is theoretically not as critical and there may be advantages in clustering the antennas together in order to minimise the area of PCB used and to minimise losses in the transmission lines.

Combined Polarisation, Pattern and Spatial Diversity

Once directional and polarised antennas have been distributed on a PCB, the three types of diversity may be combined in different ways in order to optimise performance.

1.1.5 Isolation

The antenna isolation (or coupling between antennas) must be considered during the design stage for a multiple antenna system, as it is crucial for achieving antenna-diversity schemes. According to Yu and Wang [1], mutual coupling increases the correlation of the ports and reduces the radiation efficiency of the diversity antenna solution. Thus to obtain high diversity gain in the mobile communication environment, correlation between the ports of the antennas must be small. Quantitatively, the complex cross-correlation between 2 signals (2 ports) can be obtained from the mutual coupling between the antenna ports [2], $\rho_c=r_{12}$, where r_{12} is the mutual resistance between port 1 and port 2 normalised by the input resistance of port 1.

1.1.5.1 Factors affecting isolation

Polarisation

Two linear polarised waves, one rotated 90 degrees from the other are orthogonally polarised. Waves of orthogonal polarisations do not therefore interact, antennas transmitting orthogonal polarisations will be well isolated. Also, left hand and right hand circularly polarised waves are orthogonal. In fact there are a continuum of orthogonally polarised waves. These can be found from a Poincare sphere diagram of a polarisation (refer to IEEE Std.149-1979).

Building antennas that produce only one polarisation is not trivial. Only a few types of antenna are known that generate left or right hand circular polarisation, or elliptical polarisation. None of these are small, or appropriate for small devices. We therefore must concentrate on antennas exhibiting linear polarisation. Many common antennas produce linear polarisation. Polarisation pure antennas tend to require symmetrical structures. Since small devices have the complication of the PCB and internal circuitry this is not possible in practice. However, with careful consideration, knowledge of the polarisation can be used to design the antenna with maximised isolation.

Although the polarisation of the antenna will be mixed (i.e. not pure) parts of the pattern of an antenna can be found where the polarisation is quite strongly biased. By integrating multiple antennas in such a way that the directions where the polarisation is highly biased are orthogonal this should improve the isolation between the antennas.

Antenna size

The Chu-Harrington limit sets the minimum size of an antenna. For any given frequency, bandwidth and efficiency the Chu-Harrington limit gives the minimum size of the antenna.

Part of this theory deal with polarisation. It is stated that orthogonal polarisations are independent, so restricting ourselves to only one polarisation will increases the size of the antenna.

Separation & power pattern

When two antennas as are very widely separated the coupling between them is given by the path loss equation:

Coupling = $L + G_1 + G_2$ (dB)

G_1 is the gain of antenna 1 in the direction of antenna 2

G_2 is the gain of antenna 2 in the direction of antenna 1

L is the path loss between them, given by $32.4 + 20\log_{10}(f_{MHz}) + 20\log_{10}(D_{KM})$

When two antennas are closely spaced there will be coupling caused by the reactive near field of the antennas. The direction of the highest reactive field is not necessarily the same as the direction of the far-field gain. Also, the strength of the reactive near-field contribution drops off faster with distance than the strength of the far field.

Surface wave propagation and ground plane currents

Consideration must be given to any currents set up in the ground plane. Many antennas such as monopoles and PIFAs are driven directly from the groundplane. They excite currents in the groundplane and these currents will be common to all antennas attached to it. With multiple antenna solutions this must be considered carefully as surface waves or ground plane currents are important in terms of coupling.

One way to ensure that the surface wave coupling remains low is to use a technology which confines the surface wave flow such as electromagnetic band gap (EBG) structures [3] or by design of the antenna including balanced feeding to the antenna [4]. Both of these are considered in this report.

It should also be noted that if a large portion of the groundplane is used for radiation this is likely to increase the size of the reactive near field.

Summary

When designing a multiple antenna system the following should be considered:

- Antennas should be oriented so they face each other in parts of their pattern that have low gain
- Separation distance is important. This becomes more important the closer the antennas are together
- Coupling via surface wave propagation should be minimised either by antenna design or by the introduction of features on the ground plane to inhibit current flow such as EBG structure

References:

[1] Optimum design for compact diversity wire antenna with two highly isolated ports, Yu.C., Wang.B.-Z., Xiao, S., Electronics Letters , Volume: 38 , Issue: 4 , 14 Feb 2002 Pages:154 – 155

[2] A planar diversity antenna for wireless handsets,

Ko.S.C.K., Murch.R.D., IEEE Antennas and Propagation Society International Symposium, 16-21 July 2000 Pages:968 - 971 vol.2

[3] Microstrip antennas integrated with electromagnetic band-gap (EBG) structures: a low mutual coupling design for array applications,

Fan Yang, Rahmat-Samii, Y., IEEE Transactions on Antennas and Propagation, Vol: 51, Issue: 10 , Oct. 2003 Pages:2936 – 2946

[4] Small dielectric-loaded antennas with filter response characteristics and low proximity effects for 3G and bluetooth applications
Wingfield, A.P., Leisten, O.P., Radio and Wireless Conference, RAWCON '03. Proceedings, Aug. 10-13, Pages:107 - 110

1.2 Target Antenna Specification

Antenna elements shall be developed for use on three terminal types: laptop, PDA and handset platforms. The antenna elements for the three applications shall have the same electrical characteristics and shall not exceed the dimensional requirements set out below in Table 1.1. The antenna elements shall be mounted on PCBs suitable to provide a test bed for MIMO systems.

Characteristic	
Frequency range (MHz)	5150-5275
Return loss across band (dB)	-10
Required peak gain (dBi)	1
Azimuth beam width (degrees)	120
Elevation beam width (degrees)	120
Efficiency (%)	60
Front to back ratio	5
Height (mm)	8
Width (mm)	8
Height (mm)	12

Table 1.1: Antenna characteristics

The number of antennas to be mounted on the PCB for each application is specified in Table 1.2.

Application	Number of antennas
Lap top	4
PDA	4
Handset	2

Table 1.2: Number of antennas for each application

Two development routes were taken in this research. Antenova Ltd developed the first, a dielectric resonator solution. The second, a folded loop antenna solution was developed by Queen Mary College, University of London (QMUL). These are reported on in separate sections in the following chapter - 1.3 for Antenova and 1.4 for QMUL.

1.3 High Dielectric Resonator Solution

Antenova's High Dielectric Antennas (HDA^{TM}) use ceramic dielectric material to shrink the physical size of an antenna and to improve certain other properties such as resistance to

detuning, match to 50 Ohms and radiation efficiency. With certain designs it is also possible to produce multiple resonances thereby improving bandwidth.

Dielectric materials can be used to make essentially three types of HDA™:

Dielectrically **L**oaded **A**ntennas. Here the conducting element is the radiator and the dielectric is used to reduce the physical size.

Dielectric **R**esonator **A**ntennas. Here the ceramic is the radiating element and is driven against a small groundplane. These antennas are often good on efficiency and resistance to detuning, but the bandwidths are usually modest. Large groundplanes (e.g. quarter wavelength square) can give high gain (greater than 6dBi) but bandwidths are even narrower.

Wideband **D**ielectric **A**ntennas. Again the ceramic is the radiating element but in this case it is not driven against a groundplane directly beneath the antenna. These antennas can have very wide bandwidths, but gains are modest, typically 0.5 to 2dBi, and they suffer some degree of proximity detuning.

1.3.1 Development methodology

This section outlines the description of the deployment of Antenova's High Dielectric Antennas (HDAs™) onto terminals for antenna beam switching/steering and diversity solutions. This project is part of a general strategy to look at how the implementation of multiple antennas on terminals will improve network performance.

Once the project was initialised, Antenova began the development programme. There are four aspects to the Antenova methodology for designing new antennas to meet customer specifications. These are outlined below.

1. There is a limited body of theory that may be drawn upon to define an outline approach. A number of empirical design rules have been developed at Antenova that are used to give rough estimates of the key parameters.
2. Antennas developed for other applications are considered to assess effectiveness and ease of transfer to this application
3. The Ansoft HFSS (High Frequency Structure Simulator) electromagnetic simulation program is then used to model the antenna and various design aspects are varied in order to optimise the performance of the antenna.
4. Various versions of the antenna are then fabricated and measured in the laboratory, using an anechoic chamber to measure antenna patterns. There is a considerable body of experience and 'know how' involved at this stage, especially in construction of elements from components.

In general, the design objective is to obtain good agreement between theory, simulation and practice thereby giving a high degree of confidence that the device is understood and can be readily modified to meet any changes in customer requirements.

1.3.2 Single Element Design - Simulation

Simulation of early design

Initial work using HFSS as a simulation tool for antenna development resulted in the design of an HDA™ ceramic element. A schematic of this element is given as Figure 1.3. The element was simulated in proximity to a laptop.

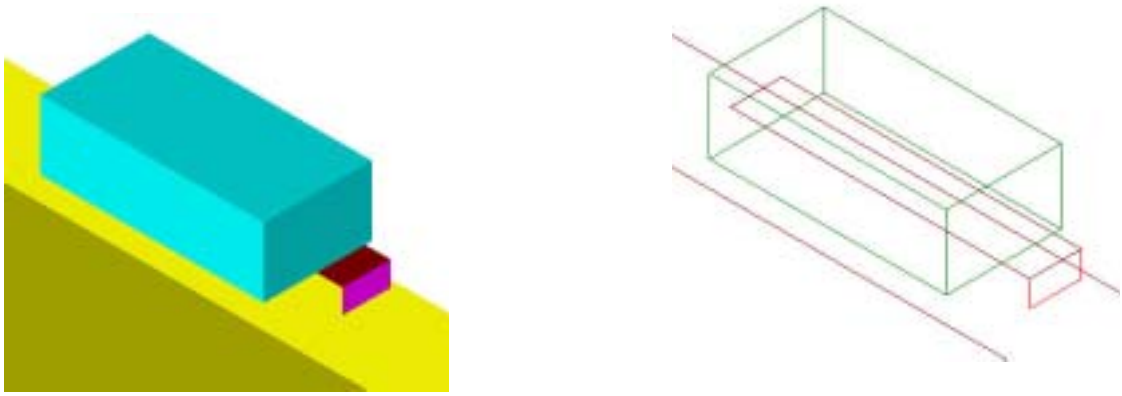

Figure 1.3: Schematic representation of single element in HFSS

The ceramic puck dimensions are 7.1mm wide, 4.6mm high 14.65 mm long and the relative permittivity of the ceramic, εr, is 40. The puck is metallised only where the microstrip runs underneath it. This ensures good electrical contact and enables a strong solder joint to be made between the PCB and the ceramic puck. The microstrip feed line is 3.2mm wide with an overhang of 2.15mm. The substrate is 1.6mm thick with εr 2.33. The centre of the microstrip is offset 1.5mm from the centre of the puck. The ground plane is the same width as the puck.

This design was shown to give extensive bandwidth: 4.8GHz to 6.0GHz at a return loss of –10dB. The graph from the simulation is enclosed as an appendix. The gain patterns of this element mounted on a laptop sized metal test fixture were also simulated. The proximity of the large ground plane associated with the lap top test fixture affects the pattern shape resulting in multiple lobes. The gain patterns are included in the appendix.

Second Generation Single Element and PCB on the PDA

Further modifications to the antenna design were performed and the size was reduced to length 11mm, width 4.8mm and height 3.2mm. Simulations using HFSS were performed

mounting the antenna centrally on a PDA sized test fixture as shown in Figure 1.4. The drawing is from the simulation software; as the antenna is symmetrical it was possible to draw half the antenna and interpolate for the second half thus reducing the solve time. The green area on the simulation is an SMA connector, the feed point for the antenna. The same element and PCB have been used in all three solutions (PDA, Handset and Laptop).

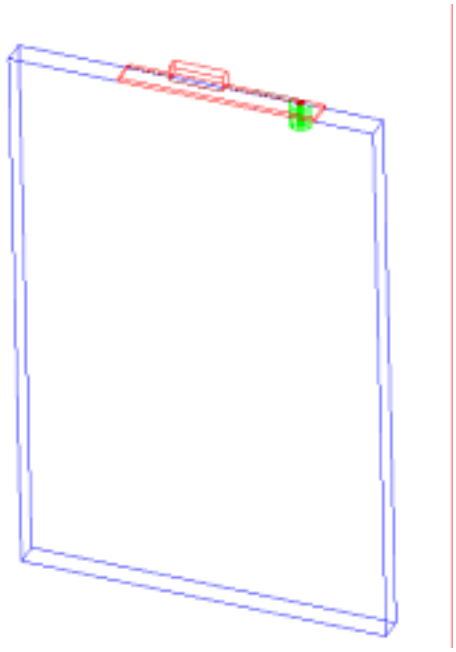

Figure 1.4: Simulated Single Element on PDA

A typical return loss plot and gain patterns from the simulation are given in the appendix. The maximum gain is away from the device with a large null in the direction of the PDA ground plane.

1.3.3 Multiple antennas on PDA - Simulation

Four symmetrical antennas on PDA

The simulations demonstrated the antenna design exceeded the required bandwidth and gave the expected directional gain patterns thus confirming this element as suitable to attempt multiple element integration. Four antennas were placed centrally on each edge of the PDA as shown in the drawing in Figure 1.5.

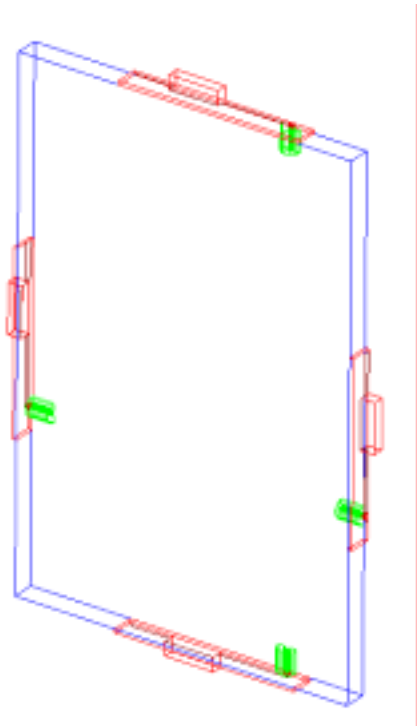

Figure 1.5: Drawing from HFSS of four symmetrical elements on PDA

Simulations with four antennas were performed and the results are in the appendix. Return loss and radiation patterns remained acceptable with the isolation between elements exceeding 24dB. Return loss, isolation, gain of a single powered antenna and the radiation pattern with all four antennas powered are included in the appendix. There are multiple peaks and troughs in the radiation pattern and these are affected by the size of the groundplane onto which the antenna is mounted so will vary with the device onto which the antenna is integrated.

Four asymmetric antennas mounted on PDA

From a practical standpoint, one or more of the antennas mounted at the centre of each face would be covered by the user's hand. This would reduce the signal strength and limit the usefulness of the multiple antenna solution. The configuration of the antennas was altered to reflect one of the possible hand positions and simulations were run. The drawing from the simulation is given as Figure 1.6.

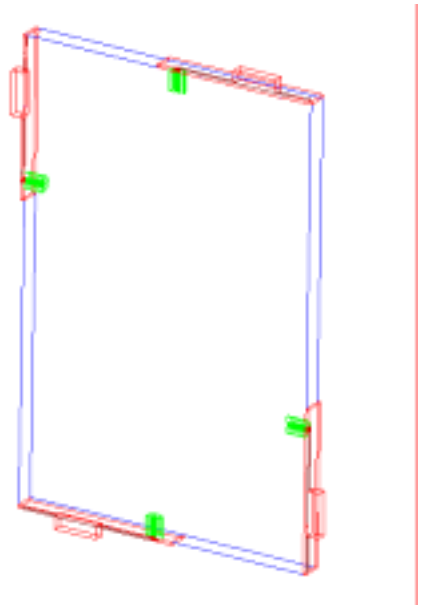

Figure 1.6: Four asymmetric antennas on PDA

A typical return loss plot for this configuration is included in the appendix and shows the elements to be well matched. As with the symmetrical version, the port-to-port isolation is better than 20dB for each combination of antennas. The radiation patterns are also included in the appendix. The radiation patterns for each of the antennas powered individually demonstrates the effect of the PDA ground plane on the direction of peak gain. Previous work by Antenova Ltd. has shown peak gain will follow the path of the longest groundplane as is also demonstrated in this case. It may thus be possible the steer the peak gain to a particular position by moving the element from a central location to one nearer the edge.

Comparison of symmetrical and asymmetrical configurations

Comparing the results from the two configurations of four elements described above we can see that the radiation patterns are affected by the size of the ground plane onto which the antennas are mounted. This is illustrated in Figure 1.7 where the red arrows indicate the direction and magnitude of the antenna radiation.

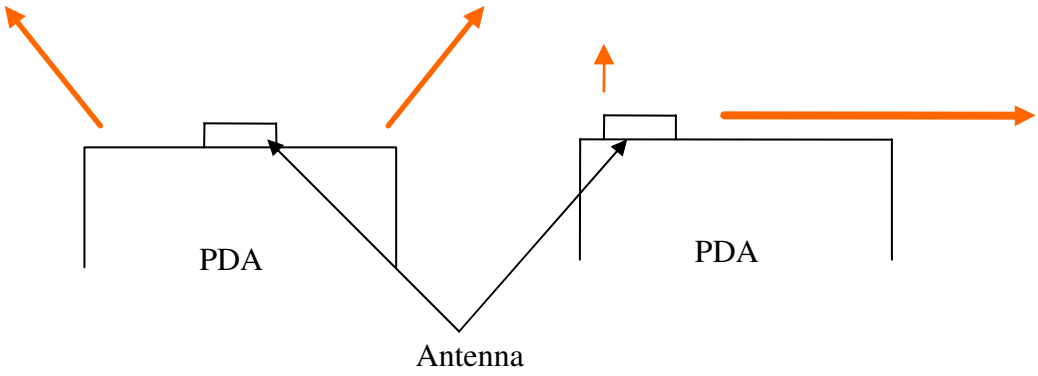

Figure 1.7: Schematic of gain 'pulled' by groundplane

With a centrally mounted antenna, the radiation fires evenly off the top of the PDA. With the asymmetrically mounted antenna, the direction of peak gain is influenced by the longest side of PDA groundplane onto which the antenna is mounted. It should be possible to select a range of intermediate element configurations and therefore change the peak direction if required. A comparison between the two PDA configurations indicates that the symmetrically configured solution gives a more omni directional pattern and therefore has more chance of receiving signal. The port-to-port isolations are similar for both solutions.

Effect of the user

No consideration has been made as to what happens when someone is holding the PDA. The proximity of the hand will have an influence on the functioning of the unit and in the case of Figure 1.4 where the elements are situated centrally on the sides of the PDA the elements on the long side may be covered by the user's hand. Obscuring the antennas will reduce the signal strength both in transmit and receive. The unit may also ramp up its transmit power to compensate, thus reducing battery life.

Moving the antennas to the top of the PDA may be one solution to avoid covering antennas, at the expense of pattern diversity as shown in Figure 1.8.

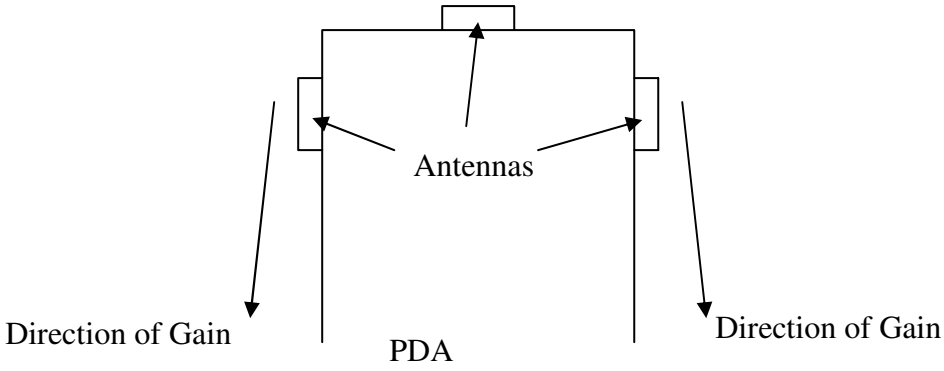

Figure 1.8: Three Elements At Top of PDA

With the antenna elements configured at the top of the PDA as shown in Figure 1.8, both the side antennas will be radiating in the direction of the user's body. The pattern diversity will be reduced but some spatial diversity will still be present. Essentially the peak gain direction is the same and some power will be lost to the user's body.

To maximise the power to free space, and maintain a high degree of pattern diversity for a PDA solution the configuration in Figure 1.9 is recommended, (for the user holding the PDA in their left hand).

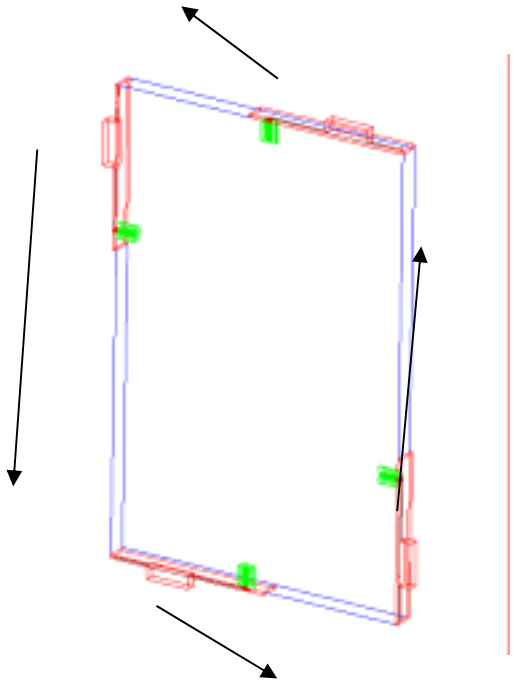

Figure 1.9: Preferred Solution with Direction of Gain Indicated

1.3.4 Practical antenna design – single element

Through an iterative process, an antenna element was designed to work on the laptop test rig. This element is shown below in Figure 1.10 and the dimensions are given in Table 1.3.

Figure 1.10: Antenna element

	Dimension/mm
PCB length	50
PCB width	10
PCB thickness	1
Ceramic length	11
Ceramic width	4.8
Ceramic height	3.2

Table 1.3: Dimensions of antenna element

The early prototypes proved to be sensitive to positioning and detuning. Further reference was made to simulations and antenna elements capable of mass production were designed. Drawings of the final antenna element are included in the appendix. The ceramics used in this research project were cut from block material and ground by hand. This resulted in some inconsistency between antennas of approximately +/-0.25mm. This non-conformance gave rise to variations in terms of central resonant frequency. Accurately produced ceramic parts can easily be produced by 'green machining' for quantities of hundred pieces, after that it is more economical to use a hard tool and press and fire the parts to size. Pressed ceramic elements are ideally suited for a mass production environment, a high degree of tolerance can be maintained as well as packing to tape and reel for use by pick and place machines. The automatically placed part will be reflow soldered to the PCB and will result in a closely toleranced part with little deviation from the central frequency.

1.3.5 Laptop design

The OEMs and ODMs of current laptop solutions require the antennas to be positioned in the lid rather than the base of the laptop unit. The laptop test rig was constructed from FR4 double-sided PCB as shown in Figure 1.11. Solder joints between the sections of FR4 were continuous. The connecting cables were RG405 semi rigid, tack soldered to the main board but also soldered to the FR4 after passing through a small hole. The outer of the cable was soldered to the groundplane of the antenna PCB with the inner soldered to the track on the topside of the antenna PCB. All four coaxial feed cables were the same length thus ensuring the losses in each one should be the equal. The cable was meandered to ensure that the cables and connectors protruding off the end of the board should be at equal distance from the last grounded point.

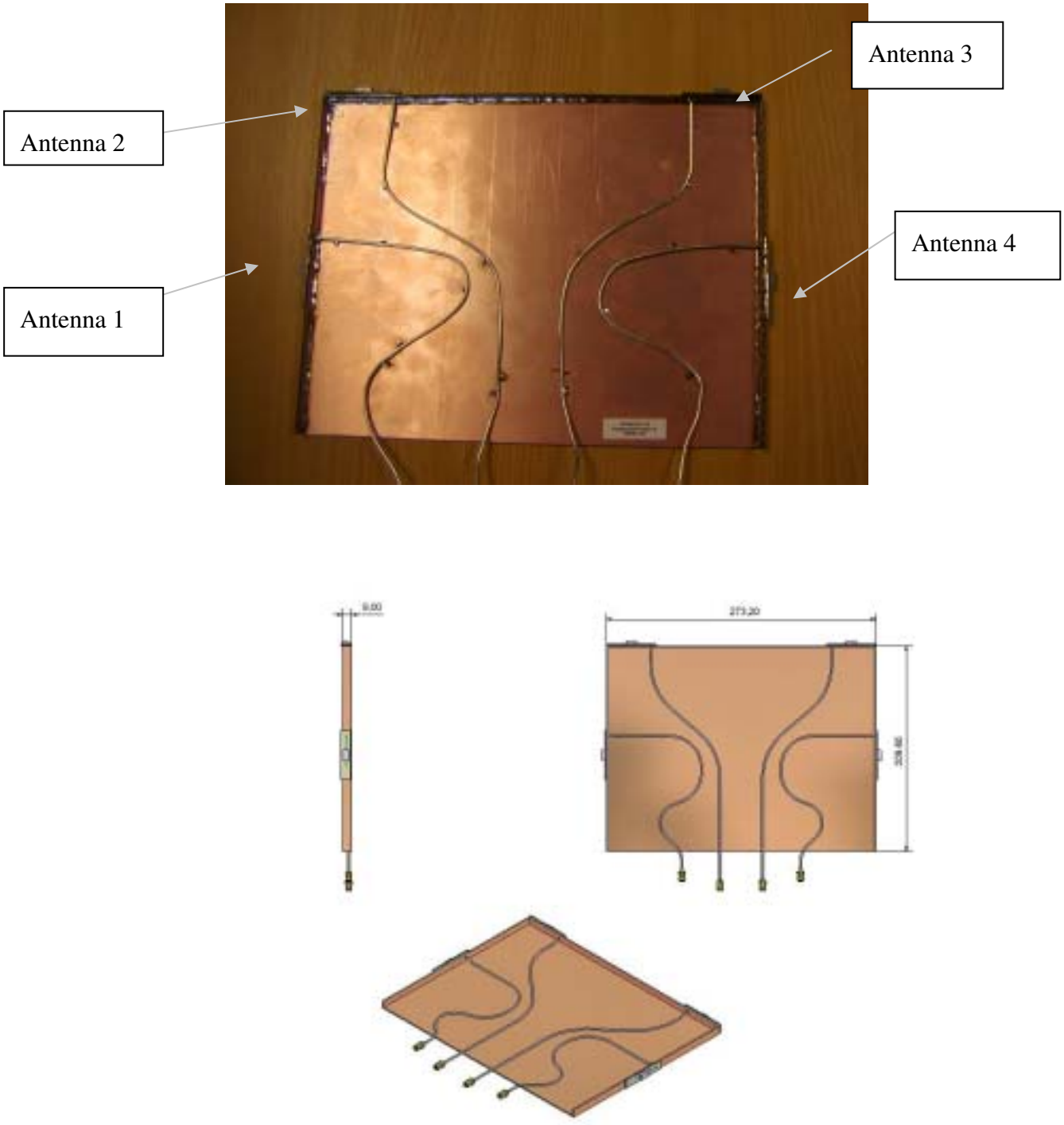

Figure 1.11: Placement of antenna elements around laptop test rig lid

Return loss

The four antennas were connected to a vector network analyser (VNA) and measurements of the return loss were made. A graph of the combined results for the four antennas is given as an appendix. All four antennas mounted on the laptop test rig meet the return loss specification of -10dB across the frequency range 5150-5275MHz. There is some variation between the antennas in terms of centre frequency but the available bandwidth ensures all are

within specification. The variation is due to the handcrafted nature of the ceramics and would not be apparent with machined parts.

Isolation

One of the outcomes of this OfCom project will be a definition of the antenna isolation requirements for MIMO. To define the baseline to which we were working, the port-to-port isolation between the antennas was measured in relation to antenna 1. A graph of the data is given as an appendix. The minimum isolation across the band is indicated for each antenna relative to antenna 1 in Table 1.4 In the worst case, the isolation between the antennas was better than 25dB. This degree of isolation is much higher than the minimum for multiple antenna systems that has been discussed with other project partners external to this research programme (10dB has been postulated).

Antenna number	Isolation relative to antenna 1/dB
2	25
3	35
4	40

Table 1.4: Port-to-port isolation on laptop

Antenna gain

The gain patterns from the laptop with four embedded antennas were measured in an anechoic chamber. The patterns were measured in the plane of the laptop lid as described schematically in Figure 1.12 with the centre of the laptop lid aligned with the centre of the receiving horn antenna. The receiving horn antenna remained stationary as the device under test was rotated.

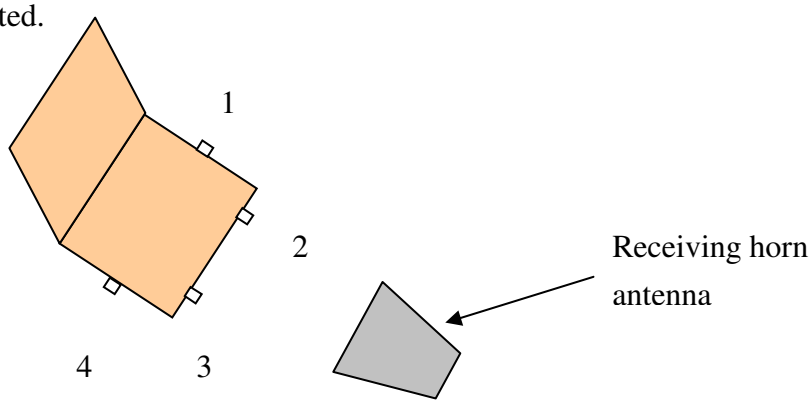

Figure 1.12: Schematic representation of receiving horn and laptop alignment

The gain patterns produced in the anechoic chamber are given as appendices. From the radiation patterns we can see effect of the large groundplane. The peak gain of each antenna is directed away from the main body of the laptop test rig - good pattern diversity. The peak gain value for the antennas varied across the frequency range and between the antennas but remained consistently between 2.9dBi and 4.1dBi. This is summarised below in Table 1.5. The high peak gain measured for these antennas reflects the directionality of the antennas.

Frequency/MHz	Antenna number			
	1	2	3	4
5140	4.1	3.0	3.5	3.9
5170	3.8	2.9	3.3	3.8
5200	3.6	3.0	3.0	3.7
5230	3.3	3.3	3.3	4.1
5260	3.4	3.5	3.2	4.0

Table 1.5: Peak gains for laptop solution

1.3.6 PDA Design

Four single elements were soldered to a PDA sized copper box to simulate the PDA environment. The antennas were distributed asymmetrically around the PDA according to the simulations described in section 1.3.4. The feed for the antennas was provided by rigid co-axial cable run inside the box section to SMA connectors on the external surface as shown below in Figure 1.13.

Figure 1.13: Photographs of PDA solution

The numbering of the antenna elements on the PDA test rig is indicated on the photograph on the right: antenna 1 is located at the top of the figure with the numbering clockwise.

Return loss

The return loss of the four antennas was measured and the results are displayed graphically as an appendix. All four antennas meet the return loss requirement of –10dB across the specified frequency range.

Isolation

The port-to-port isolation referenced to antenna 1 was better than 20dB across the frequency band with the maximum isolation demonstrated between antennas 1 and 4 that are spaced furthest apart. A graph is included as an appendix.

Antenna gain

The gain of the four antennas on the PDA was measured in an anechoic chamber. 2-dimensional measurements were taken in the three principle planes around the centre frequency of 5.2GHz. The gain patterns are included as appendices. The plots presented are composites for the total polarisation i.e. the vertical and horizontal components are summed. The connectors for the antennas were mounted on the underside of the device and their position is annotated on the schematics included with the plots as required.

The patterns measured show the diversity of the antenna patterns with the nulls of one antenna being filled with the peaks of another. The peak observed gains measured for the antennas in the 3 principle planes are given in table 1.6 below.

Frequency/MHz	Antenna number			
	1	2	3	4
5140	3.8	5.9	3.2	5.1
5170	3.8	6.1	3.2	5.5
5200	3.8	6.2	3.6	5.3
5230	4.1	6.3	3.6	5.4
5260	4.1	6.1	3.1	5.1

Table 1.6: Peak gains for PDA solution in horizontal polarisation (dBi)

The simulations of the radiation patterns for the PDA indicate the presence of detailed structure. With only the 3 principle planes measured it is possible that the maximum gain would be missed. From the 3 polar plots of composite gain it is seen the antennas radiate in different directions. For example in the plane of the PDA (Cut 1) the radiation patterns for

antennas 2 and 4 are directed to the left and right respectively and antennas 1 and 3 contribute to null filling.

It should be noted that the antenna teams at University of Bristol also measured the PDA unit in the Bristol anechoic chamber. Their 3d measurements confirmed the radiation patterns to be directed in the positions expected.

1.3.7 Handset Design

Two single elements were soldered to a handset sized copper box to simulate the handset environment. The elements were located on either side of the box with co-axial cable running inside the box section to SMA connectors on the external surface of the box as shown below in Figure 1.14.

Figure 1.14: Photographs of handset solution

Return loss

The return loss for the two antennas mounted on the handset was measured and is shown graphically as an appendix. The bandwidth is easily covered at –10dB.

Isolation

The port-to-port isolation was measured on a VNA. A graph showing this is given as an appendix. The isolation was better than 25dB across the band of interest.

Antenna gain

2-dimensional gain measurements were taken in the three principle planes of the device under test around the centre frequency of 5.2GHz. The antenna gain plots, with the vertical and horizontal components of polarisation summed, are included as appendices. Schematic diagrams to enable visualisation of the orientation of the handset are given alongside each composite plot. The connectors for the handset were located at the end of the handset as shown in the photographs in Figure 1.14 and are annotated on the composite plots where appropriate.

From the antenna gain patterns we can see that the null of one antenna pattern is covered by the peak of the other, giving good all round coverage. The peak gains measured for the antennas are given in Table 1.7. The high peak gains measured for these antennas indicate the directivity of the patterns.

Frequency/MHz	Antenna number	
	1	2
5140	4.6	4.3
5170	4.3	4.2
5200	4.3	4.2
5230	4.2	4.2
5260	4.2	4.1

Table 1.7: Peak gains for handset horizontal polarisation (dBi)

1.3.8 3-dimensional pattern correlation

Antenova Ltd. has previously correlated antenna gain patterns using the Excel "correl" function. Two patterns are compared by measuring in one plane and one polarisation and correlating data points at eight degree intervals.

This method could be extended to form a correlation matrix showing how different patterns and polarizations are related. In order to do this, the measurement planes must be defined. Figure 1.15 shows a 4-element layout. Each element needs to be measured in 2 planes and in 2 polarisations, resulting in 16 antenna patterns. When the patterns are correlated peak gain of each antenna should appear in at least one of the cuts. The xz and yz planes are considered below, however, the most appropriate coordinate system would be defined once the design of the antenna was finalised.

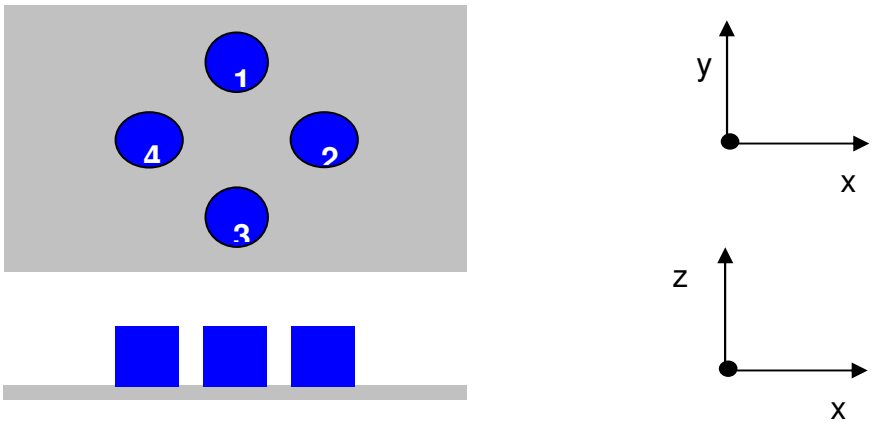

Figure 1.15: Definition of measurement planes

Defining the 2 measurement planes A and B and the 2 polarisations which can be measured for each plane theta (T) and phi (P) a matrix of possible combinations is produced, shown in Figure 1.16. Not all of the combinations of correlations are relevant, but there are still 24 useful correlation coefficients shown in blue.

	1AT	1AP	1BT	1BP	2AT	2AP	2BT	2BP	3AT	3AP	3BT	3BP	4AT	4AP	4BT	4AP
1AT																
1AP																
1BT																
1BP																
2AT																
2AP																
2BT																
2BP																
3AT																
3AP																
3BT																
3BP																
4AT																
4AP																
4BT																
4BP																

Figure 1.16: Matrix of possible correlation coefficients; blue squares denote useful correlation measurements, grey squares show duplication or self-correlation.

3D Correlation theory

If the far field radiation pattern is defined as being composed of orthogonal theta and phi components of E as defined in Equation 1, then the signal correlation, ρ_e is defined as in Equation 2, see reference [1,2]. Since a correlation is defined for mean zero data we must first subtract the average value of E from the data.

$$E_m(\theta,\phi) = E_\theta(\theta,\phi)\hat{\theta} + E_\phi(\theta,\phi)\hat{\phi}$$

Equation 1

$$\rho_c = \frac{X[A_{12}]}{\sqrt{X[A_{11}] \bullet X[A_{22}]}}$$

Equation 2

Where A_{mn} is defined as in Equation 3

$$A_{mn}(\theta,\phi) = \Gamma E_{\theta,m}(\theta,\phi)E^*_{\theta,n}(\theta,\phi) + E_{\phi,m}(\theta,\phi)E^*_{\phi,n}(\theta,\phi)$$

Equation 3

Γ is the ratio of incoming polarisations to the antenna

X[] is the expectation operator defined as in Equation 4. It should be noted, since we are correlating across the surface of a sphere, the integral can be defined either as a double integral across theta and phi or as a closed surface integral. The factor of 41,253, equivalent to 4π steradians, normalises our data so we get the expectation value for the surface of a sphere.

$$X[A_{mn}(\theta,\phi)] = \frac{1}{41{,}253}\int_{\phi=0}^{2\pi}\int_{\theta=0}^{\pi} A_{mn}(\theta,\phi)d\theta d\phi = \frac{1}{41{,}253}\oint_S A_{mn}(\theta,\phi)dS$$

Equation 4

The expectation operator can accordingly be evaluated in one of two ways described here as case 1 and case 2.

Case 1

If N evenly distributed points are defined on a sphere, indexed by i, then the surface integral can be performed as a summation as in Equation 5, below, where ΔS is equal to 4π/N steradians. Substituting equation 5 into equation 2 gives equation 6.

$$X[A_{mn}(\theta,\phi)] = \frac{1}{41{,}253}\oint_S A_{mn}(\theta,\phi)dS \approx \frac{1}{N}\sum_{i=1}^{N} A_{mn}(\theta_i,\phi_i)$$

Equation 5

$$\therefore \rho_c \approx \frac{\sum_{i=1}^{N} A_{12}(\theta_i,\phi_i)\Delta S}{\sqrt{\sum_{i=1}^{N} A_{11}(\theta_i,\phi_i)\Delta S \bullet \sum_{i=1}^{N} A_{22}(\theta_i,\phi_i)\Delta S}} = \frac{\sum_{i=1}^{N} A_{12}(\theta_i,\phi_i)}{\sqrt{\sum_{i=1}^{N} A_{11}(\theta_i,\phi_i) \bullet \sum_{i=1}^{N} A_{22}(\theta_i,\phi_i)}}$$

Equation 6

A problem with this method is that evenly distributing N points on a sphere is a not a trivial task. A reasonable approximation can however be achieved relatively easily as expressed in Figure 1.17.

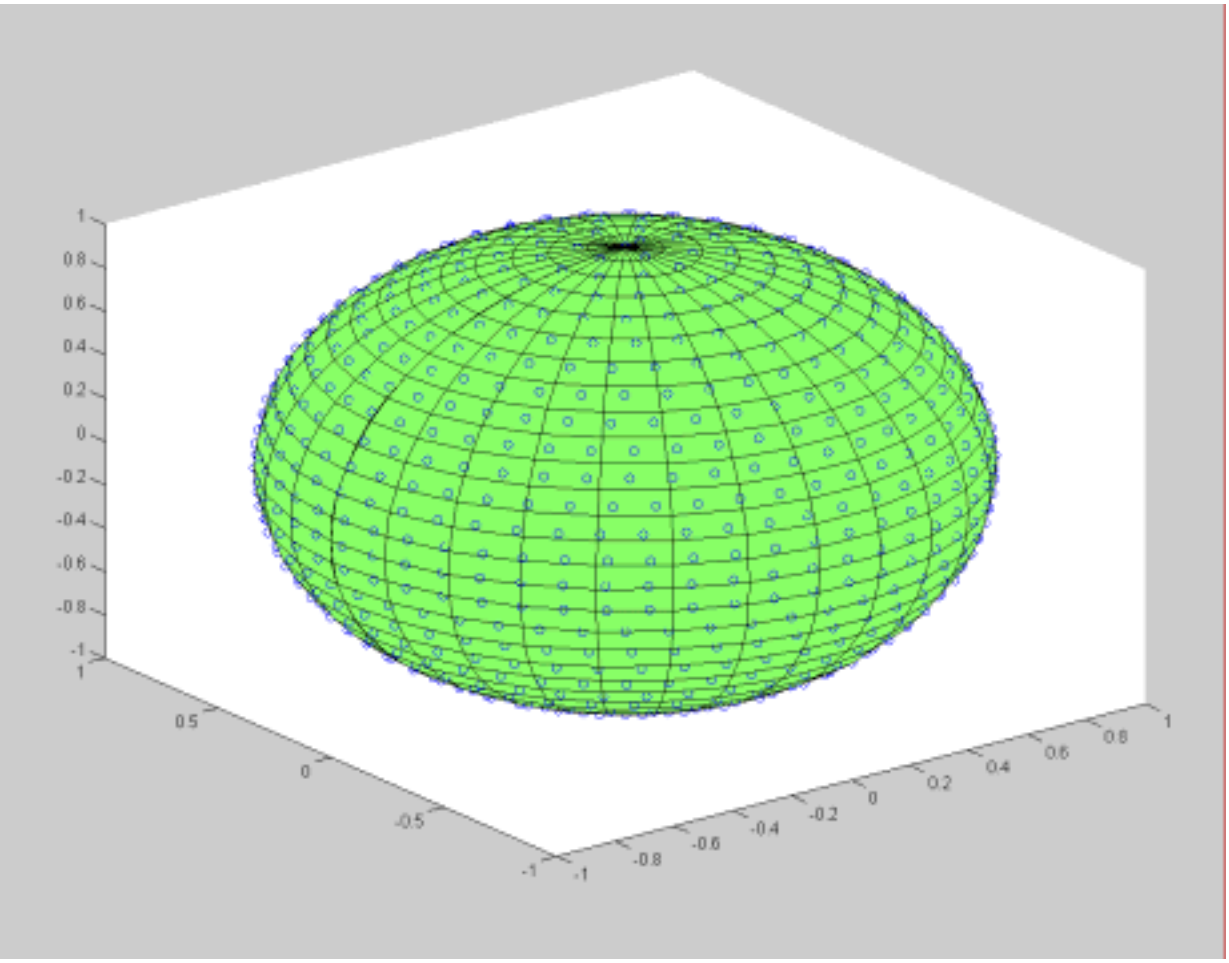

Figure 1.17: Measurement points distributed evenly over the surface. The correlation is now uniformly weighted over the sphere.

Case 2

In this case the integral is performed by summing over data that is regularly spaced over theta and Phi but therefore not evenly distributed on the sphere. The data points are then weighted in the summation of Equation 6 to reflect this uneven distribution. This has the advantage that the distribution of points is likely to arise from many sorts of measurements. Note that in the equations below we have chosen to work in degrees rather than radians since this is the likely form of the data we will be working with.

$$X[A_{mn}(\theta,\phi)] = \frac{1}{41{,}253}\oint_S A_{mn}(\theta,\phi)dS = \frac{1}{41{,}253}\sum_{u=1}^{360}\sum_{v=1}^{180} A_{mn}(\theta_v,\phi_u)Sin\,\theta_v$$

Equation 7

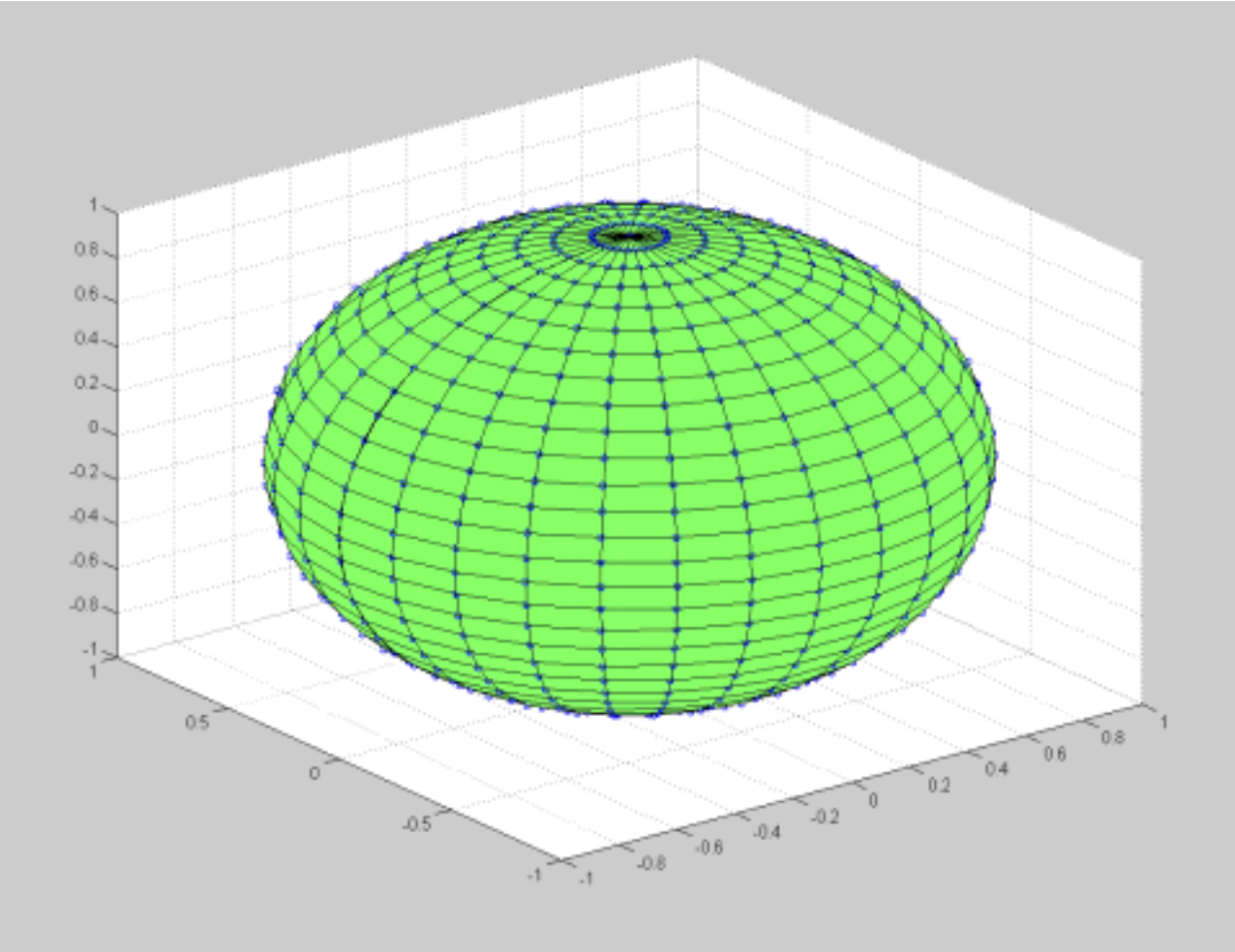

Figure 1.18:measurement points distributed evenly in theta and phi. Points lie on the intersection of the lines of latitude and longitude. Point density is highest at the top and bottom of the sphere, over emphasizing the importance of pattern differences at these points. The data must therefore be weighted by Sin theta.

Substituting Equation 7 into Equation 2 gives Equation 8.

$$\therefore \rho_c \approx \frac{\sum_{u=1}^{360}\sum_{v=1}^{180} A_{mn}(\theta_v,\phi_u)Sin\theta_v}{\sqrt{\sum_{u=1}^{360}\sum_{v=1}^{180} A_{mn}(\theta_v,\phi_u)Sin\theta_v \bullet \sum_{u=1}^{360}\sum_{v=1}^{180} A_{mn}(\theta_v,\phi_u)Sin\theta_v}}$$

Equation 8

Summary of theory

In diversity receiving systems the important parameter is the difference between the voltage signals at the output terminals of the antennas. The difference is a function of both how the radio signals are distributed in time and space, which in turn is a function of the multipath environment, and the difference between the antenna gain patterns. The multipath variation in the radio signals will be different in every location and will also change with time. The effect of spatial diversity is therefore difficult to measure and is usually assessed by statistical experimental methods by gathering data in different environments such as the office, laboratory, outdoors, etc. However, the beam and polarisation diversity of two antennas can be assessed much more directly by measuring the full 3D cross-correlation coefficient of the 3D gain patterns of the two antennas.

Of the two methods of 3D cross-correlating measurements outlined above, it is our intention to use the method in case 2 as it does not require the data to be re-interpolated on to a new set of points. The term , in equation 3, means we must either define the ratio of theta and phi polarizations of the incoming wave, or graph the effect of varying on the correlation coefficient. For the sake of simplicity we will quote the correlation coefficient for the case of equal theta and phi polarized signals.

Results from 3-dimensional radiation patterns

The correlation of the antenna gain patterns for the PDA solution were calculated according to the method described above using data measured in the Bristol anechoic chamber. The 3D patterns are included as an appendix. These data are displayed in table 1.8 for both the magnitude of the E-field (Mag E) and for the phase.

Mag E				
Element	1	2	3	4
1	1	0.0429	0.0333	0.0487
2	0.0429	1	0.0402	0.0195
3	0.0333	0.0402	1	0.0174
4	0.0487	0.0195	0.0174	1

Phase				
Element	1	2	3	4
1	0	-56.961	-13.674	-87.777
2	56.961	0	-41.189	23.175
3	13.674	41.189	0	30.759
4	87.777	-23.175	-30.759	0

Table 1.8: Cross correlation coefficients for the PDA antennas using the Antenova algorithm

These correlation figures show a significant level of de-correlation between the antennas on the PDA device. They are probably an order of magnitude better than the level required for MIMO operations.3 The University of Bristol group also have a 3D cross-correlation algorithm which they applied to the same data set. These results are shown in table 1.9. It can be seen that although the correlation coefficients are not the same, they are of a similar magnitude overall and confirm that the de-correlation between the antennas is excellent.

	Mag E			
Element	1	2	3	4
1	1	0.0495	0.0087	0.0221
2	0.0495	1	0.0189	0.008
3	0.0087	0.0189	1	0.0385
4	0.0221	0.008	0.0385	1

Table 1.9: Cross correlation coefficients for the PDA antennas using the Bristol University algorithm

It is also possible to correlate the simulated 3D antenna gain patterns. Here the results might be expected to be slightly better than for the measured gain patterns because there are no cables radiating or chamber problems that contaminate them. Antennas 1-2 have a cross-correlation coefficient of 0.0094, 1-3 have 0.0226 and 1-4 have 0.0380. These have the same magnitude as the correlations based on measured data and the results for 1-3 and 1-4 lie between the Antenova and Bristol values. Once again these results confirm that the de-correlation between the antennas is excellent and they are suitable candidates for diversity and MIMO systems.

1.3.9 The cost of Antenova MIMO antennas

The antennas developed by Antenova for this project were designed from the outset to be suitable for high volume manufacture. It is a very simple design to make and a single automated assembly line would be able to manufacture about 200/minute. There are many factors influencing the cost of antennas, but in large volumes the manufacturing cost might be expected to be less than one dollar, given the following factors:

- No connector or cable is supplied with the antenna.
- The PCB is made from Duroid.
- The volume is 1 million pieces or greater.

The Antenova antenna is small enough for several to be used in small space. Because the stored energy inside the dielectric is very high, the antennas tend not to couple to each other strongly and so good diversity can be obtained from them, even when they are electrically

close. They are also efficient and suitable for integration with RF modules and so, with the low manufacturing cost, represent a good candidate for future MIMO system antennas.

1.3.10 Conclusions- HDA™

The antenna element designed using Ansoft high frequency simulation software (HFSS) performed as the simulations predicted on all three data terminals. The bandwidth exceeded the specified requirement at –10dB.

The DRA solution was not adversely affected by the three different sizes of ground plane onto which the multiple antennas were mounted. The same single element could therefore be used on each of the three applications without modification.

The antenna was designed to be directional in nature with the peak gain away from the terminal. The placement of the antennas on opposing sides of each terminal ensured that the direction of maximum gain was different for each antenna. This provided good coverage in all directions and combined with the minimal current in the ground planes ensured good isolation between the antennas.

Radiation pattern measurements taken at Bristol University and at Queen Mary, University of London confirm the antenna gains measured by Antenova.

Signification de-correlation was shown for the antennas both with the simulated and measured data. The de-correlation calculated from the simulations was greater than the measured data due to the perfect environment of the simulation. The team at Bristol University confirmed the magnitude of the de-correlation. This should ensure that the antennas are suitable for integration into MIMO enabled terminals.

1.4 Folded Loop and Photonic Bandgap Structures

Conventional MIMO terminals with multiple antennas often use co-polarised linear arrays based on space diversity. This set-up is suitable for a base station scenario but not for a compact mobile terminal. There are wide research and development efforts into compact antenna arrays for MIMO wireless communication terminals. The essential requirements for this system are that the antennas must be diverse, i.e. they must be capable of receiving different signals even though they are closely spaced. At the moment, the use of multiple antennas on compact mobile terminal (laptop, PDA or handset) for the MIMO communication systems still remains a challenge. There are two main reasons for this. First, it is difficult to implement multiple antennas in something as small as a handset. Second, the performance of the handset antenna will be degraded by the effects of inter-antenna coupling, envelope cross-correlation and coupling to biological tissues in the user's head and/or hand. When multiple antennas are involved, either at different frequencies or at the same frequency

as in a diversity solution, the technical challenges are even more complex. Antenna-diversity techniques generally fall into four categories. Spatial diversity involves the use of physically separated identical antennas. Pattern diversity uses co-located antennas that are of different size, shape, or orientation having dissimilar radiation patterns and their signals are combined in phase due to their collocation. Polarization diversity uses two antennas oriented at 90° to each other. Finally, transmit/receive diversity schemes employ separate antennas for transmit and receive functions.

The following sections report the simulations and experimental work performed by Queen Mary College University of London (QMUL) on balanced antenna designs (folded loop antennas) and the application of electronic bandgap structure on groundplanes. The simulations were performed with CST Microwave Studio, an electromagnetic software based on the Finite Integral (FI) method which is similar to the Finite Difference Time Domain (FDTD). Measurements are carried out in the anechoic Chamber at QMUL's Antenna Lab.

1.4.1 Development methodology – Folded loop

The antenna element chosen is a double folded dipole/folded loop antenna [1]. The double folded dipole originated from folding the folded dipole as shown in Figure 1.19a and 1.19b. The folded loop antenna is essentially a two-wire transmission line, folded at about a quarter-wavelength to form an equivalent half-wave double folded dipole. At the same time it appears as a loop antenna, from which the antenna is referred to as folded loop. The surface currents of the folded dipole are in-phase for the two main branches while anti-phase for the two shorter branches thus cancelling each other as shown in Figure 1.19c. The radiation is mainly caused by the two main branches. Moreover, the current in the two main branches reduces at the end of the turn. By folding the folded dipole near this end, the currents are not greatly affected as shown in Figure 1.19d. The effective area of the antenna also increases.

1.4.1.1 Groundplane currents

In a mobile terminal such as a laptop/PDA/handset, the antenna is usually in close proximity with the PCB board of the device. This PCB board acts as a ground plane. With antennas such as a dipole being fed by a coaxial cable, currents on the ground plane are generated by the outer coaxial cable due to its unbalanced nature. In practical use, when a person is in close proximity or is in contact with the device, the currents on the ground plane vary significantly. This reduces the gain and affects the frequency of operation of the antenna. However, because the folded loop antenna has a one-wavelength loop structure, no unbalanced current is likely to be produced on the feed line i.e. the antenna is a self-balanced

structure, which is useful to reduce the current flow on the ground plane. In order to show that there is very little current distribution on the ground plane for a folded loop antenna, a comparison is made between the folded loop antennas with balanced and unbalanced feeding. The folded loop is designed to resonate at 5.2GHz. Figure 1.20a and 1.20b shows the currents on the ground plane with balanced and unbalanced feeding, respectively. Only slight difference is seen around the feed point between the current distribution in both the balanced and unbalanced system. The rest of the current distribution has almost similar amplitudes for both systems. This shows that the folded loop is indeed a balanced structure by itself generating very little current on the ground plane disregard of its feeding method.

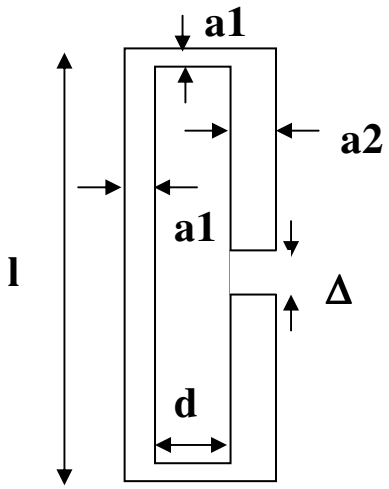

A: Folded dipole

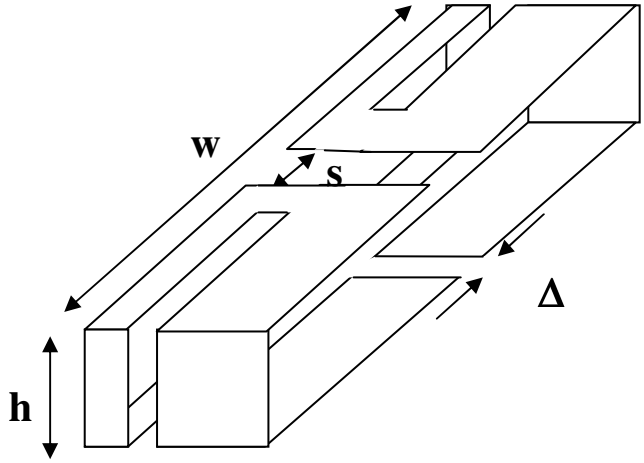

B: Folded Loop

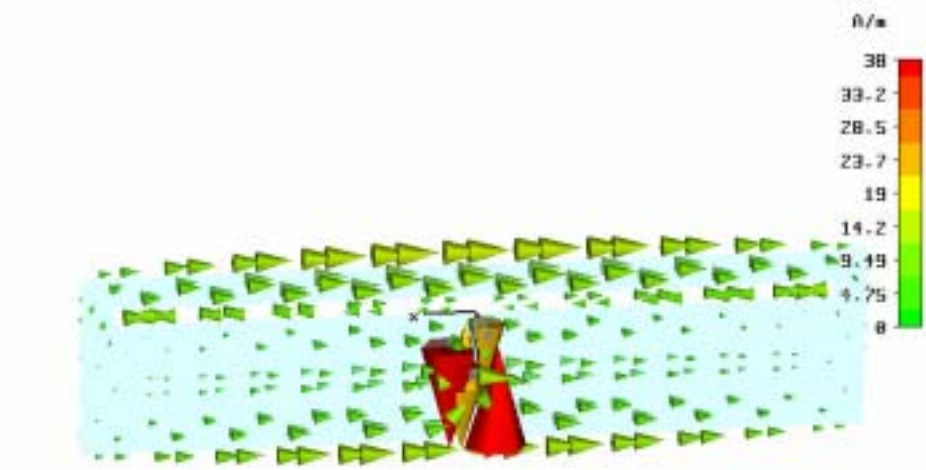

C: Surface current of folded dipole

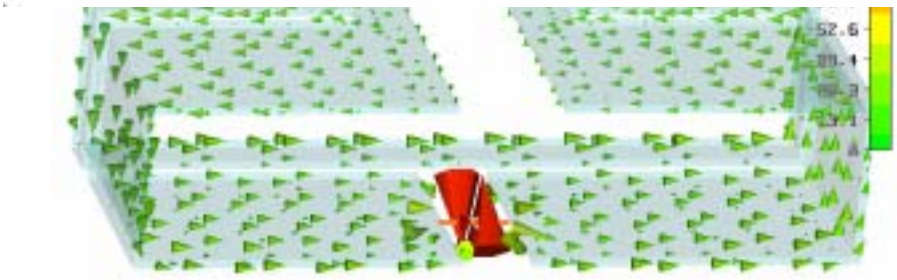

D: Surface current of double folded dipole

Figure 1.19; Description of dipole

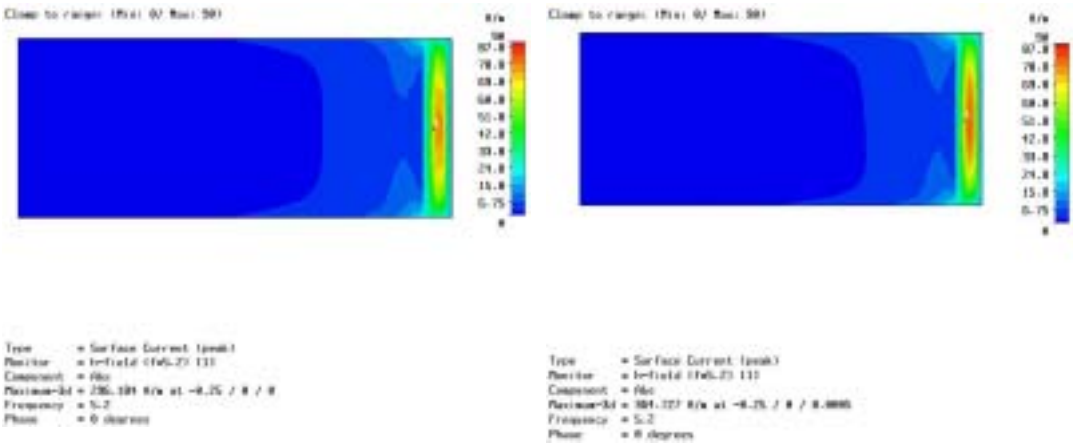

(a) (b)

Figure 1.20 Folded loop at 5.2GHz above a ground plane with (a) Balanced feeding; (b) Unbalanced feeding

1.4.2 Development methodology – Dielectrically filled folded loop

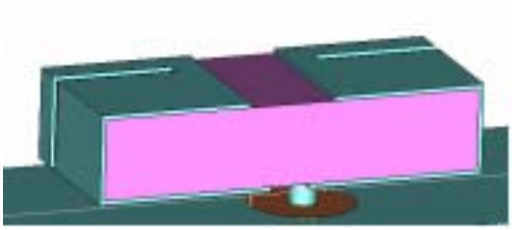

Figure 1.21: Dielectric loaded double folded dipole

The double folded dipole has a length of approximately λ/4 which is about 14.4mm at frequency 5.2GHz. In order to reduce the size of the antenna and also for mechanical support [2][3], the antenna folds around a dielectric slab of the same dimension as the antenna. The dielectric slab used is a piece of low loss fibreglass (εr =4) and a piece of ceramic (εr =6). The feeding method employed on the antenna is unbalanced and no balun was used to form a balanced feed. One of the reasons is because a balun such as a sleeve balun at 5.2GHz is narrow-band. Moreover, the folded loop antenna does not induce a lot of current on the ground plane below, whether fed in a balanced or unbalanced mode. The reducing of

induced currents on the ground plane provides a good isolation between the antenna with its adjacent elements in a multi-antenna system.

1.4.3 Laptop Design

Two designs were made for the MIMO laptop solution. The differences lie in the dimensions and orientation of the folded loop on the laptop. The folded loop was not mechanically rigid enough and thus it was designed to include a support (fibreglass GRP ε_r=3.99). The fibreglass not only supports the folded loop but also helps to reduce the antenna size. The laptop lid was manufactured from 0.4mm thick copper and the folded loop was made of 0.2mm thick copper. Figure 1.22 shows the first MIMO laptop design with its antenna element design shown in Figure 1.23. The antenna element has a dimension of 13.2mm x 5.5mm x 2.9mm and the laptop size is 270mm x 210mm x 10mm. Figure 1.24 shows the second MIMO laptop design with its antenna element design shown in Figure 1.25. The antenna element has a dimension of 10mm x 5.5mm x 6.5mm and the laptop size is 270mm x 210mm x 10mm.

The antenna elements size and orientation in the two designs are different. In Design 1, the antennas are placed with the two main branches in parallel with the laptop screen (large ground plane) while in Design 2, the antennas are placed with the two main branches orthogonal to the laptop screen. The two designs have been made to investigate the effects on the antenna performance with respect to its orientation.

1.4.3.1 Design 1

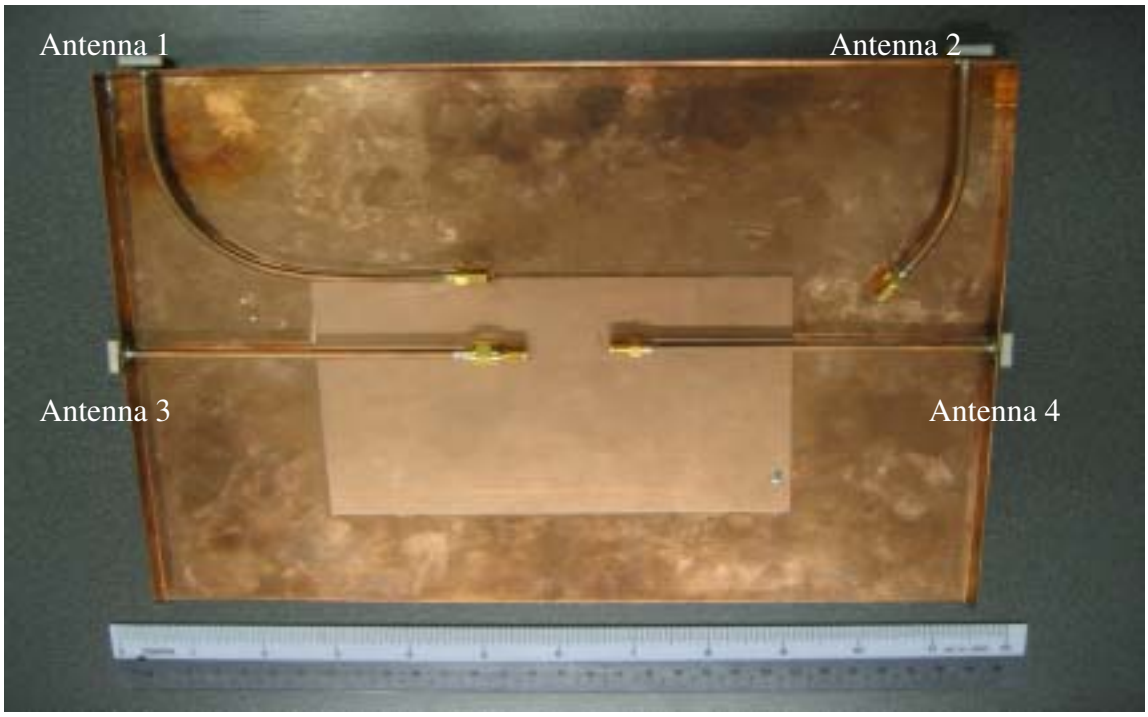

Figure 1.22: Design 1: Four antennas on laptop lid for MIMO application

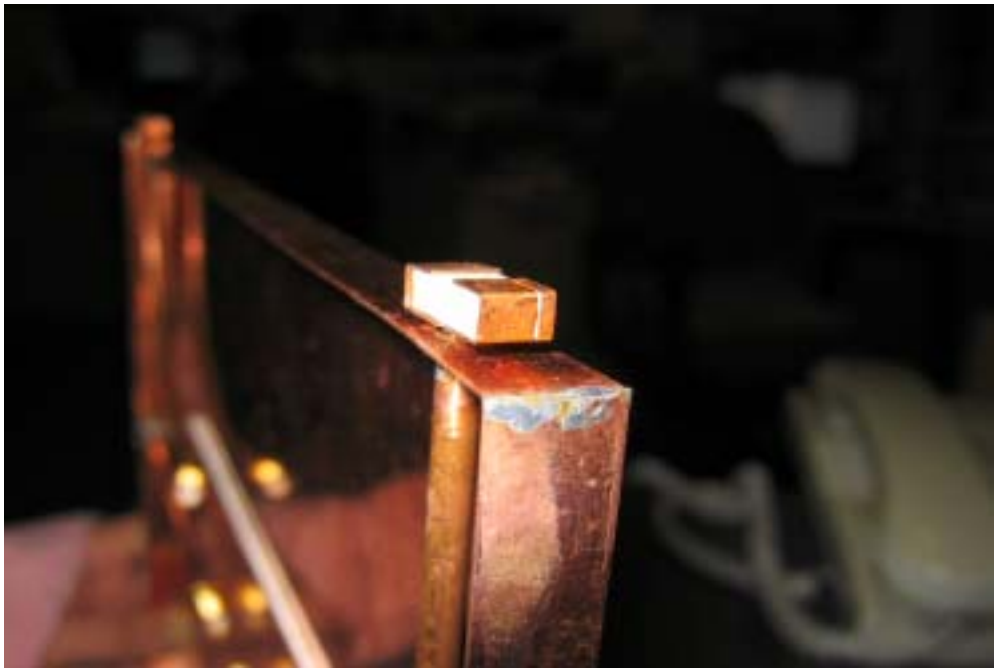

Figure 1.23: Antenna element (Size : 13.2mm x 5.5mm x 2.9mm)

Return loss

The return loss and isolation measurements were performed with a HP 8720ES 50MHz-20GHz network analyser. The graphs are recorded as appendices. Simulations using CST were also performed and these results are also plotted in the graphs for comparison. The results agree well, the discrepancy is due to the fact that the calibration was not de-embedded up to the antenna port (not including the losses due to the coaxial connector). The dotted lines indicate the bandwidth below -10dB according to the required specification. Both the simulated and measured bandwidths are approximately double the requirement of 120MHz in the specification.

Isolation

Port to port isolation was measured and result is plotted as a series of graphs as appendices. The isolation is better than -20dB. Because of the presence of noise floor and that rigid coaxial cable was used (coupling between the cables unavoidable), the measured isolation is higher between Antenna 3 and Antenna 4 as they have less than about -50dB calculated isolation. The measured and simulated isolation do not agree as well as the results for the return loss and this is due to the fact that the rigid coaxial cables couples with each other besides the antennas. The results agreement could be improved with semi-rigid coaxial cables. Spatial diversity is easily employed in this design among all the antennas due to the big laptop screen which is more than half a wavelength at 5.2GHz.

Antenna gain

The radiation patterns were measured in an anechoic chamber. The transmitting source is a quad ridge horn with dual-polarisation capability. The MIMO laptop design was mounted on turntable aligned to the centre of the horn. Co- and cross-polar gain patterns measured for the E-plane and H-plane for all four antennas are included as appendices. The measured patterns are in good agreement with the simulated results.

To compare the calculated peak gain and measured gain, a 10dB standard gain horn was first measured. The horn was replaced by the laptop antenna and the peak gain for Antenna 1 was measured. The calculated peak gain for Antenna 1 was 7.05dBi and the measured was 6.75dBi. However, only the peak gain for Antenna 1 was measured at the time but the peak gain for the rest of the antenna should be close to the calculated. The calculated peak gain for Antenna 3 is 6.98dBi.[1] The calculated efficiency for all the antennas is about 97%. The 3-D calculated co- and cross-polar patterns of Antenna 1 and Antenna 3 are also included in the appendix.

[1] Antenna 1 is similar to Antenna 2 and Antenna 3 to Antenna 4

1.4.3.2 Design 2

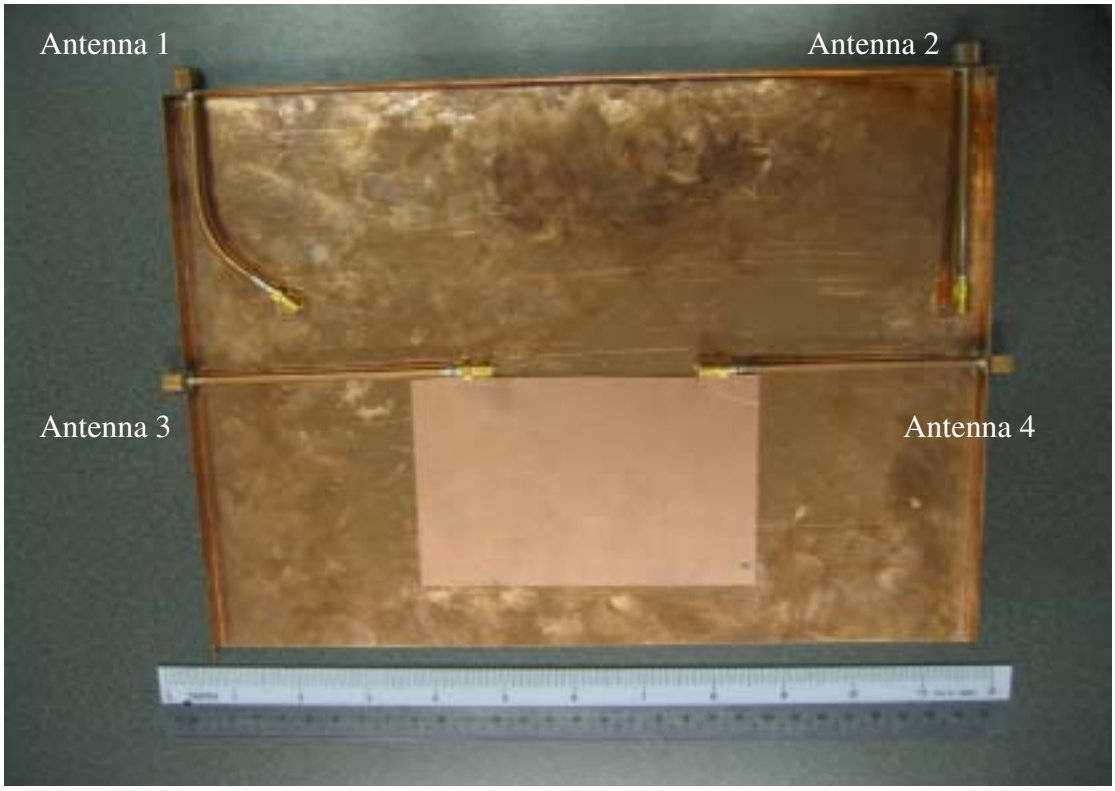

Figure 1.24: Design 2: Four antennas on laptop lid for MIMO application

Figure 1.25: Antenna element (Size : 10mm x 5.5mm x 6.5mm)

Return loss and isolation

The return loss and isolation measurements were again performed with a HP 8720ES 50MHz-20GHz network analyser. The CST simulated return loss compared to the measured results is shown graphically as an appendix. The dotted lines show the bandwidth below -10dB according to the required specification. The resonance for Antenna 2 has slightly shifted down by about 0.2GHz and this is due to the fact that all the antennas were manufactured by hand with possible distortion of the dimension during the folding process. Again the measured and simulated bandwidth is twice or more than 120MHz.

Graphs showing the isolation between the antennas are included as appendices. Overall the isolation is better than -20dB. The measured isolation is slightly higher than the calculated for S41 and S34 as they have less than -50dB calculated isolation. Again, spatial diversity is employed in this design among all the antennas due to the big laptop screen that is more than half a wavelength at 5.2GHz.

Antenna gain

The radiation patterns were measured as before. The MIMO laptop design was mounted on turntable aligned to the centre of the horn. Co- and cross-polar gain patterns measured for the E-plane and H-plane for all four antennas are included as appendices. The calculated peak gain for Antenna 1 is 4.66dBi and Antenna 3 is 2.98dBi.[2] Overall, the measured pattern and simulated are in very good agreement with only slight discrepancy for the cross-polar level as it is known to be difficult to measure cross-polar patterns due to their low level. The calculated efficiency for Antenna 1 is 96% and for Antenna 3 is 98%. The 3-D calculated co- and cross-polar patterns of Antenna 1 and Antenna 3 are given in the appendix.

By comparing the performance of the two designs, Design 1 has better radiation patterns because the maximum directivity of the elements direct away from the laptop. With spatial diversity as the main diversity technique employed in the laptop design, more antenna elements can be placed on the laptop by implementing polarisation diversity etc.

1.4.4 PDA Design

The PDA solution is shown in Figure 1.26. The folded loop is filled with a slab of ceramic (εr=6), which supports the folded loop and also reduces its size further. The PDA is made of

[2] Antenna 1 is similar to Antenna 2 and Antenna 3 to Antenna 4

0.4mm thick copper and the folded loop is made of 0.2mm thick copper. The folded loop has dimensions of 12mm x 5.5mm x 2mm and the PDA size is 75mm x 110mm x 10mm.

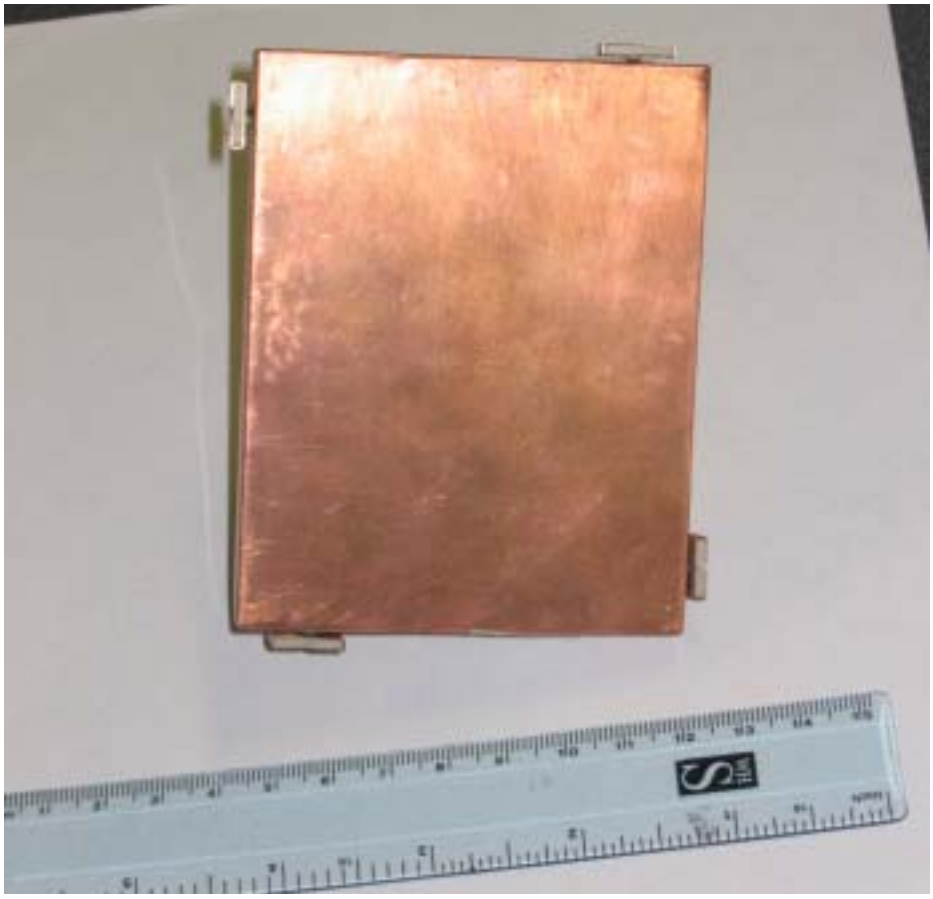

Figure 1.26: Folded loop design filed with ε_r=6

Return loss

The return loss and isolation measurements were performed with a HP 8720ES 50MHz-20GHz network analyser. The graphs are recorded as appendices. Simulations using CST were also performed and these results are also plotted in the graphs for comparison. The results agree well, the discrepancy is due to the fact that the calibration was not de-embedded up to the antenna port (not including the losses due to the coaxial connector). The dotted lines indicate the bandwidth below -10dB according to the required specification.

Isolation

Port to port isolation was measured and result is plotted as a series of graphs as appendices. Polarisation diversity is employed in this design between Antenna 1 and Antenna 3 (also between Antenna 2 and Antenna 2) while spatial diversity for Antenna 1 and Antenna 2 (also between Antenna 3 and Antenna 4). Overall the isolation is better than -20dB.

Antenna gain

The radiation patterns were measured in an anechoic chamber. The MIMO PDA design was mounted on turntable aligned to the centre of the horn. Co- and cross-polar gain patterns measured for the E-plane and H-plane for all four antennas are included as appendices. The calculated peak gain and efficiency for Antenna 1 is 5.27dBi and 94% while the peak gain and efficiency for Antenna 3 is 6.12dBi. and 95%[3]. Overall, the measured pattern and simulated are in very good agreement again with slight discrepancy for the cross-polar level. The calculated co- and cross-polar 3-D patterns are also included as appendices.

1.4.5 Handset Design

The handset solution is shown in Figure 1.27. The folded loop is filled with a slab of ceramic (εr=6). The handset is made of 0.4mm thick copper and the folded loop is made of 0.2mm thick copper. The handset has dimension of 40mm x 100mm x 10mm while the folded loop has dimensions of 12.5mm x 5.5mm x 4mm.

Figure 1.27: Folded loop filled with ceramic of er=6

Return loss and isolation

The return loss and isolation measurements were performed with a HP 8720ES 50MHz-20GHz network analyser. Measurements and simulations are included as appendices. The results agree quite well with a slight discrepancy due to the fact that the calibration was not de-embedded up to the antenna port (not including the losses due to the coaxial connector). The dotted lines show the bandwidth below -10dB for the return loss according to the required specification while about -20dB for the isolation. Polarisation diversity is employed in the handset between Antenna 1 and Antenna 2.

Antenna gain

The radiation patterns were measured in an anechoic chamber. The MIMO handset design was mounted on turntable aligned to the centre of the horn. Measurements of the co- and cross-polar patterns of Antenna 1 and Antenna 2 in the plane parallel to the handset and perpendicular to the handset are included as appendices. The calculated peak gain for Antenna 1 and Antenna 2 is 4dBi. Again, the measured copular patterns are in good agreement while slight difference for the cross-polar patterns. The calculated peak gain for Antenna 1 and Antenna 2 is 4dBi. The efficiency of Antenna 1 is 96%. The 3-D calculated co- and cross-polar patterns of Antenna 1 and Antenna 3 are also included as appendices.

1.4.6 Electronic Band-Gap (EBG)

Electromagnetic band gap (EBG) materials are periodic structures which exhibit useful characteristics such as frequency stop-bands, pass-band and band-gaps when interact with electromagnetic waves. EBG structures are formed by introducing periodic perturbations such as holes, dielectric rods and patterns in waveguides and PCB substrates. Many EBG structures have been reported such as holes on ground plane, mushroom-like EBG, uniplanar compact EBG (UC-EBG) [4]-[6] etc. EBG structures have been used as ground planes to achieve low profile antenna designs [4]. They have been integrated with patch antennas to suppress surface waves further enhancing its performance [6]. EBG structures when combined with antennas offer a wide range of application. These include image rejection, gain improvement, suppression of surface waves, ripple suppression in antenna pattern and antenna bandwidth.

Low profile antenna placed above EBG structures result in complicated interactions between the antenna and EBG structure. To ensure an effective application of the EBG structure on these low profile antenna, the frequency band of the EBG structure must provide good return loss and radiation efficiency for the antenna. In EBG structures, the surface wave propagation is inhibited within the stopband. This study focuses on one of the simplest EBG structures i.e.

---

[3] Antenna 1 is similar to Antenna 2 and Antenna 3 to Antenna 4

periodic holes on ground plane. When multiple antennas share the same ground plane, surface currents can cause unwanted mutual coupling. The goal of the analysis is to study the effect of the EBG structures on the folded loops whether the antenna performance is enhanced and also if the isolation is decreased.

1.4.6.1 EBG Structures

The circular hole EBG on ground plane is show in Figure 1.28. The design criteria was that the period of the EBG equals half a wavelength while the ratio of the radius of the hole to the period is about 0.25.

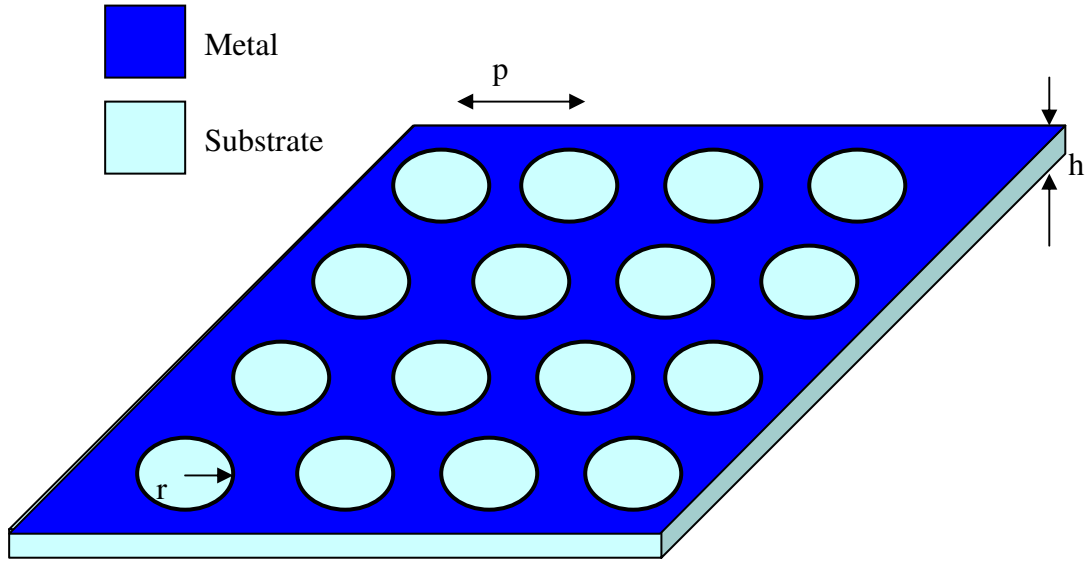

Figure 1.28: Circular holes EBG. Circular holes are etched on ground plane

1.4.6.2 PBG Evaluation

The EBG structures were tested on a PDA. In the analysis, the ratio of the radius of the hole to the period is approximately 0.14. The return loss and isolation are compared with the PDA and handset without EBG. The EBG structures are not placed below the antenna because the unbalanced feed is relatively large and would have destroyed the periodicity of the EBG. Figure 1.29a and 1.29b show the PDA without EBG and with EBG, respectively. Figure 1.30 shows the antenna location on the PDA.

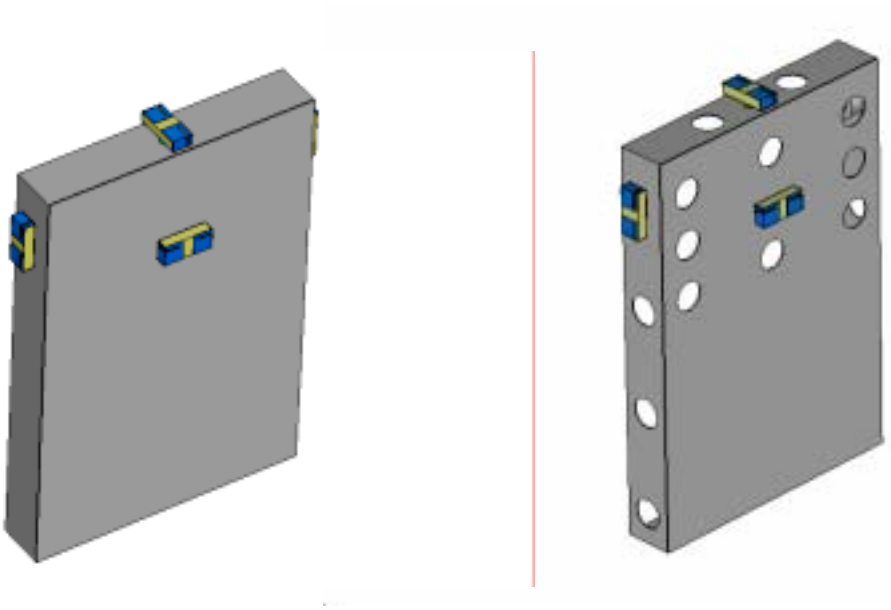

(a) (b)

Figure 1.29 (a) PDA without EBG (b) PDA with EBG

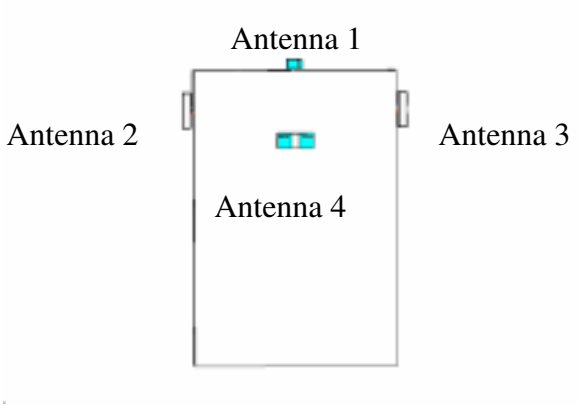

Figure 1.30: Antennas location on PDA

Return loss and isolation

The return loss and isolation were measured and graphs are included as appendices. For Antenna 1 and Antenna 4, the return loss with circular holes on ground plane improves by about 15dB and 8dB, respectively. However, no improvement is seen on the return loss for Antenna 2 and Antenna 3.

The isolation is similar for all with about 2-3dB difference. From the results, the implementation of EBG does not guarantee better isolation for all the antennas.

The EBG structure only takes effect when placed beside the two main branches, as there is more current along them (Figure 1.31). This is the case for Antenna 1 and Antenna 4. Antenna 1 has better improvement in return loss than Antenna 4 because the antenna has more current flowing beside the two main branches due to the narrower ground plane.

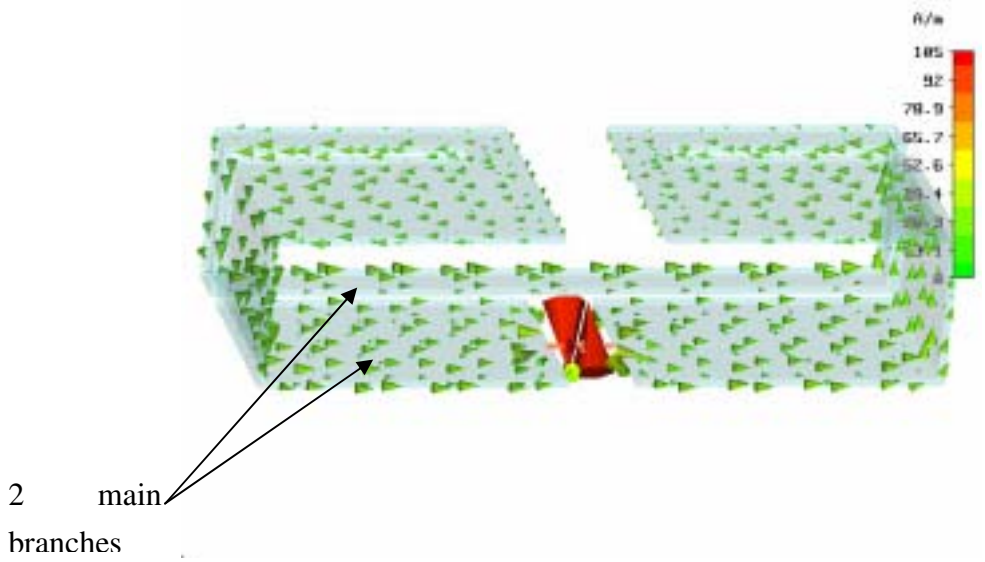

Figure 1.31: EBG more effect when placed this side and opposite side of the two main branches (if there is space on the ground

The above study shows that the EBG structures if placed at suitable locations respective to the folded loop antenna can increase the return loss. However, the isolation does not improve among the antennas. This is because the current induced on the ground plane by the folded loop antenna is localised and does not spread a lot towards the surrounding antenna. Generally speaking, EBG structures could improve the performance of conventional antenna elements, but it is not necessary when the antennas already have good isolation.

1.4.7 Conclusion - Folded loop and EBG

This report has shown that the dielectrically folded loop antenna is a suitable candidate for laptop, PDA and handset antenna in MIMO application. The folded loop filled with dielectric meets the requirements such as small size, low profile and lightweight. A representative laptop, PDA and handset have been designed, built, measured and compared with simulation (CST Microwave Studio). The antenna has been optimised to meet the required specification. The antennas have very high degree of isolation among each other and the gain patterns are reasonable broad and maximum directivity of each antenna is away from each other and also from the mobile device. Spatial and polarisation diversity are employed in the design. Furthermore, the return loss of the folded loop improves when incorporated with EBG structures at certain locations on the device. The isolation remains roughly the same because the folded loop does not induce a lot of currents on the ground plane. The isolation among the antennas is optimised when the induced currents on the ground plane are well suppressed. With the folded loop antenna design, the implementation of periodic holes EBG is not necessary since the isolation with or without the periodic holes EBG is almost the same. However, more complicated EBG structures such as mushroom EBG might improve the isolation and also the gain of the antenna elements.

1.4.8 References

[1] H. Morishita, Y. Kim and K. Fujimoto, 'Design concept of antennas for small mobile terminals and the future perspective', IEEE Antenna and Propag. Mag., vol 44, # 5, 30-43 (2002).

[2] J.P. Casey and R.Bansal, 'Dielectrically loaded wire antennas', IEE Proc. vol 135, Pt H, #2, 103-110 (1988).

[3] O.Leisten, et al, 'Miniature dielectric-loaded personal telephone antennas with low user exposure', Electronics letts, vol.34, #17, 1628-1629, (1998).

[4] R. Cocciolli, F.R.Yang, K.P.Ma and T.Itoh,'Aperture-coupled patch antenna on UC-PBG substrate',IEEE Trans. Microwave Theory & Tech., vol.47, #11, 2123-2130 (1999).

[5] F.Yang, Y.Rahmat-Samii,'A low profile circularly polarized curl antenna over EBG surface',Microwave Opt. Tech. Letters, vol. 3, #3, 165-168 (2001).

[6] Y.Horii, M.Tsutsumi,'Harmonic control by photonic bandgap on microstrip patch antenna',IEEE Microwave & Guided Wave Lett., vol. 9, #1, 13-15 (1999).

[7] F.Yang, Y.Rahmat-Samii,

'A low profile circularly polarized curl antenna over EBG surface',

Microwave Opt. Tech. Letters, vol. 3, #3, 165-168 (2001).

1.5 Conclusions

The HDA™ and folded loop antenna solutions described in this chapter were designed using HFSS and CST simulation software packages. There was good agreement between the simulations and the measured results in terms of resonant frequency, bandwidth and radiation patterns.

The antennas employed spatial, polarisation and pattern diversity to reduce coupling between multiple antennas. The de-correlation measured from the 3-D radiation patterns confirms the low coupling between antennas. Due to the inherent high isolation between the antennas, the introduction of electronic bandgap (EBG) structure on the ground plane did not give a useful improvement in performance. However, with less well-isolated antennas it is believed that EBG would give technical advantage.

The antennas presented in this study were small, lightweight and in the case of the HDA™ designed for mass production. The antennas were integrated on laptop computer, PDA and handset platforms and the performance in each situation was found to be similar. The maximum radiation from the antennas was directed away from both the common groundplane and the other antennas thus ensuring isolation and de-correlation between antennas was maintained.

.

1.6 Recommendations

Generally speaking, there is insufficient published study available to guide the design of MIMO systems involving antenna arrays at the user terminal. Further studies should be carried out to fully understand the fundamental limitations of antenna elements in MIMO system, such as the close proximity to the human bodies, etc. Exploring the creation and placement of multiple, identical or dissimilar antennas on a mobile terminal (laptop, PDA or handset) while maintaining good performance and low overall cost is the current research trend on MIMO systems. No antenna offers a perfect diversity solution. It is usually a combination of the different types of diversity, which is put into practice, especially on small, handheld devices, where the antennas are in close proximity to one another, and the human body. The most critical parameter regarding the correlation factor in any type of diversity solution is the coupling between the different antennas. The location of the antenna elements on the terminal device would be one of the main problems faced by antenna design engineers to overcome the problem of good isolation as the number of MIMO increases. The antenna isolation must always be considered during the design stage, this is crucial to achieve the implementation of antenna-diversity schemes into MIMO systems. Surface waves remain one of the most important issues. One way to ensure that the surface waves coupling remain low is to use a technology that confines the surface waves flow such as EBG structures. Low profile antennas with simple feeding networks would bring great advantage to the MIMO systems.

2 APPENDIX - DIELECTRIC RESONATOR TECHNOLOGY

2.1 Simulation Development work

2.1.1 Early development of Single Element

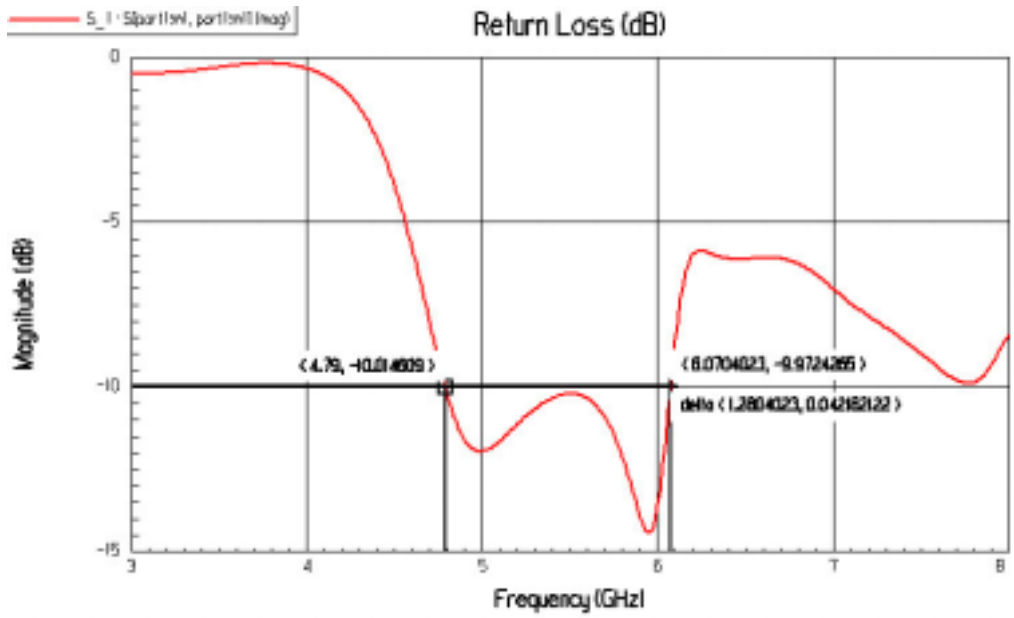

Appendix 1: S11 response for element used in Figure 1. 5

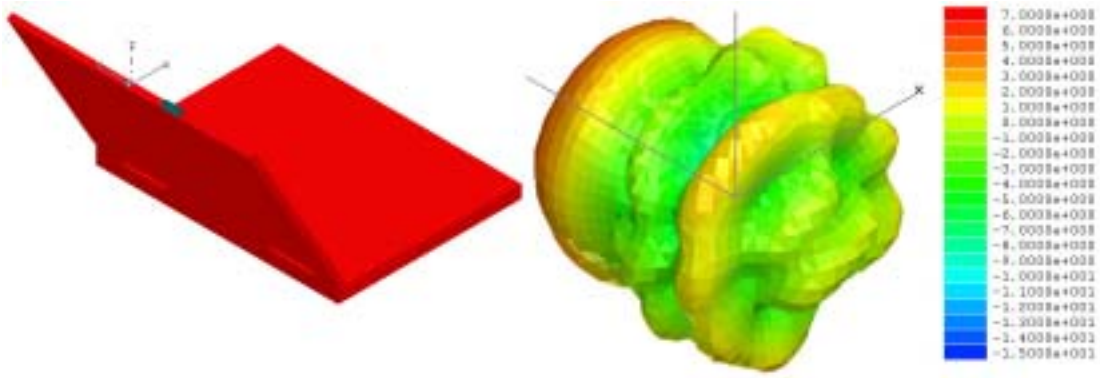

Appendix 2: Gain pattern and schematic of single antenna on laptop lid

	Antenova results (HDA™)	Specification
Centre frequency	5395 MHz	5437.5 MHz
Bandwidth (-10dB S11)	1210 MHz (22%)	575 MHz
Peak Gain	>5 dBi	1 dBi
Size (height×width×length)	4.6mm×7.1mm×14.65mm	8mm×8mm×12mm

Appendix Table 1: Summary of results from simulation of single antenna on laptop lid

2.1.2 Simulated Second Generation Single Element and PCB on the PDA

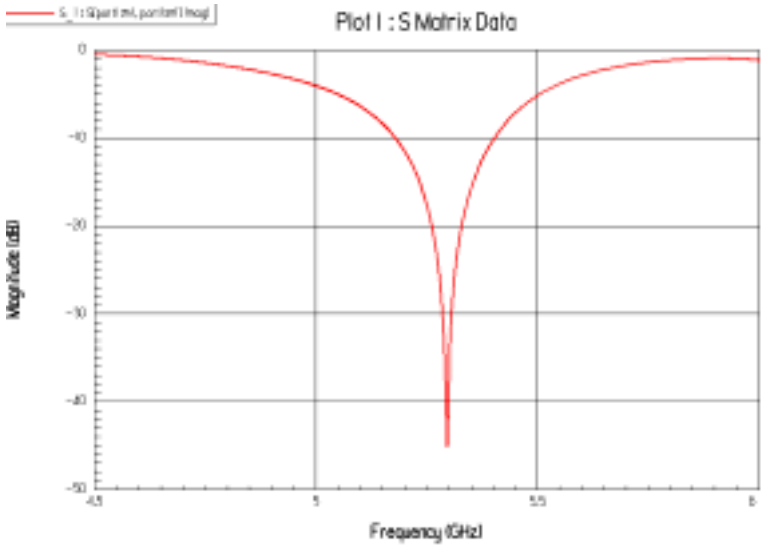

Appendix 3: S11 Return Loss - Single Element on PDA

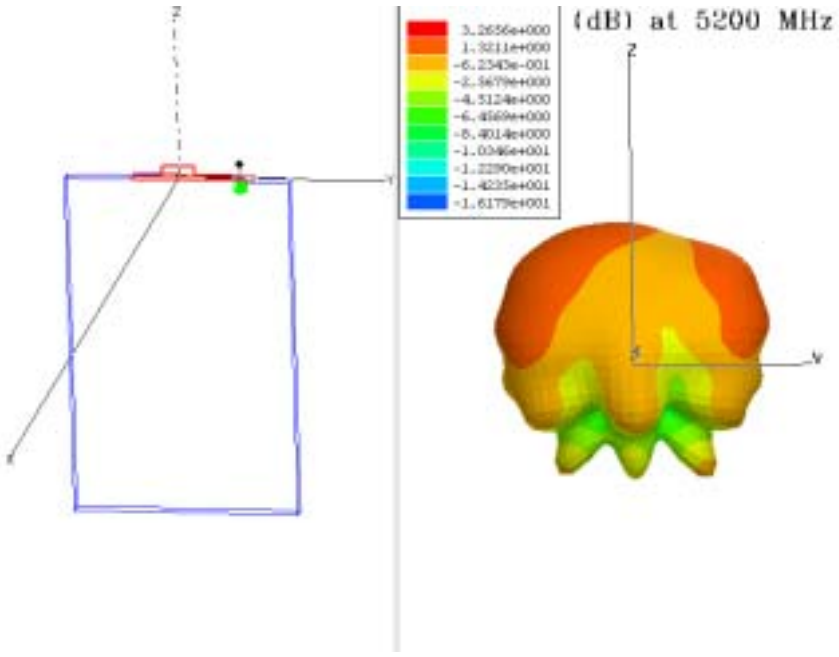

Appendix 4: 3D Gain Pattern of a Single Element on a PDA

Appendix 4 shows the 3D gain pattern of the single element, the orientation of the PDA and pattern are the same. The red areas show the highest gain, which is emanating largely vertically to the left and right side of the PDA, with a null towards the base.

2.1.3 Simulated Second Generation Four Elements and PCBs on the PDA

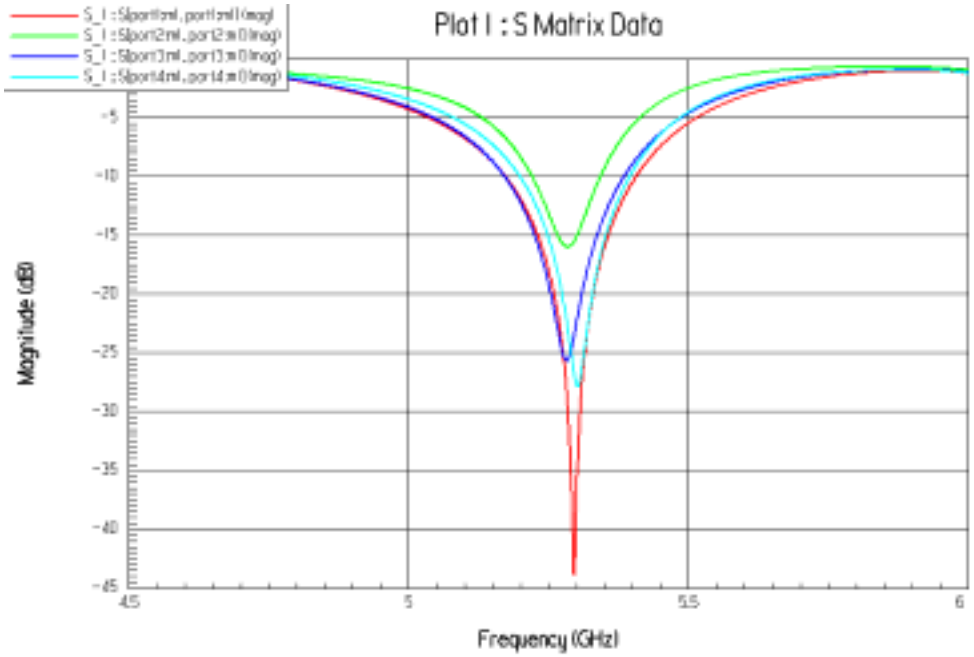

Appendix 5: S11 Return loss for each of the elements

The return losses are all centred a round a narrow frequency band but the magnitudes are different. Due to the logarithmic scale, the benefits of the extra match between the worst and best will be slight.

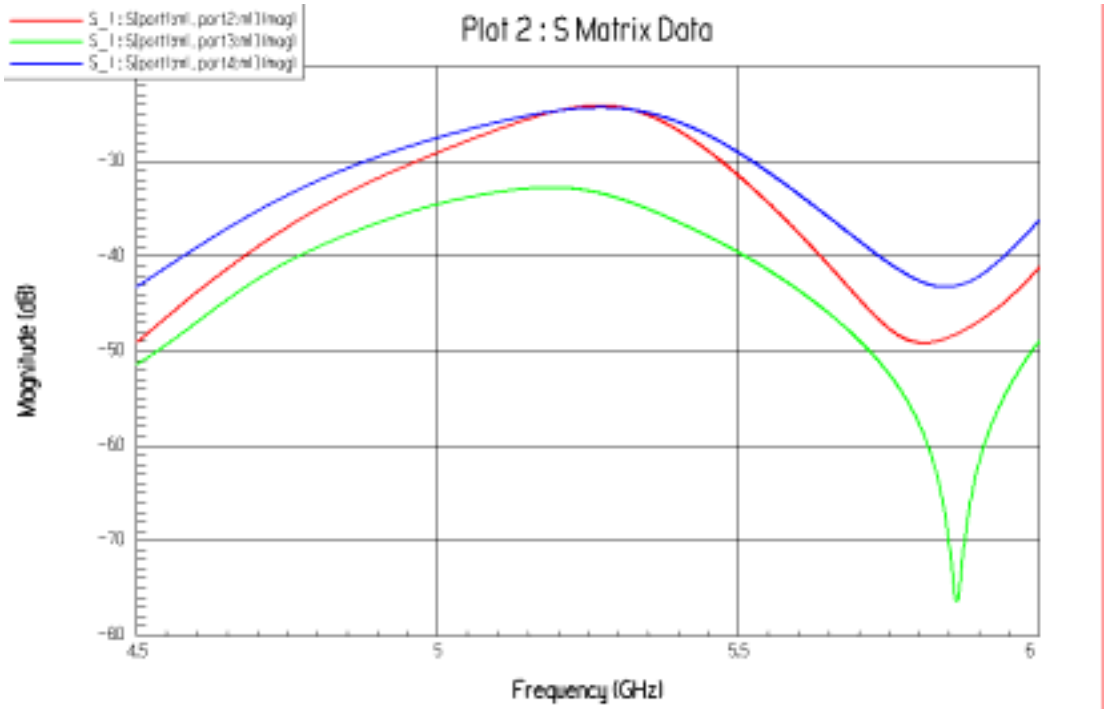

Appendix 6: Port to Port Isolation: Red=1to2, Green=1to3, Blue=1to4

In Appendix 6 the difference in port-to-port isolation is seen because the path length between the elements differs.

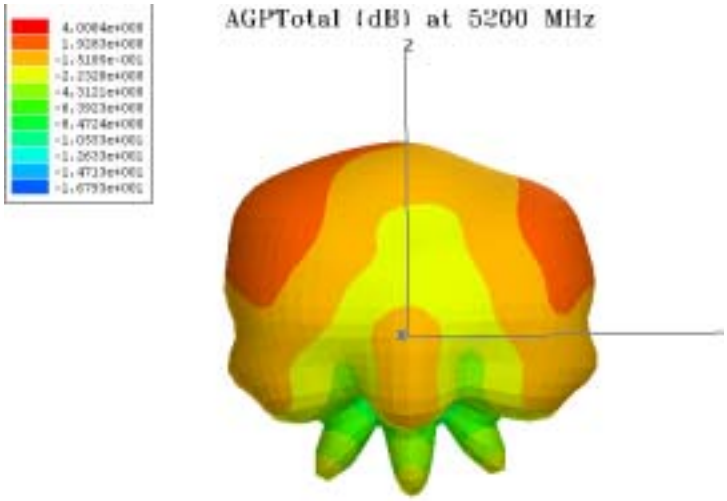

Appendix 7: Simulated 3D Gain Pattern Top Element 1

Appendix 7 shows the simulated gain where only one element was present.

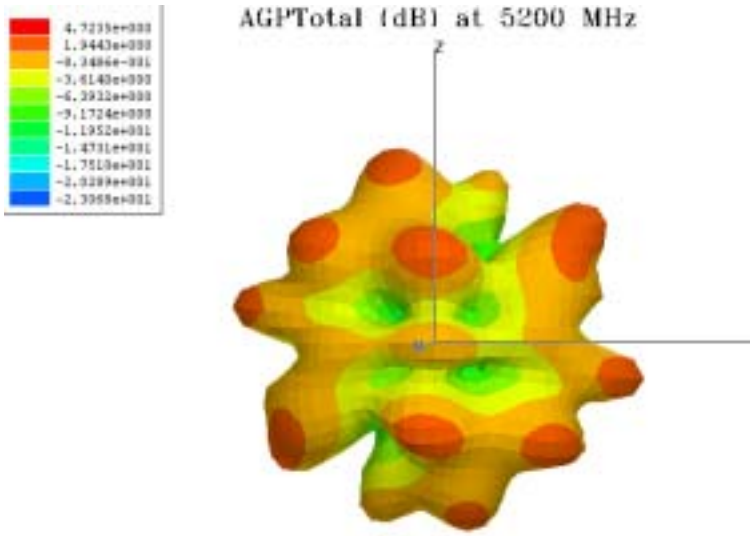

Appendix 8: Simulated 3D Plot of All Elements Active at Once

When all the PDA elements are powered at once, a different gain pattern is seen as shown in Appendix 11. The red areas represent the highest gain, the high gain component at the edges of the plot extend round to the opposite site. There are many peaks and nulls, but because there are so many high gain peaks it is likely that any incident radiation would be detected.

2.1.4 Simulated 4 Antenna asymmetrically positioned on PDA

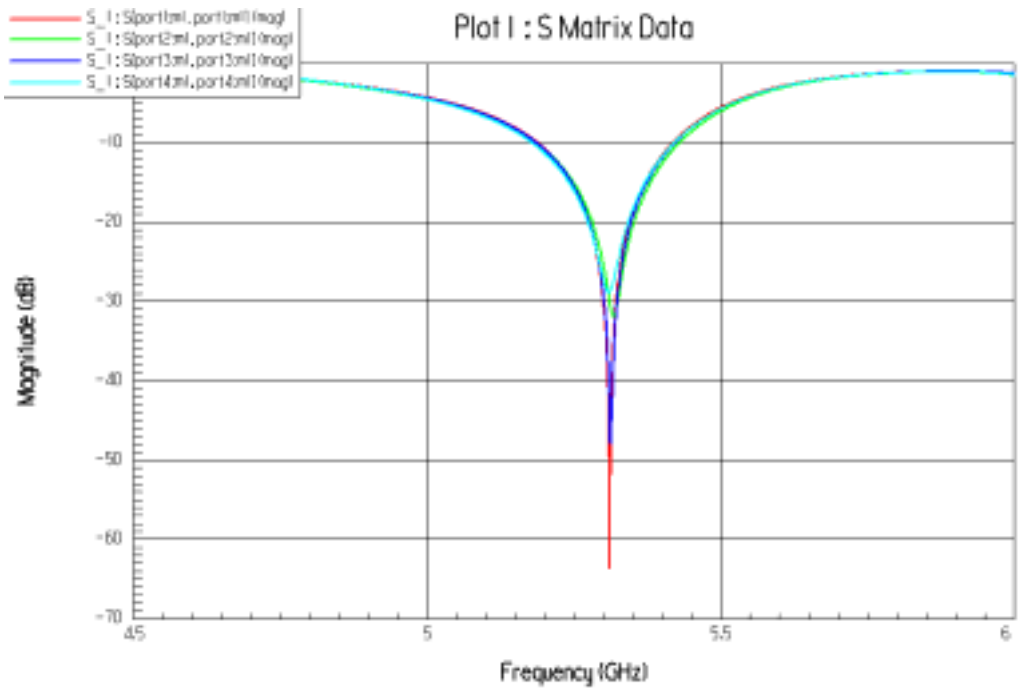

Appendix 9:Simulated S11 return loss four Asymmetric Elements

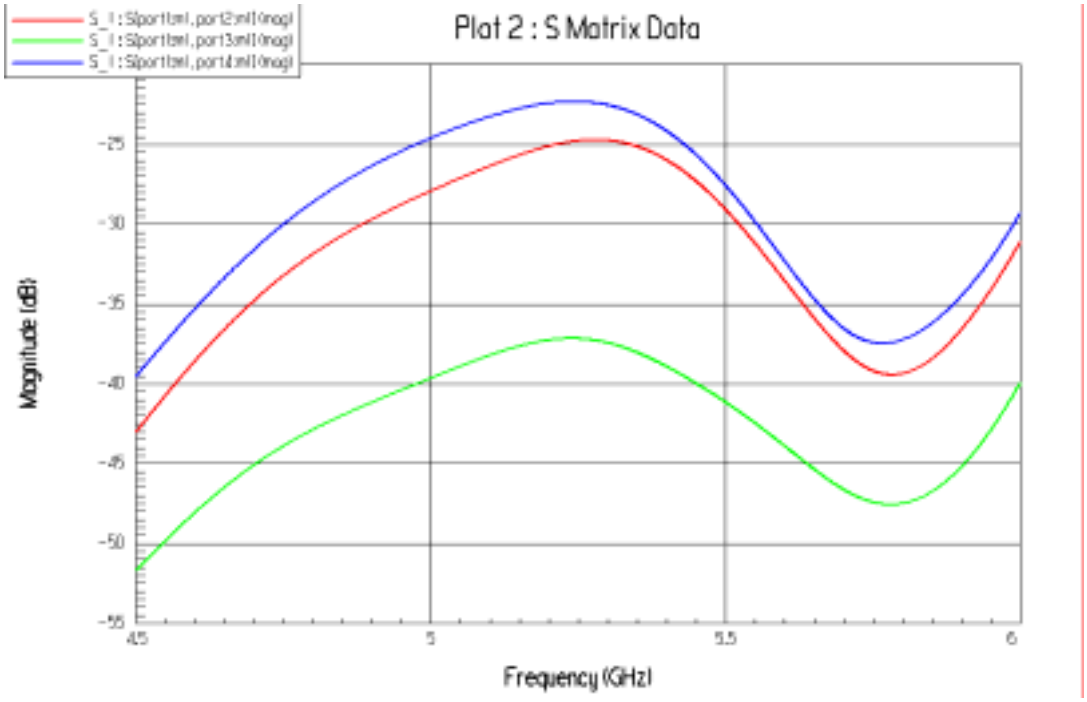

Appendix 10: Port-to-Port Isolation Four Asymmetric Elements

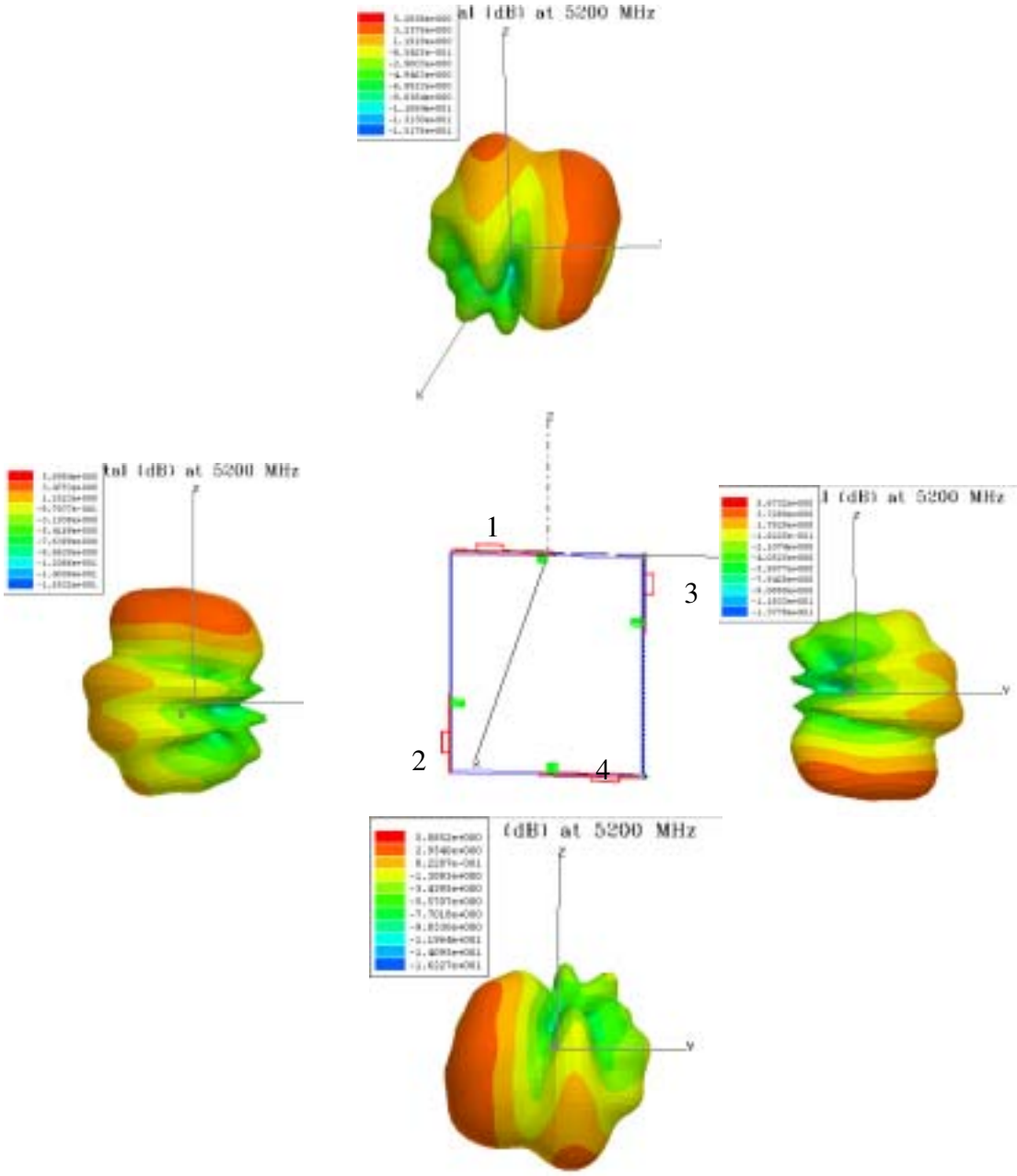

Appendix 11: Simulation of the directionality of each element when only one is exited at a time.

Appendix 11 shows the PDA at the centre of 4 gain patterns each pattern opposite corresponding antenna element. The magnitude of the gain is represented in colour with red being the peak gain then orange, yellow and green. Antenna 1 shows the peak gain predominantly to the right side of the element with a small component vertically. Antenna 2 shows the peak gain is now nearly all in the vertical direction. The component that would have been to the left hand side has been directed by length of the longer side of the groundplane.

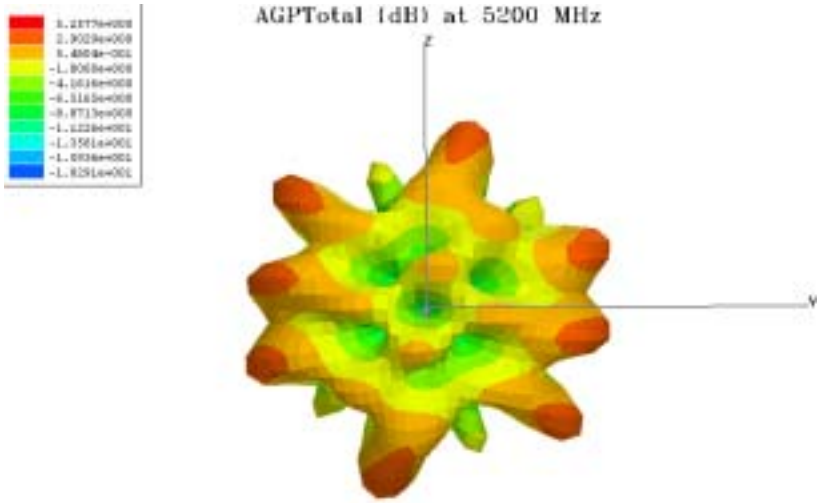

Appendix 12: Simulated PDA with all Four Asymmetrically Elements Radiating At The Same Time

2.2 Drawings of Antenna Element

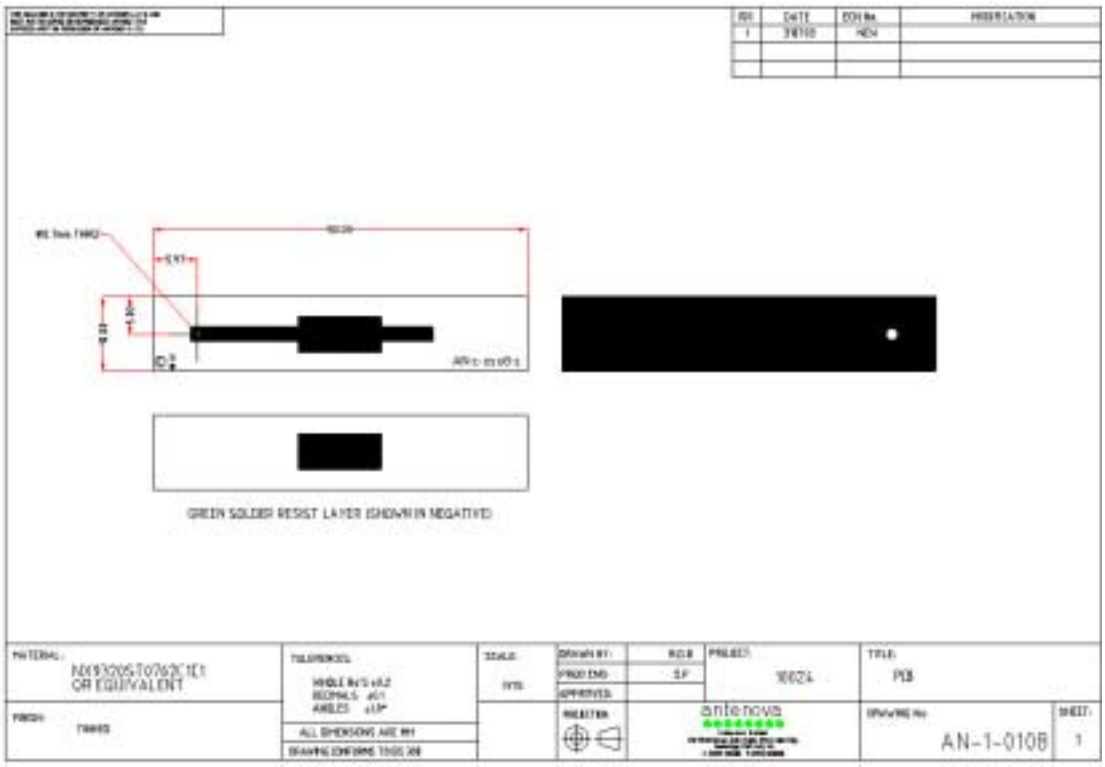

Appendix 13: Antenova drawing of PCB for antenna element

The final drawing for the single element PCB design resulting from the simulations is given as Appendix 16. The PCB is PTFE with a relative permittivity of 3.2 and thickness 0.8mm. The central rectangular pad locates the ceramic element and is soldered to it. A semi rigid co-axial cable is use to carry a signal to the PCB, with the cable outer being soldered to the ground (base of board, solid black rectangle). The cable inner passes through the 0.7mm diameter hole and is cut slightly proud of the surface and soldered to the track.

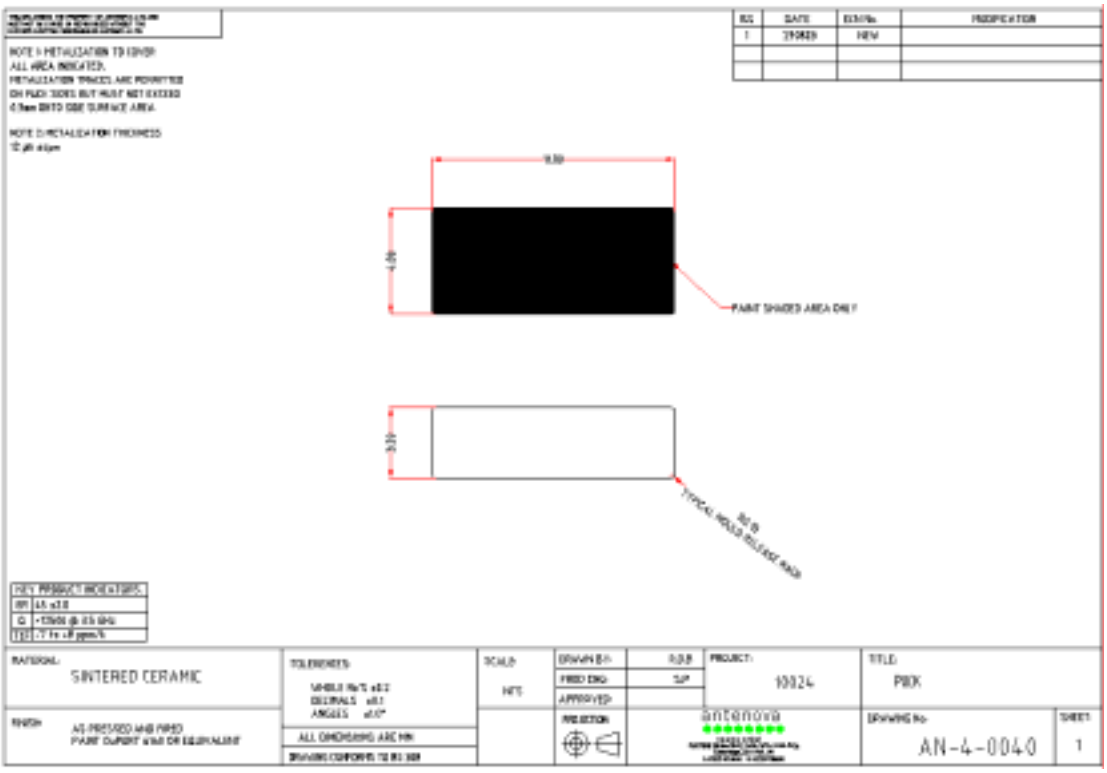

Appendix 14: Antenova drawing of Ceramic Element

Appendix 14 gives the drawing of the ceramic element to be used in conjunction with the PCB Appendix 13. The element is made from ceramic with relative permittivity of 45 that has been metallised on one face.

2.3 Laptop Design – Measurements

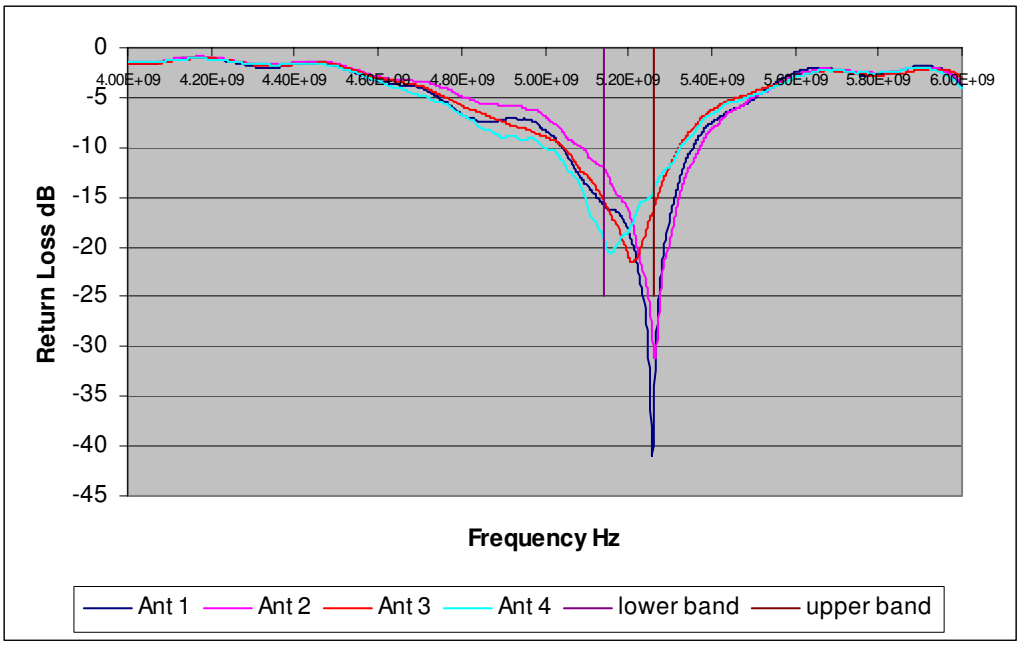

Appendix 15: Return Loss of Laptop Design

This figure illustrates the return losses measured for the four antennas integrated onto the laptop test rig.

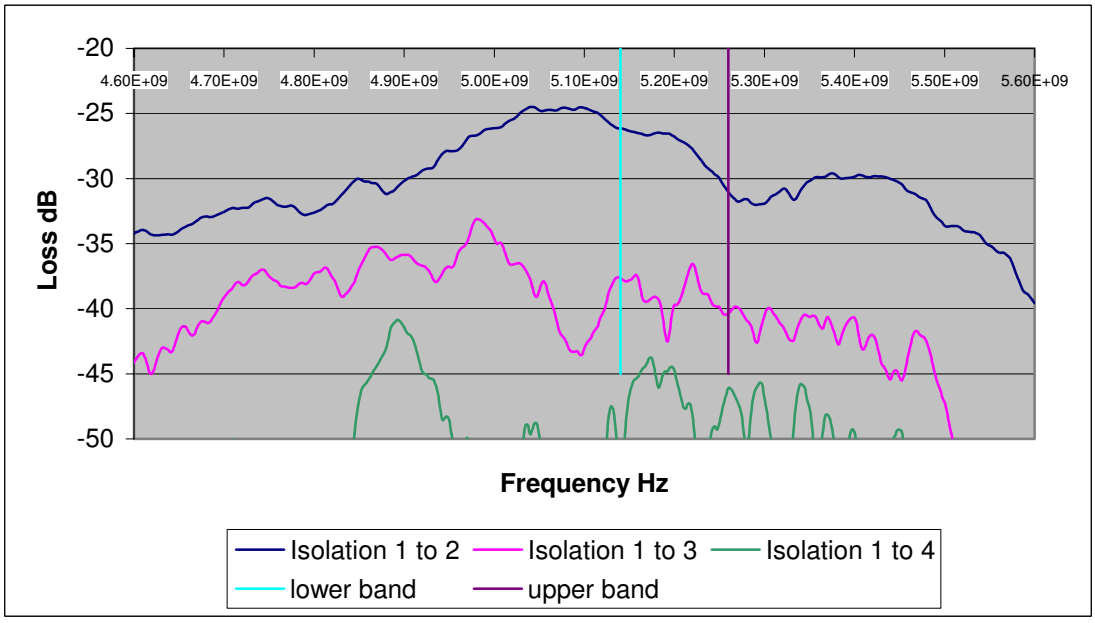

Appendix 16: Isolation Measurement on Mock-up Laptop

The figure above shows the port-to-port isolation on the mock-up laptop. Each antenna was measured relative to antenna 1. The band edges are marked on the graph with vertical lines. The isolation between the two furthest spaced elements, 1 and 4, was the highest.

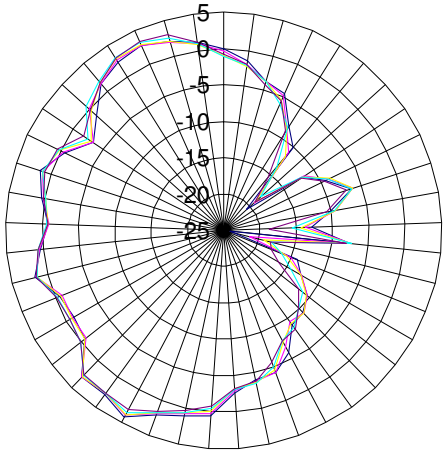

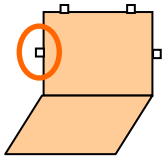

Appendix 17: Gain pattern for antenna 1 on laptop

The gain pattern shown in Appendix 17 has a large null to the right and peak gains to the left. The antenna in conjunction with the metal of the laptop lid has produced a field pattern that emanates way from the laptop. The peaks of which are to the top and bottom left of the pattern. There is also a smaller component which is centre left of the pattern indicating the element is radiating of the top. The isolation measurement was good because the field pattern is not in the direction of the other antenna.

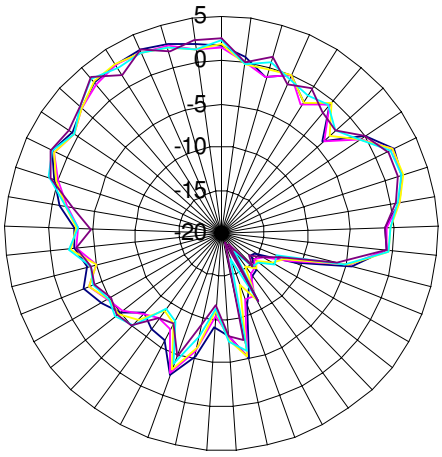

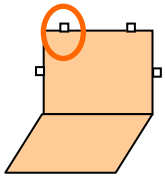

Appendix 18: Gain pattern for antenna 2 on laptop

Appendix 18 shows the peak gain of the pattern towards the top left and a small component to the right, toward antenna 3.

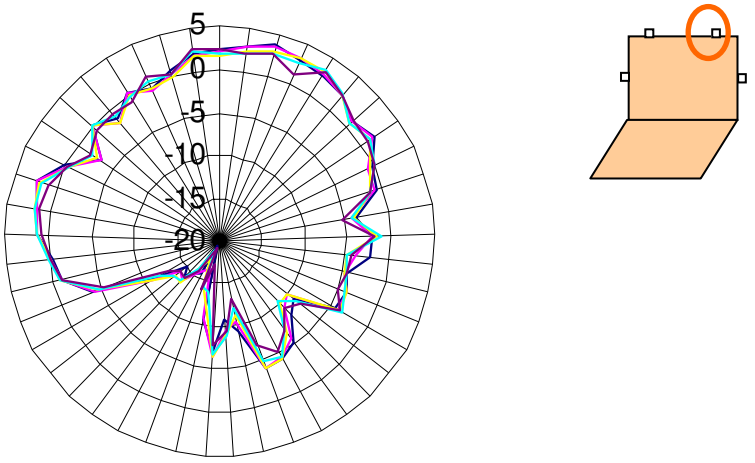

Appendix 19: Gain pattern for antenna 3 Mock-up Laptop V2

The pattern in Appendix 19 appears to be a mirror image of Appendix 18. Again there is a small component of gain directed at the antenna in the same plane, antenna 2. The isolation between antennas 2 and 3 reflects this.

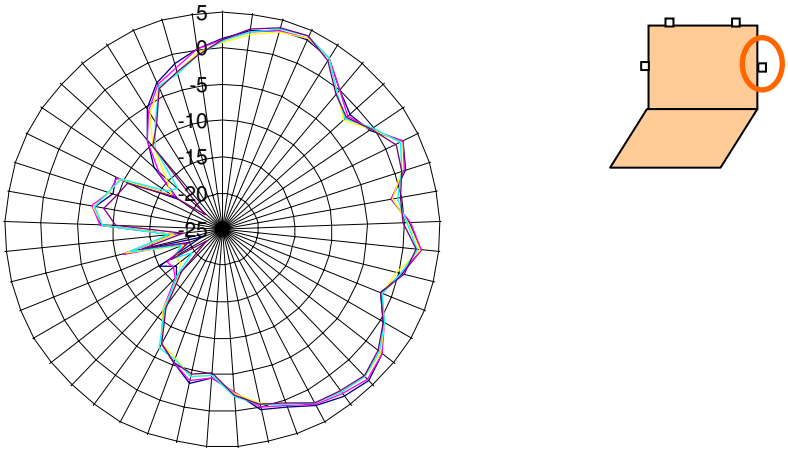

Appendix 20: Gain pattern for antenna 4 Mock-up Laptop V2

The pattern in Appendix 20 is similar to Appendix 17 but mirrored reflecting its position on the laptop, with the peak gain directed away from the groundplane of the laptop.

2.4 PDA Design – measurements

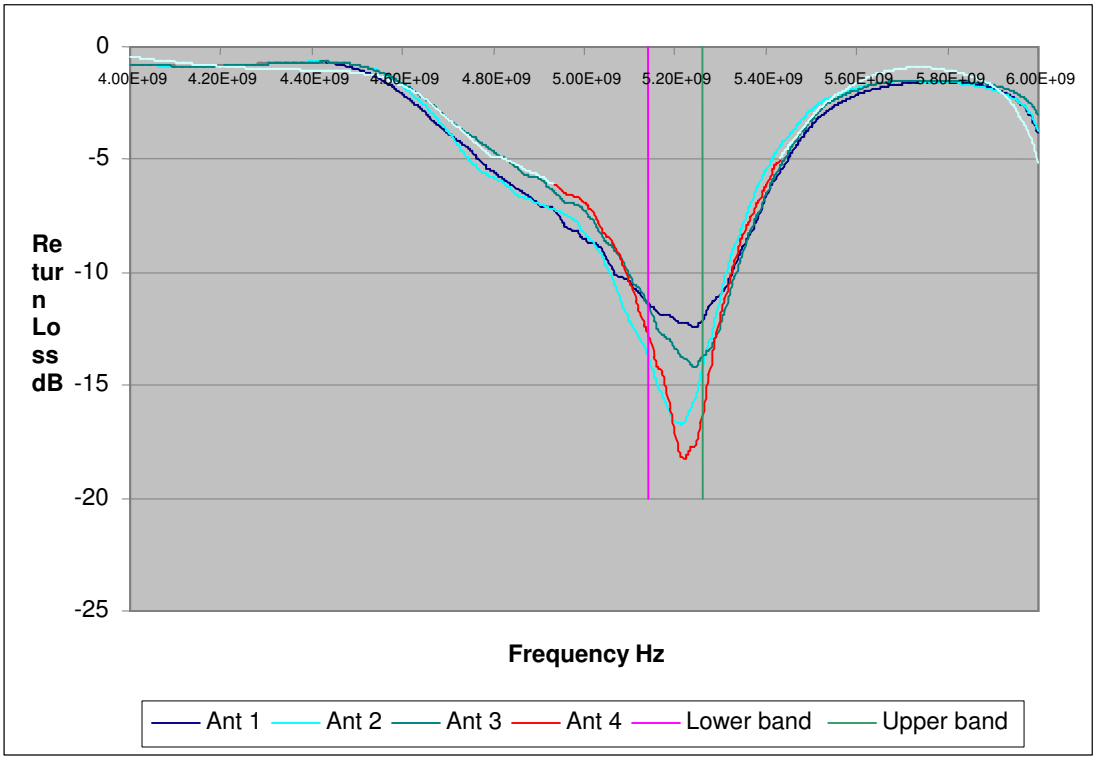

Appendix 21: PDA Return Loss

The return losses of the four PDA antenna elements are shown in Appendix 21. All are matched to better than –10 dB, for the frequency band denoted inside the two vertical lines. The return losses are not as well matched as those of the laptop, and this is likely to be due to the physical length of the metal work the antenna sits on, i.e. the longer the better and the hand made ceramic.

Appendix 22: PDA Showing Element Positions

Appendix 22 shows the element numbering clockwise; SMA connectors are also shown at the centre. Element 1 is at the top of the picture.

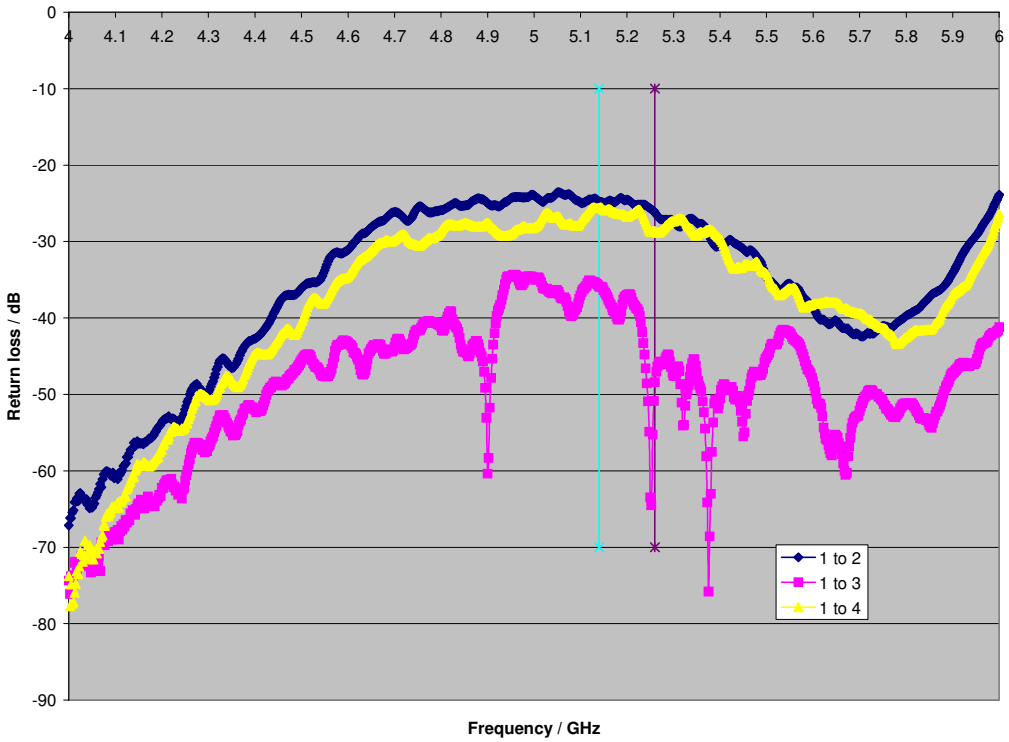

Appendix 23: PDA Isolation

Antennas 1 to 2 and 1 to 4 have similar Isolations at better than –23 dB and 1 to 3 is better than –33 dB. So as in the case of the laptop the isolations are good. So the power received at the ports is 200 and 2000 time less respectively.

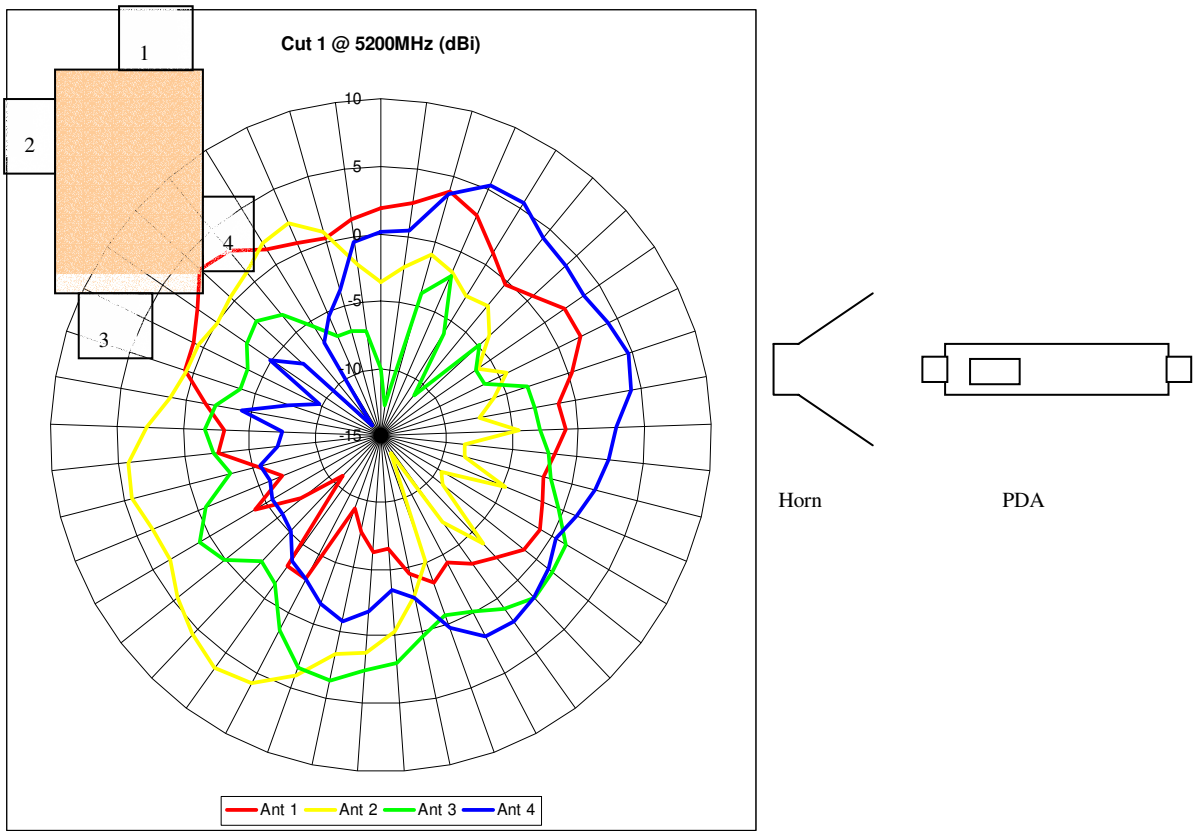

Appendix 24: Composite gain pattern for PDA (Cut 1)

Appendix 24 shows the gain pattern for 'Cut1', with both polarisations added together – the 'composite' gain pattern. 'Cut1' describes the orientation of the PDA relative to the receiving horn. The horn is positioned centrally in front of the PDA, and the PDA is revolved left to right (x-y plane) on a turntable to record the field pattern generated. The peak gains reached in this orientation were approximately 5 dBi

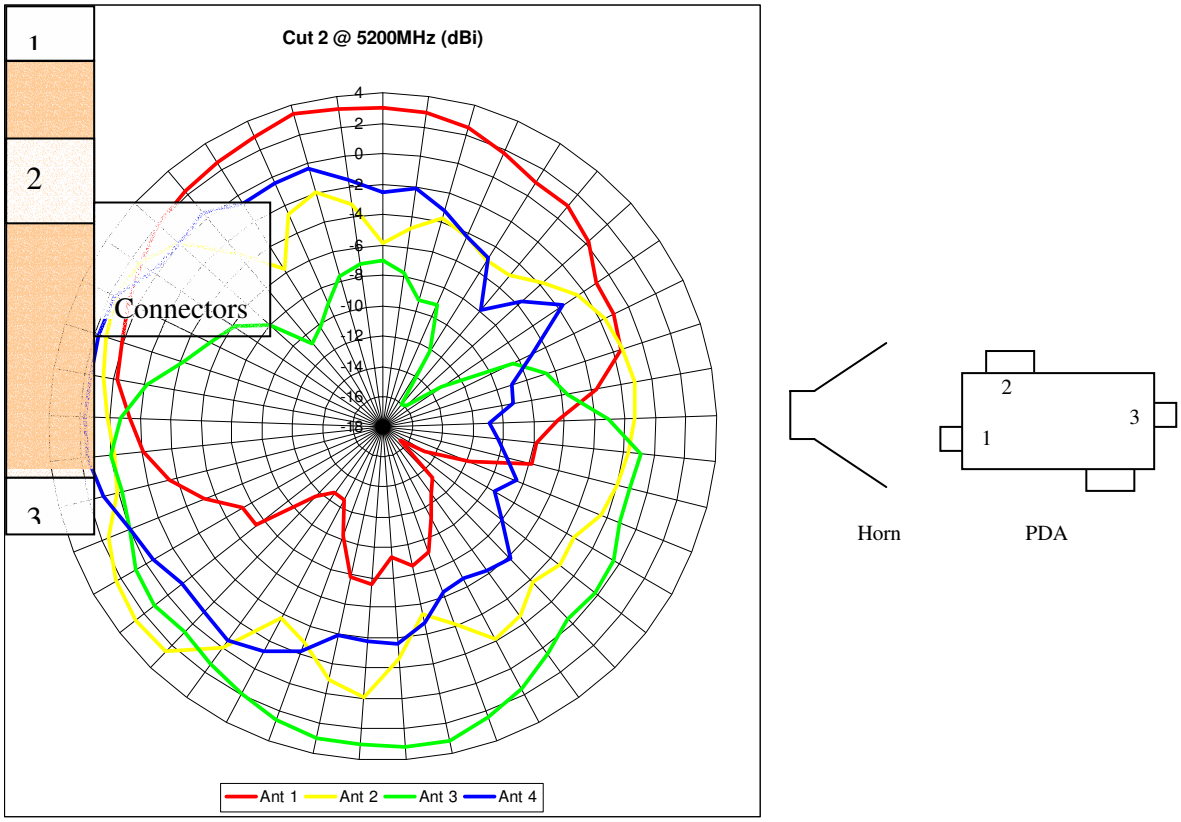

Appendix 25: Composite gain pattern for PDA (Cut 2)

In this plane (Cut 2) looking at the narrow end of the PDA so element 1 is initially facing the horn with antennas 2 and 4 in the vertical plane facing up and down respectively. The PDA is again spun left to right (x-y plane) with the receiving horn located centrally in front of the PDA. This shows that now the major contribution is coming from 1 and 3 with little benefit from 2 and 4, the opposite case than in Cut 1. The peak gains reached in this orientation were approximately 3.5 dBi. The polar plot insert shows the orientation of the PDA when looking down from above in relation to the plot.

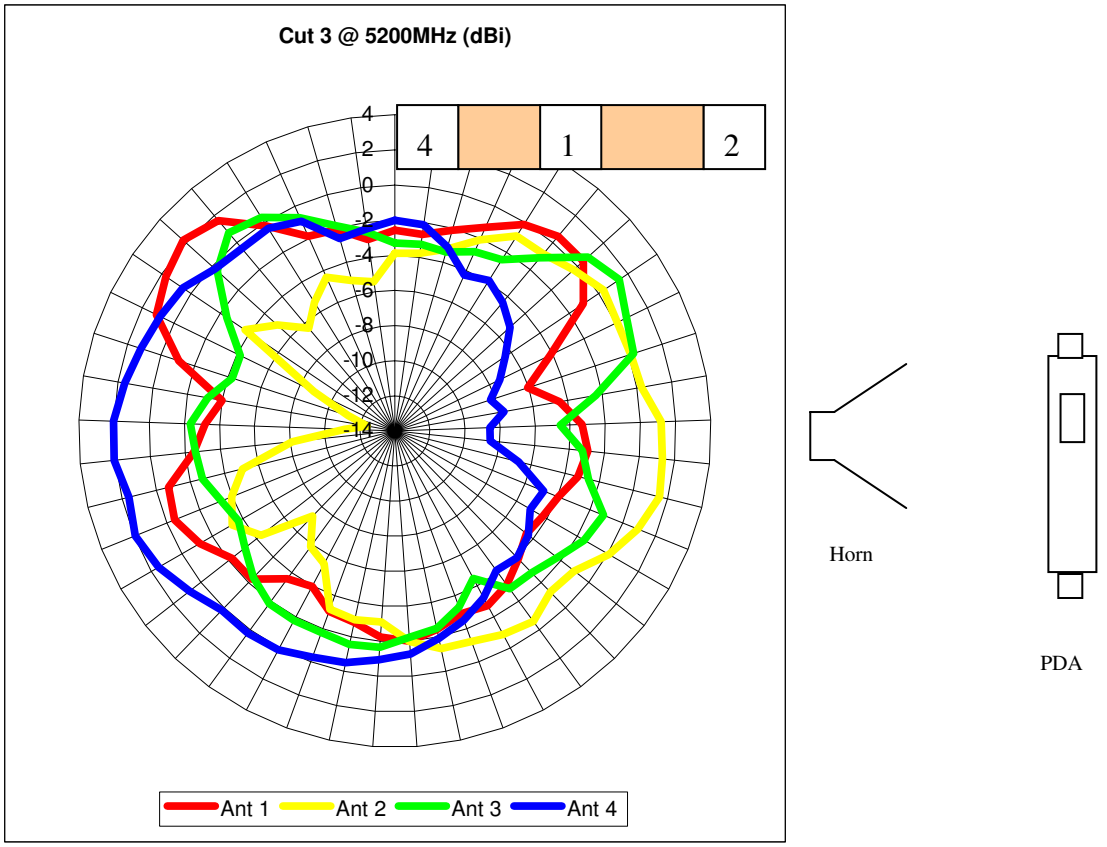

Appendix 26: Composite gain pattern for PDA (Cut 3)

In this view the PDA is vertical with antenna 1 pointing up with 4 and 2 in and out of the page; again the receiving horn is located centrally. The peak gain contribution is from antennas 4 and 2 with a lesser contribution from antennas 1 and 3. The peak gains reached in this orientation were approximately 2 dBi. The insert in the polar plot shows antenna orientation with respect to the patterns when viewed from above.

2.5 Handset Design – Measurements

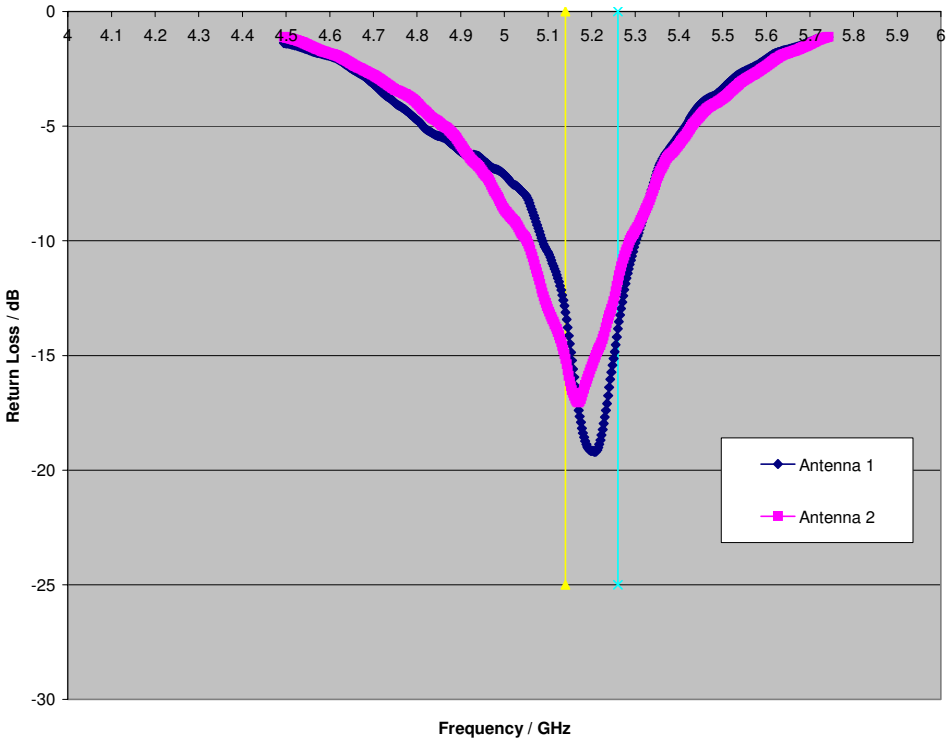

Appendix 27: Return loss plots for handset solution

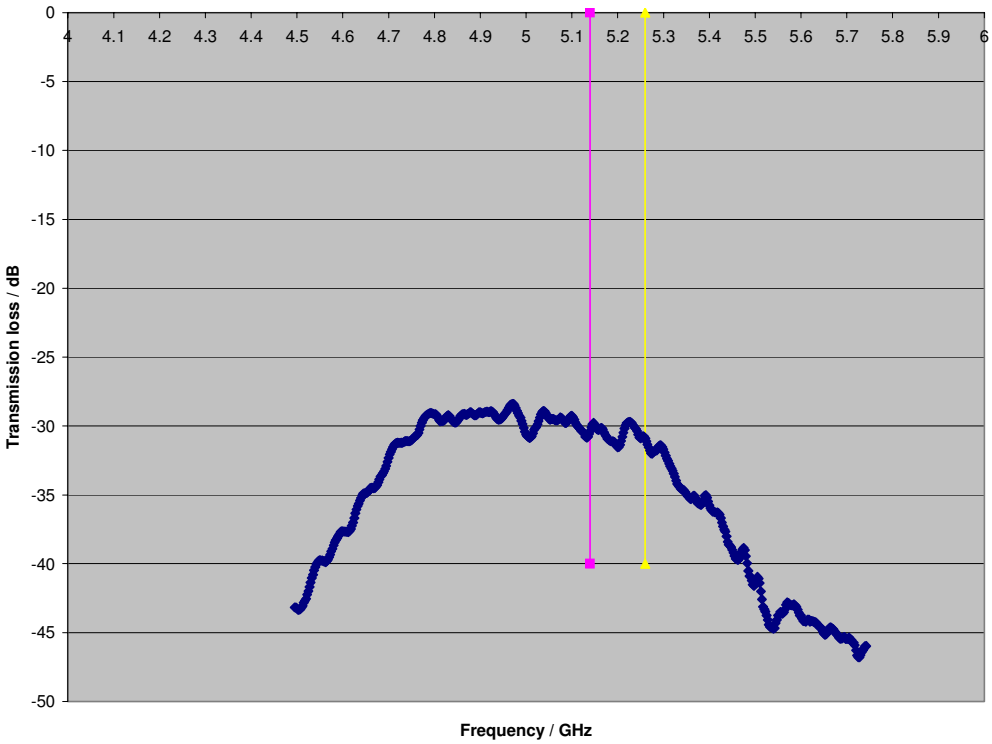

Appendix 28: Isolation for handset solution

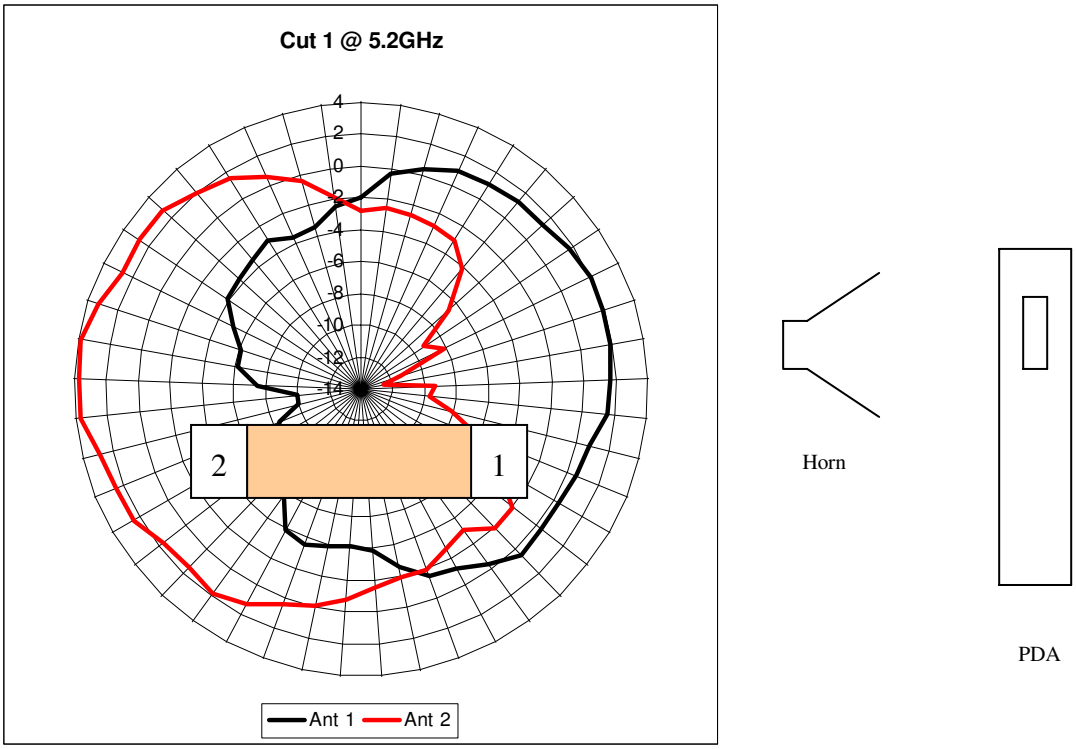

Appendix 29: Composite Gain Pattern for the Mock-up handset

These patterns show good diversity as the peak gains are away from each other with values of 4 and 2 dBi and the nulls are approximately 10 dB down. In this cut the handset is vertical with an antenna on either side. The handset is rotated in the x-y plane, left – right. The nulls correspond to the front and back of the handset. The insert in the plot shows orientation looking down from above.

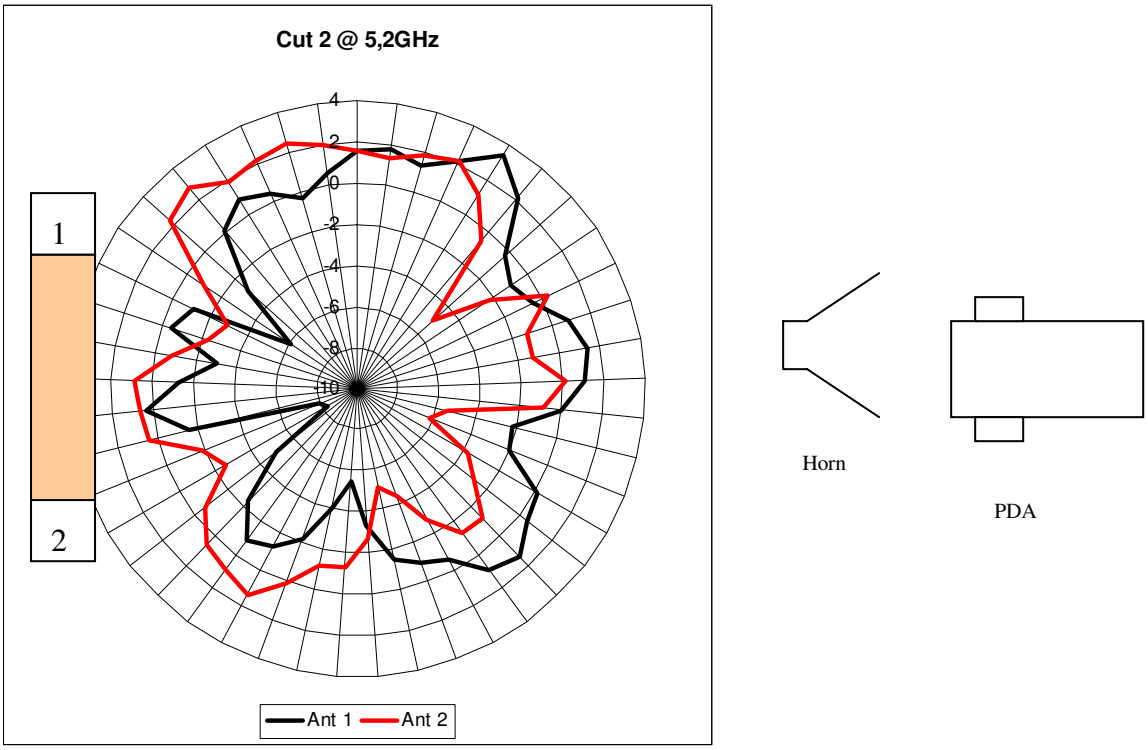

Appendix 30: Composite Gain Pattern for Mock-up Handset (cut 2)

In this cut the handset is on it's side, so the antennas are the situated on the top and bottom when looking from the end, we would not expect to see much diversity in this cut as both elements equally see the receiving horn antenna. The patterns for the two antennas are similar but reversed with peak gains around 2 to 3 dBi.

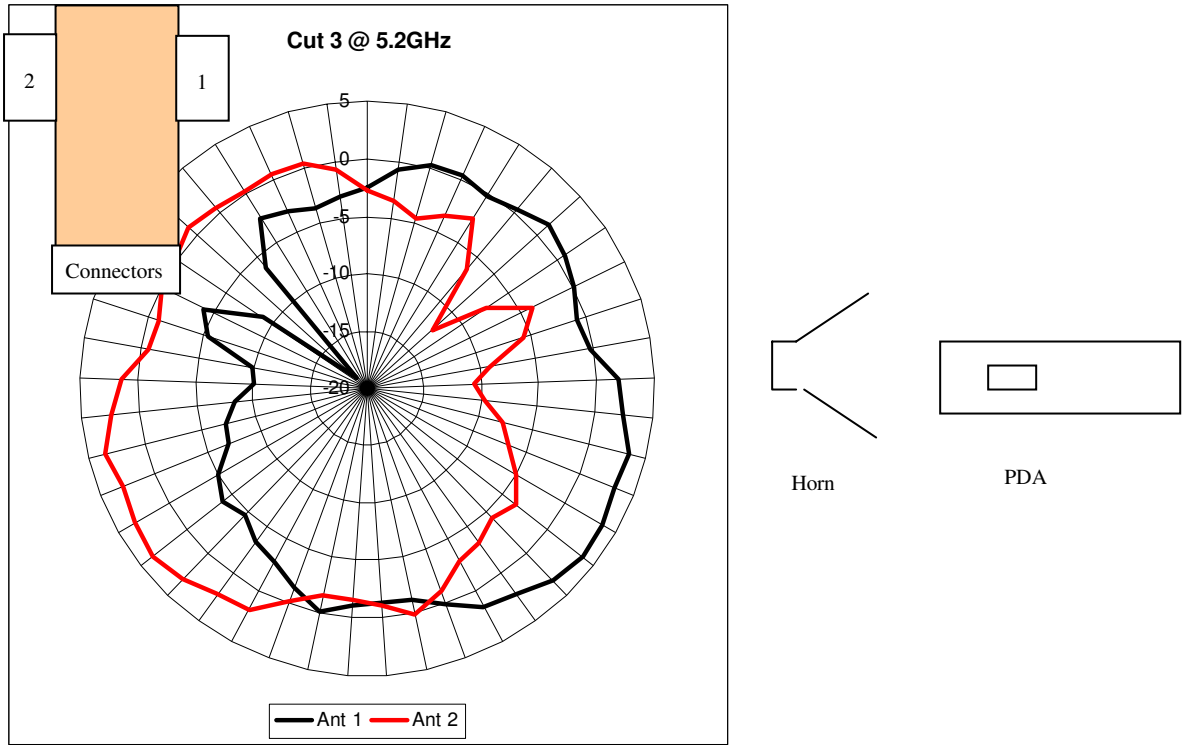

Appendix 31: Composite gain pattern for handset (cut 3)

In this plane the handset is placed flat on the turntable relative to the horn (see sketch) and again rotated around the x-y plane. The insert in the polar plot is orientated the same way as the polar plot (looking down on to it), so the peak gain is emanating from the bottom of the handset, peaking at over 3.5 dBi.

2.6 3-Dimensional Correlation from Measurements on PDA

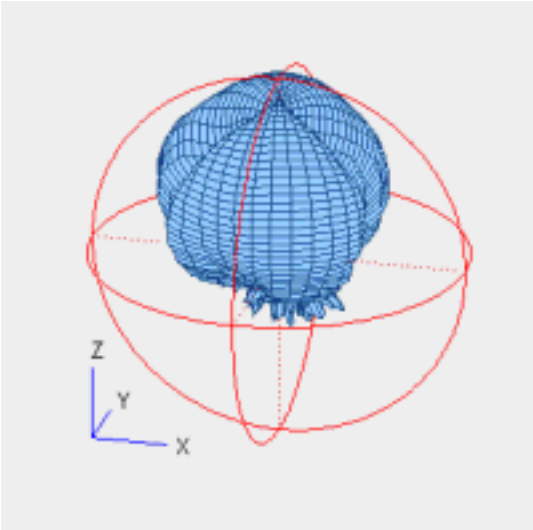

Element 1 – Horizontal Polarisation

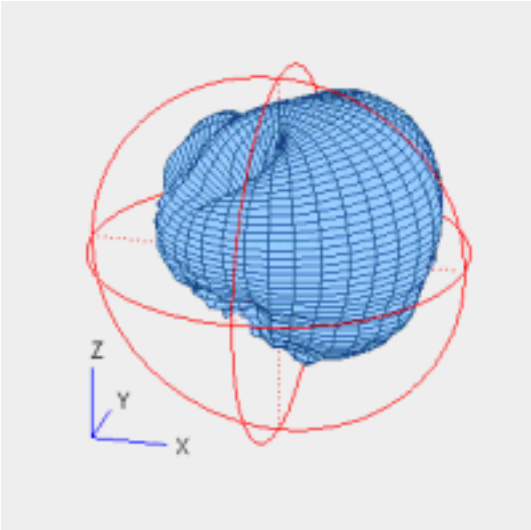

Vertical Polarisation

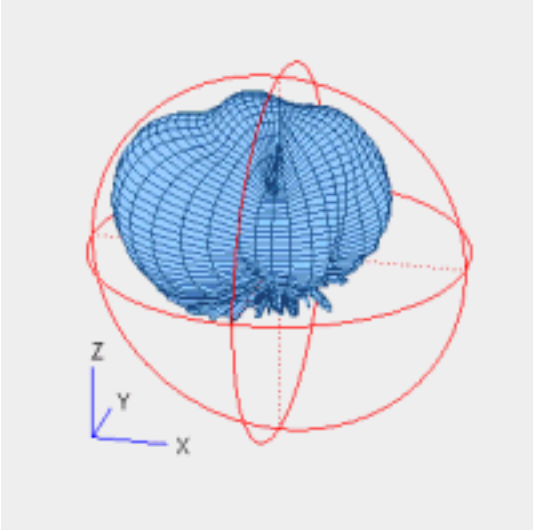

Element 2 – Horizontal Polarisation

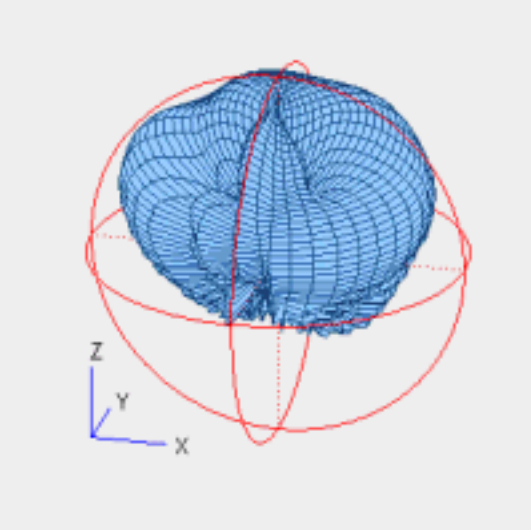

Vertical Polarisation

Appendix 32: Measured 3-D Patterns of Elements 1 and 2 on the PDA (used for correlation)

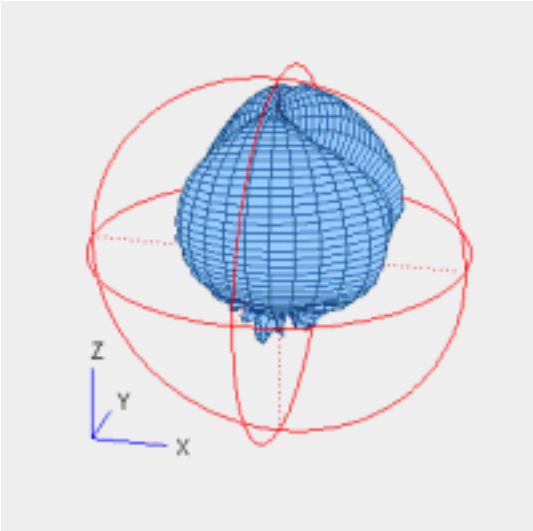

Element 3 – Horizontal Polarisation

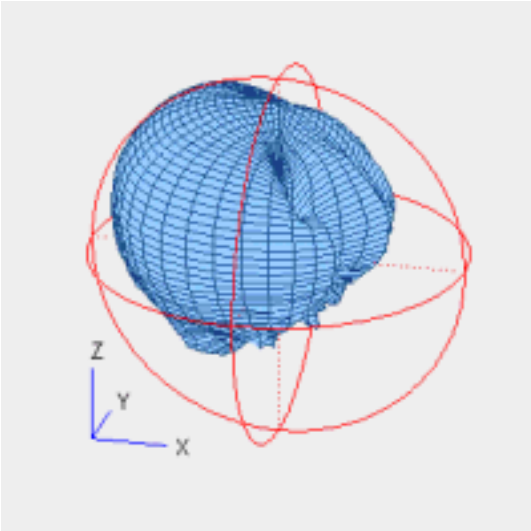

Vertical Polarisation

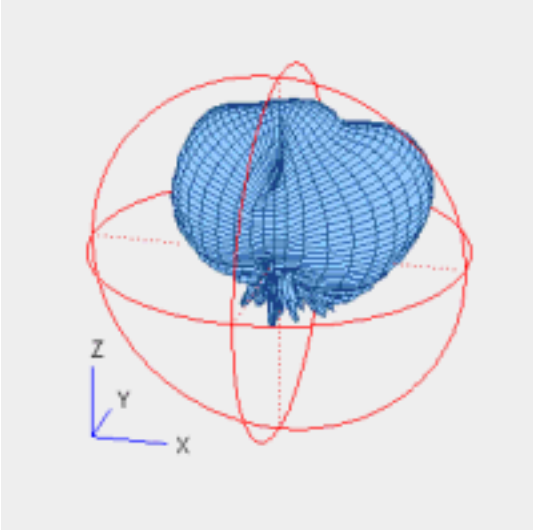

Element 4 – Horizontal Polarisation

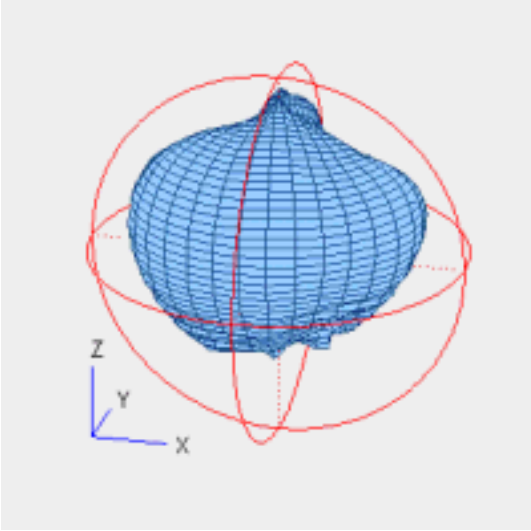

Vertical Polarisation

Appendix 33: Measured 3-D Patterns of Elements 3 and 4 (used for correlation)

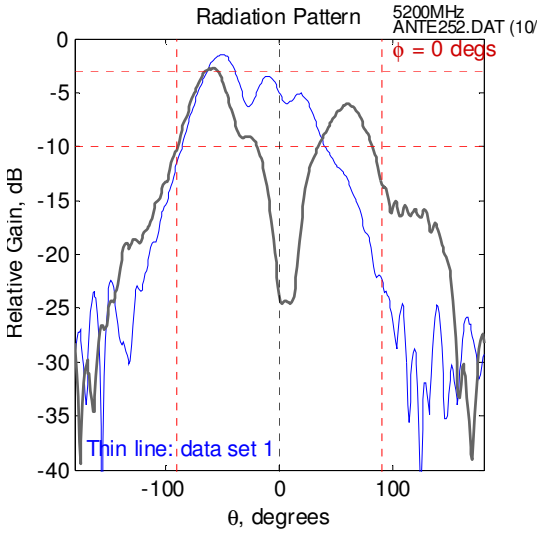

Element 2 – Principal planes

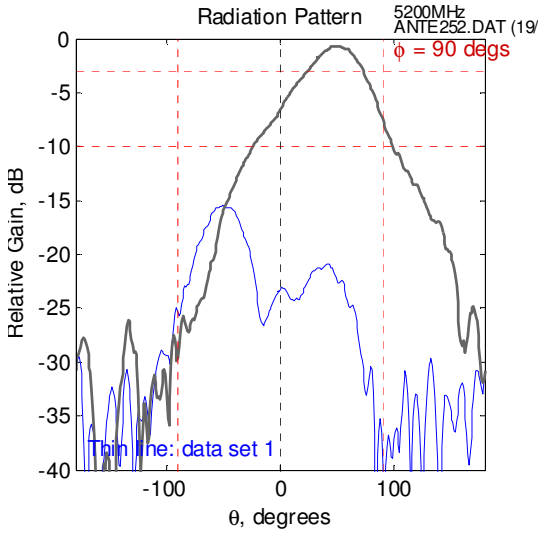

Blue is Horizontal Polarisation,

Black is Vertical Polarisation

Appendix 34: Cartesian Plots of Antenna gain

Elements	**1**	**2**	**3**	**4**
1	**1**	0.0495 ∠51.8°	0.0087 ∠117.6°	0.0221 ∠67.3°
2		**1**	0.0189 ∠-172.3°	0.0080 ∠-76.7°
3			**1**	0.0385 ∠-23.4°
4			0.0385 ∠23.4°	**1**

Appendix Table 2 Correlation between elements 1 to 4, mock-up PDA

Element	**D, dBi**	@ °	@ ϕ°
1	7.1	+50	+50
2	7.8	-55	-10
3	7.2	-51	+60
4	7.8	+52	-80

Appendix Table 3: Maximum gain (regardless of polarisation), 4 element mock-up PDA

3 APPENDIX - FOLDED LOOP AND ELECTRONIC BAND-GAP

3.1 Laptop Design 1

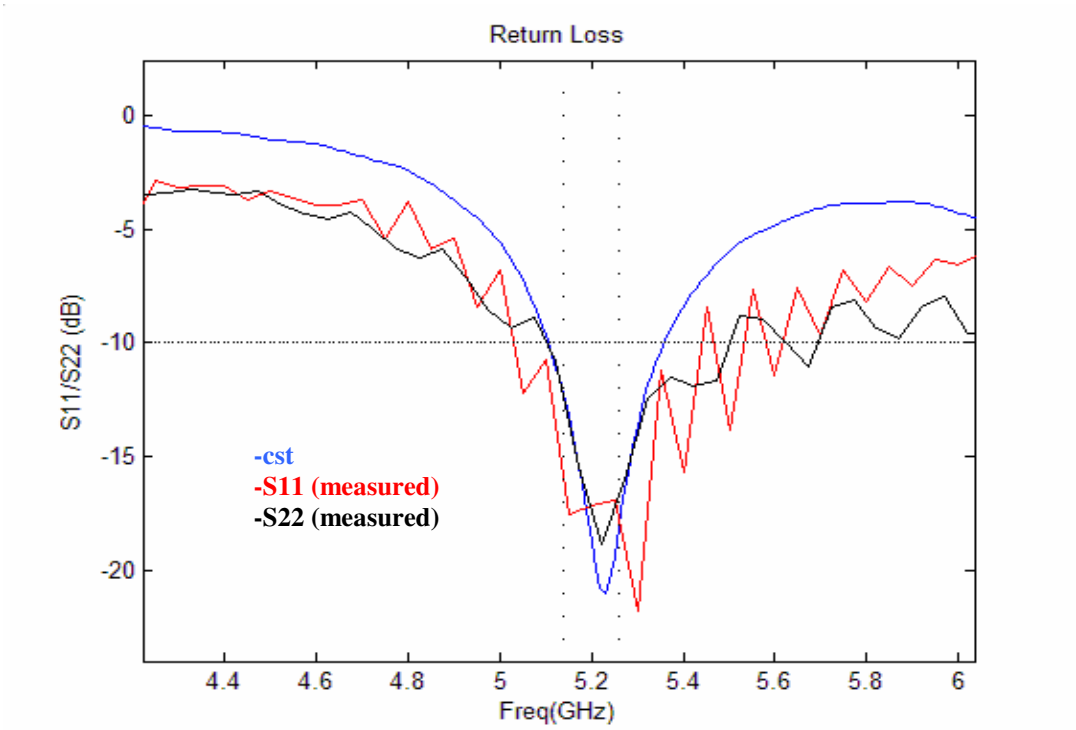

Appendix 35: Return loss of Antenna 1 and Antenna 2

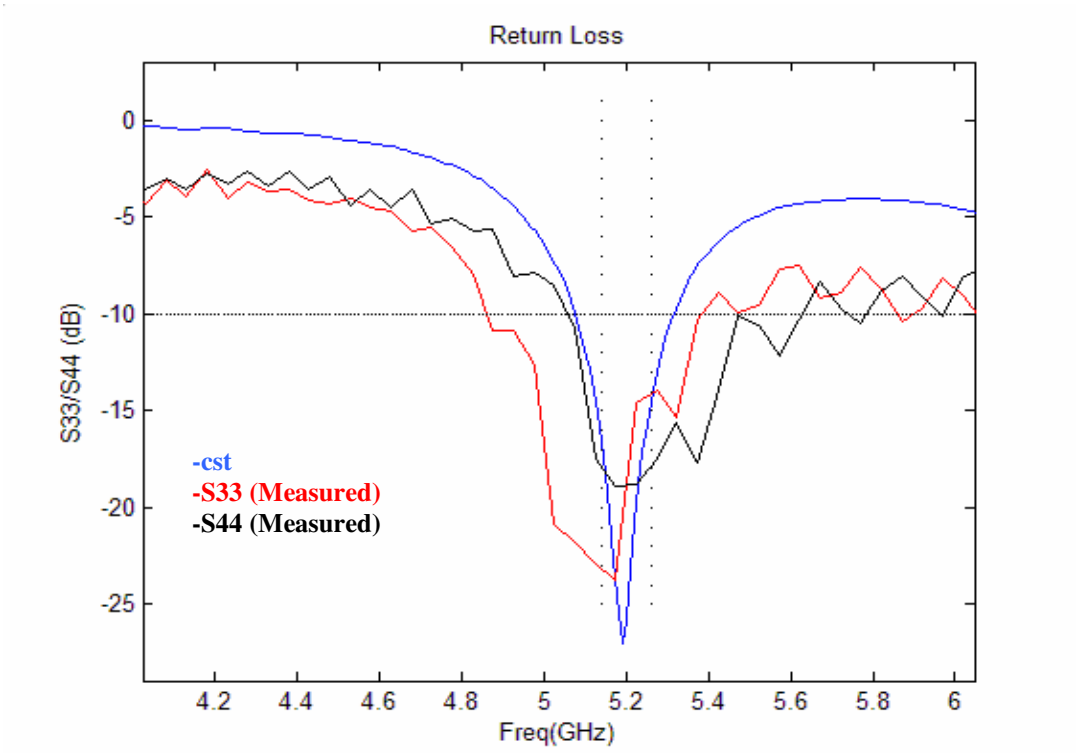

Appendix 36: Return loss of Antenna 3 and Antenna

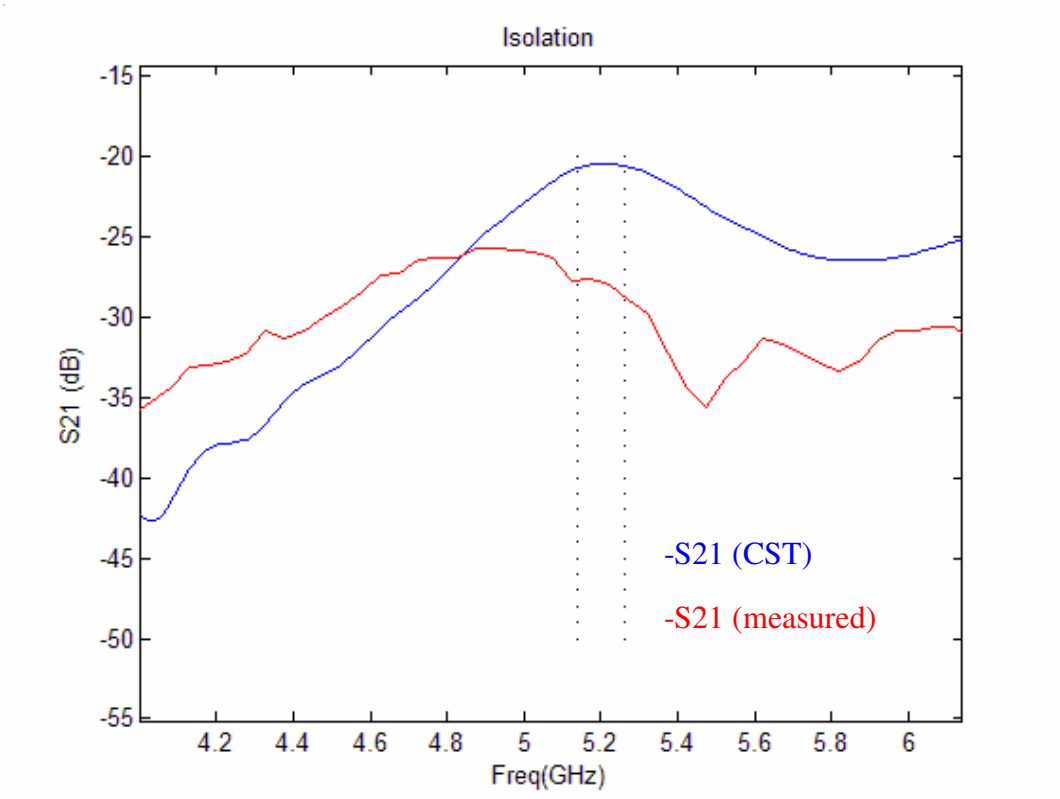

Appendix 37: Isolation between Antenna 1 and Antenna 2

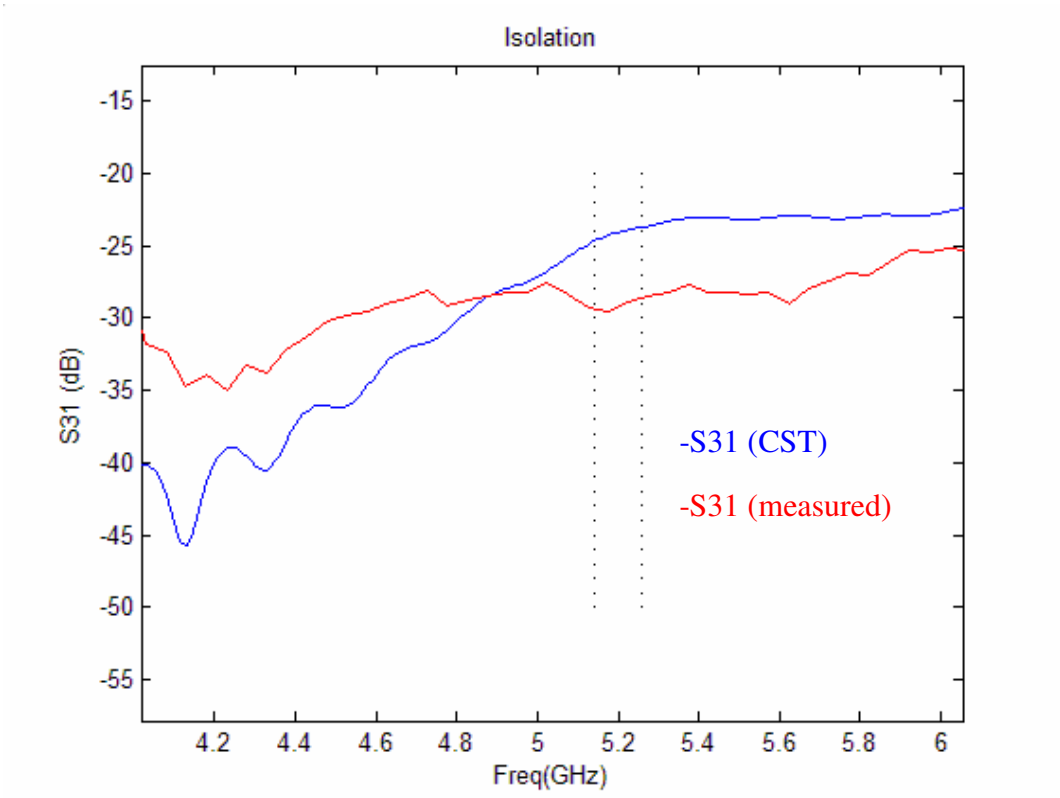

Appendix 38: Isolation between Antenna 1 and Antenna 3

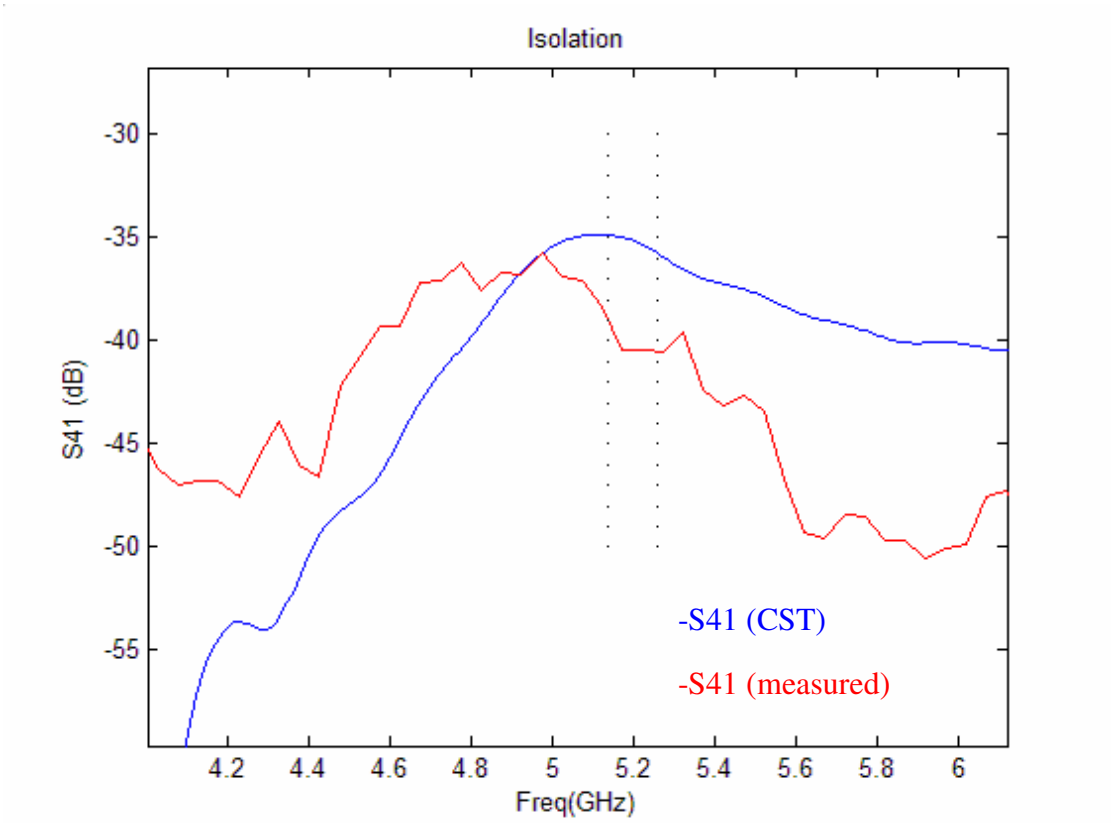

Appendix 39: Isolation between Antenna 1 and Antenna 4

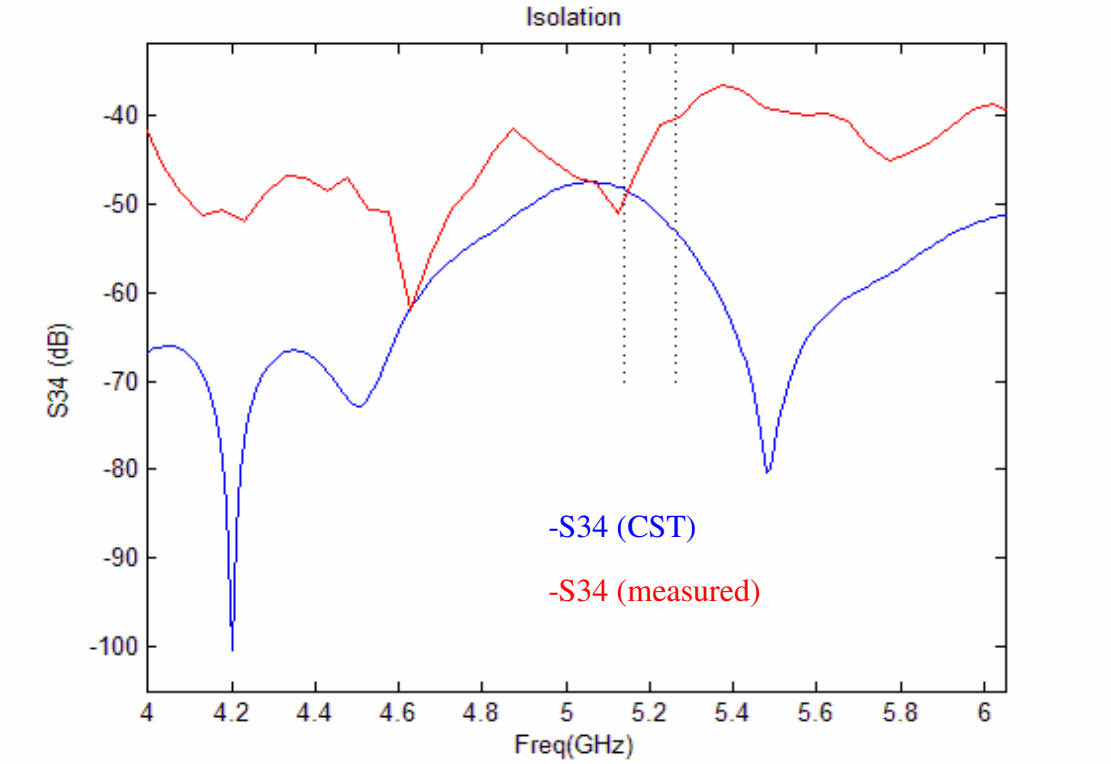

Appendix 40: Isolation between Antenna 3 and Antenna 4

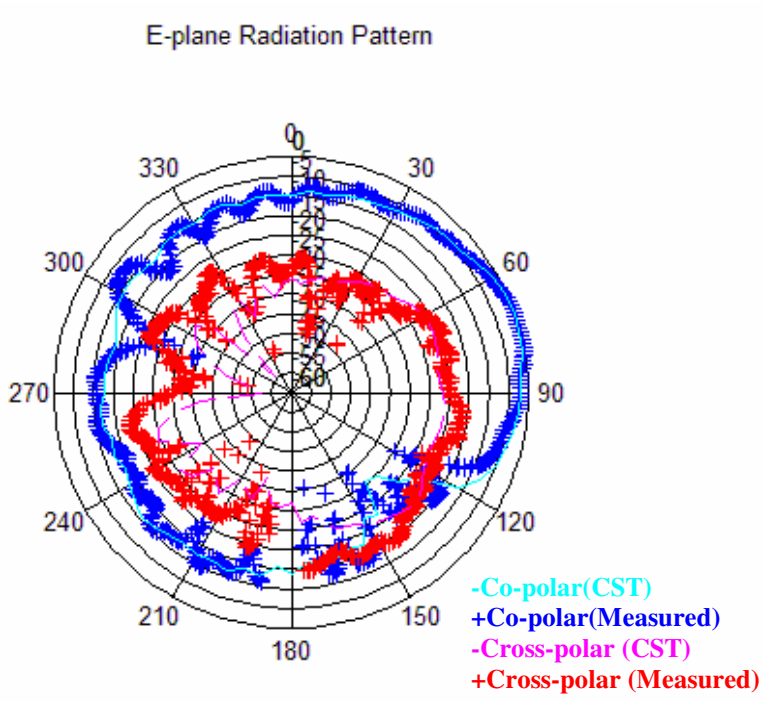

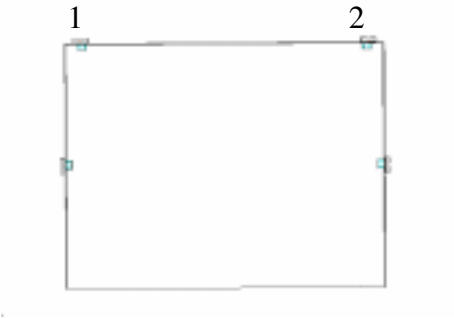

Appendix 41: E-plane co- and cross-polar of Antenna 1

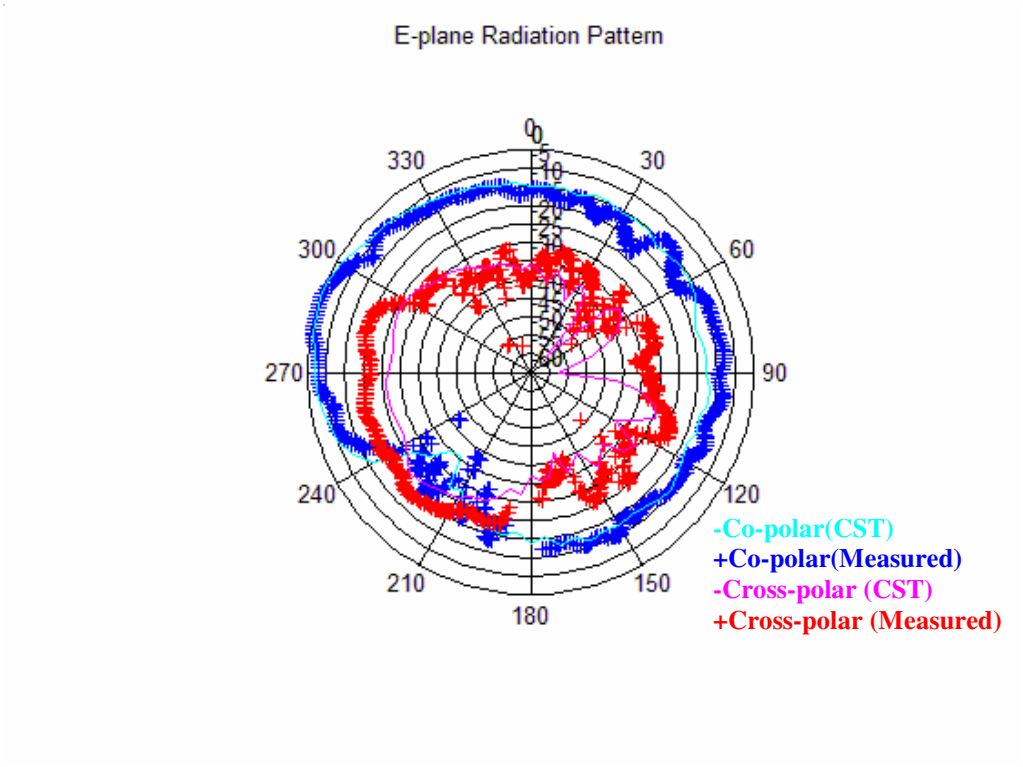

Appendix 42: E-plane co- and cross-polar of Antenna 2

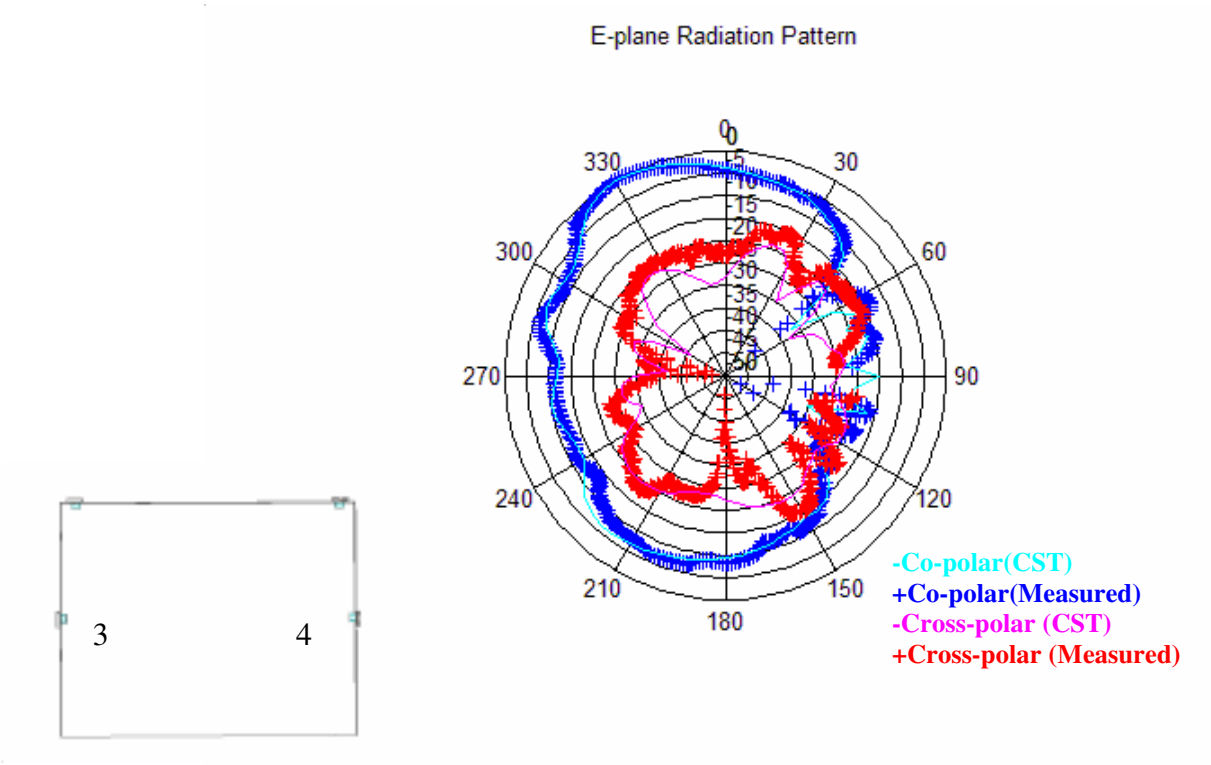

Appendix 43: E-plane co- and cross-polar of Antenna 3

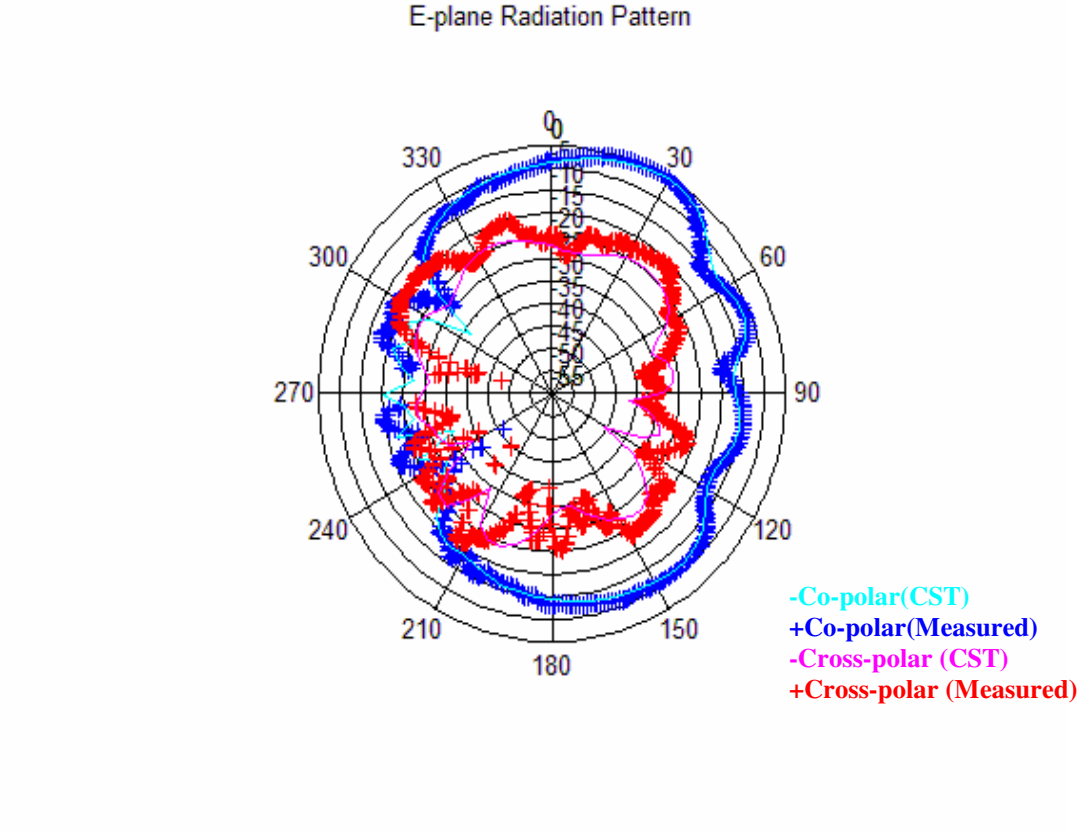

Appendix 44: E-plane co- and cross-polar of Antenna 4

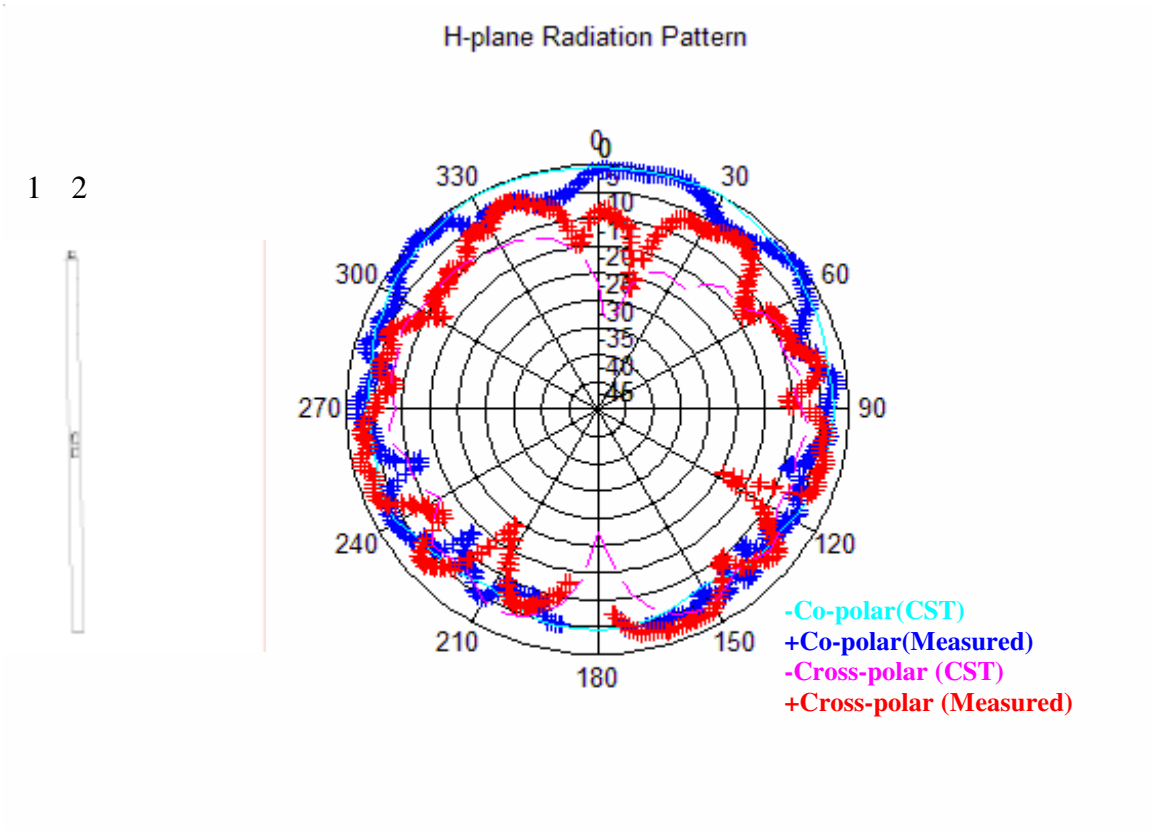

Appendix 45: H-plane co- and cross-polar of Antenna 1

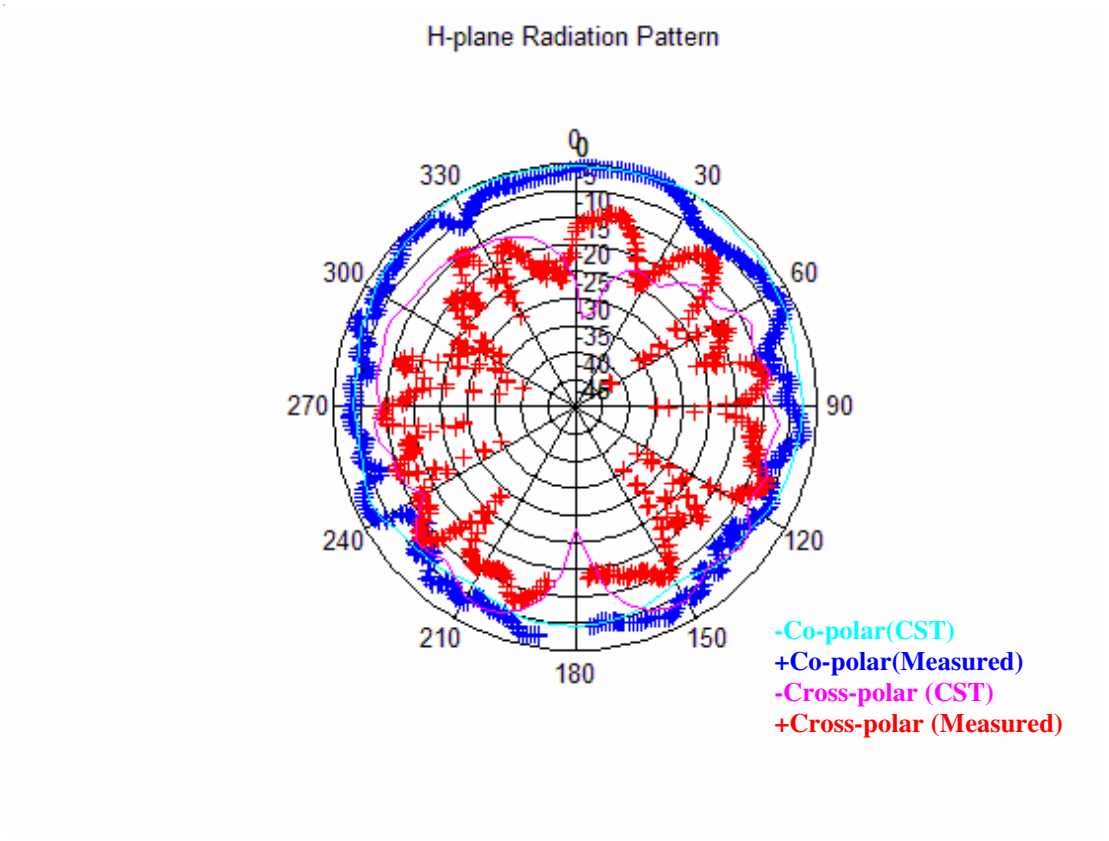

Appendix 46: H-plane co- and cross-polar of Antenna 2

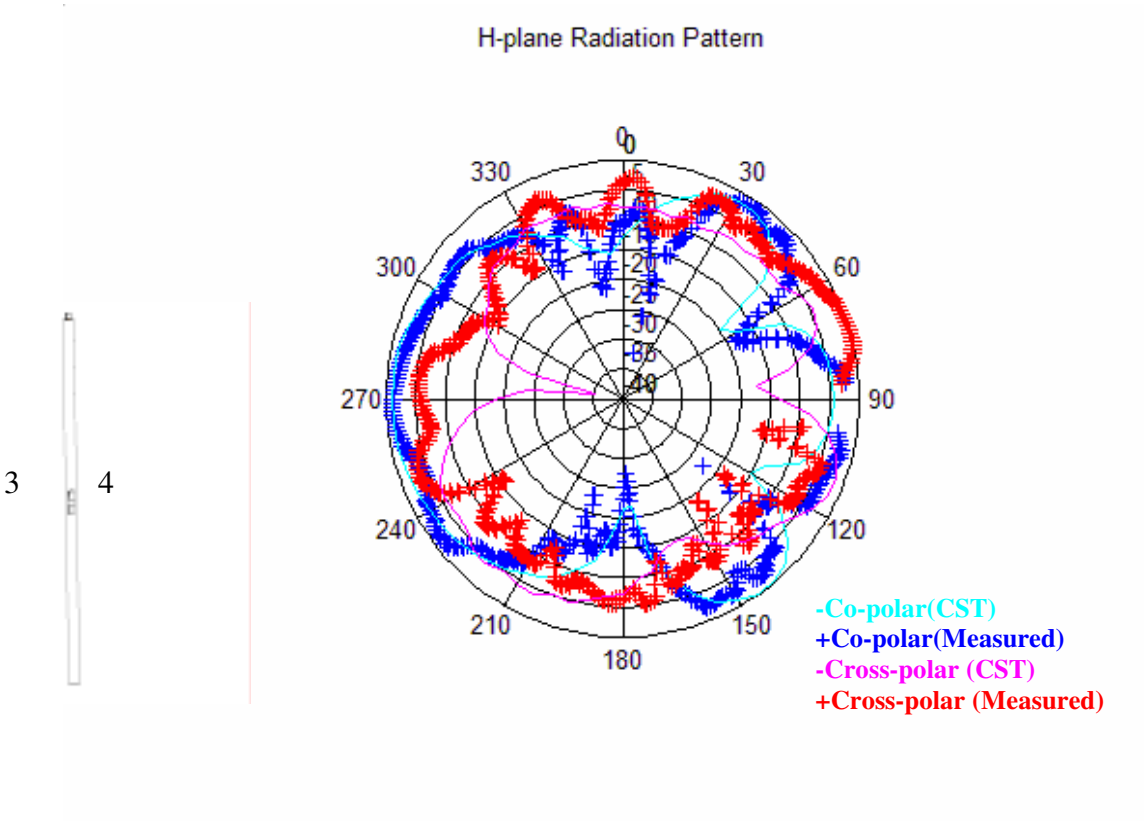

Appendix 47: H-plane co- and cross-polar of Antenna 3

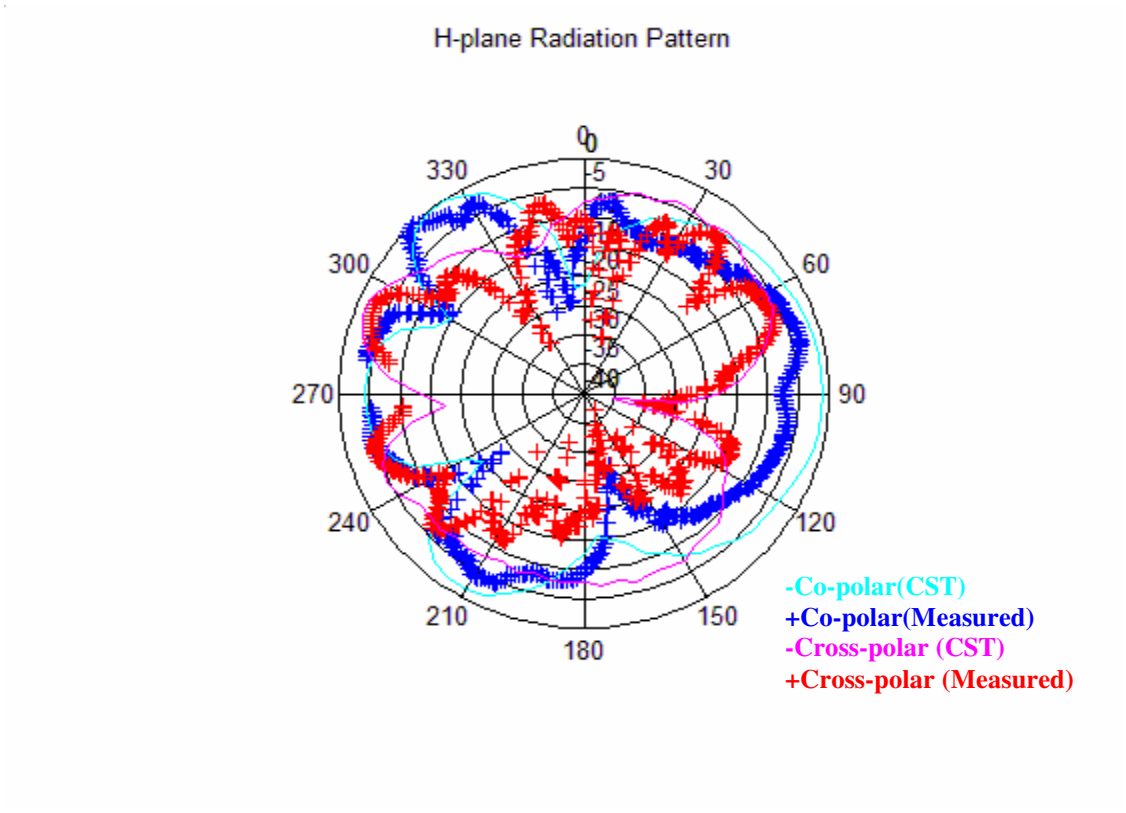

Appendix 48: H-plane co- and cross-polar of Antenna 4

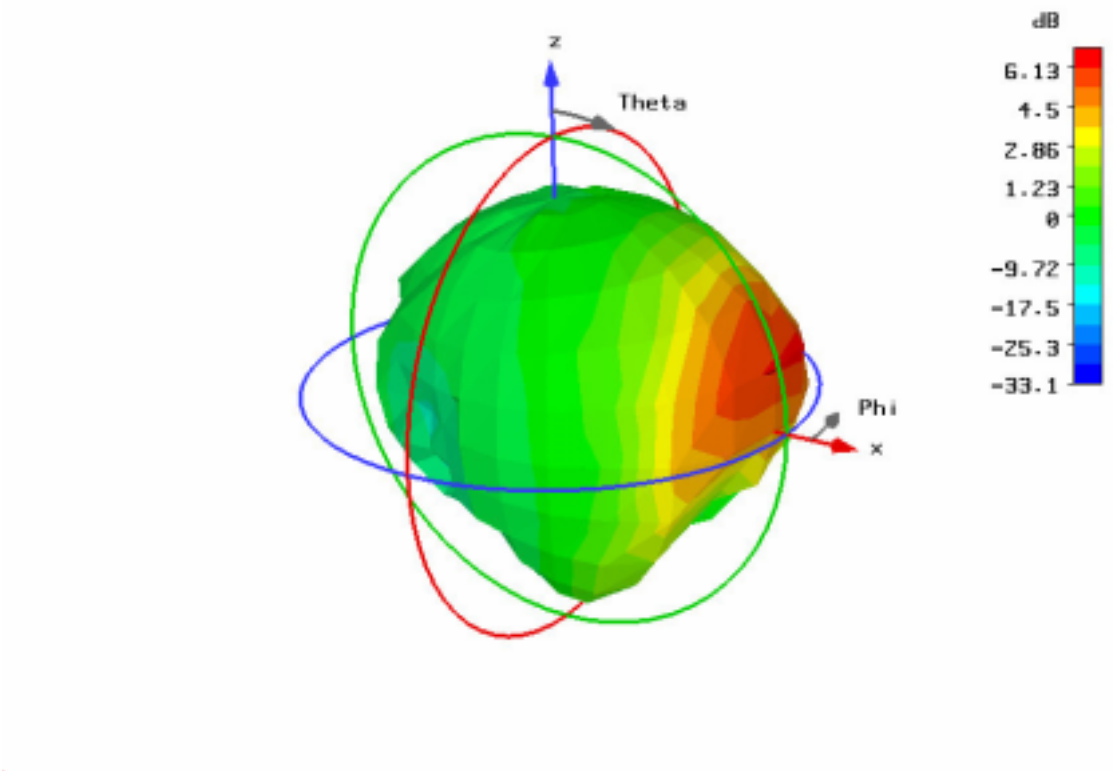

Appendix 49: 3-D co-polar of Antenna 1

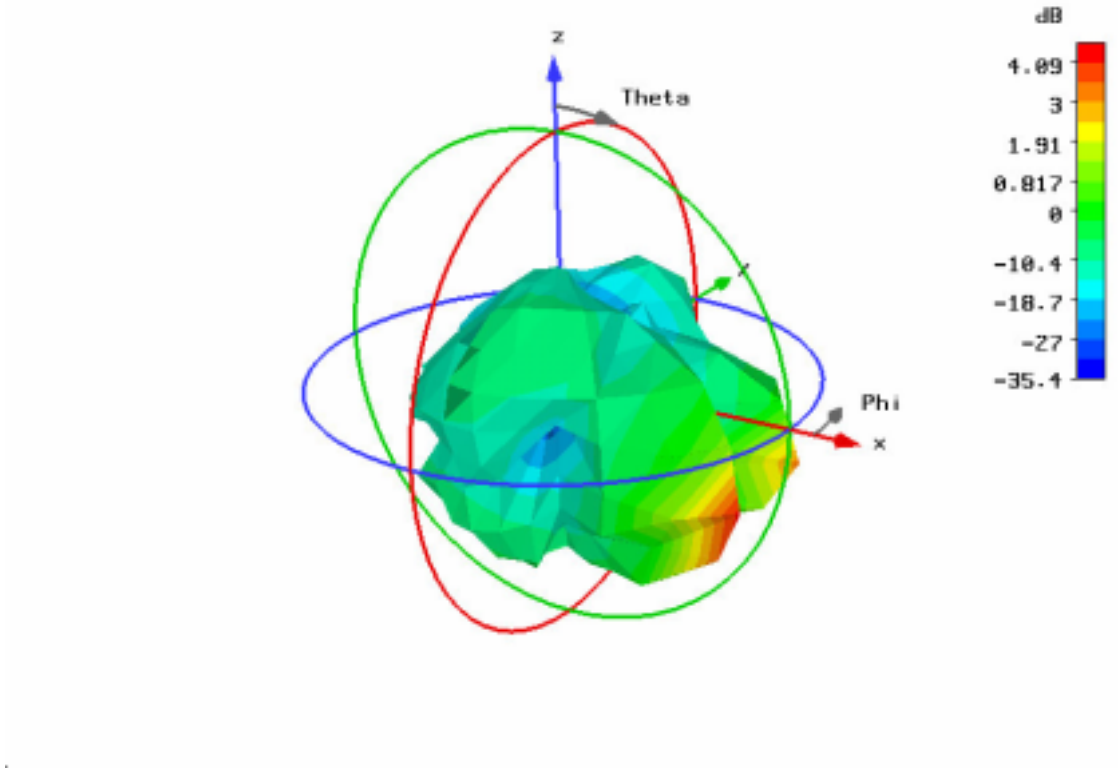

Appendix 50: 3-D cross-polar of Antenna 1

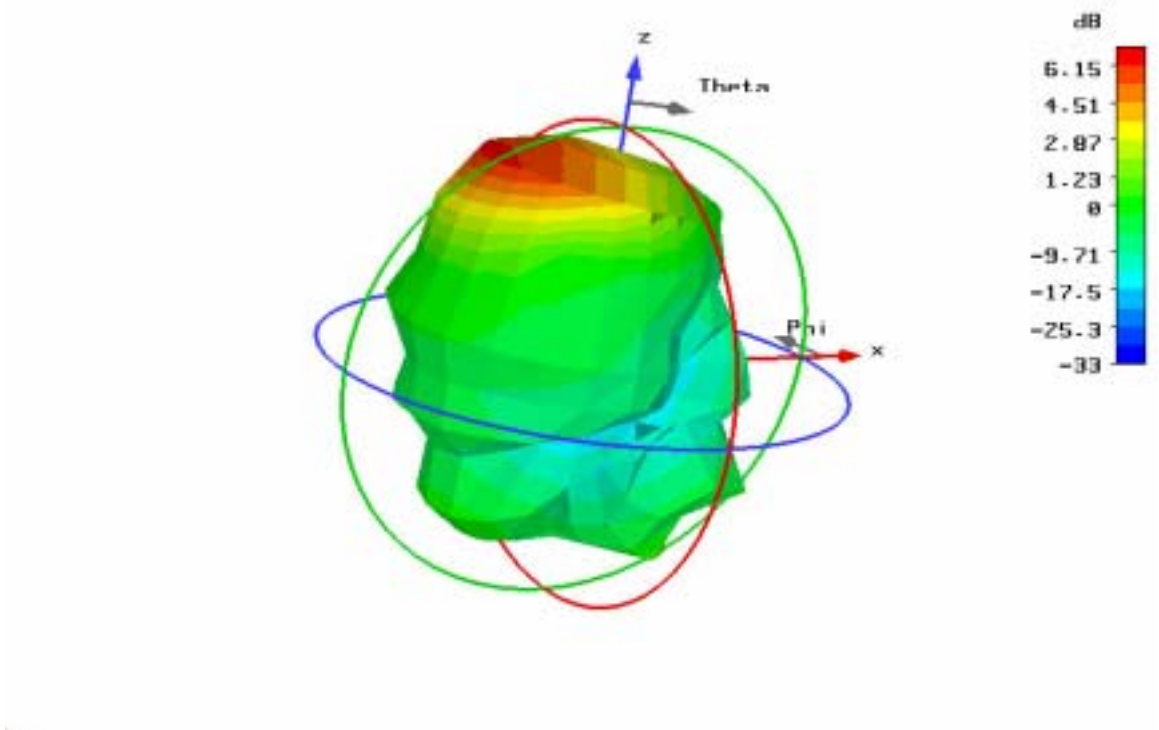

Appendix 51: 3-D co-polar of Antenna 3

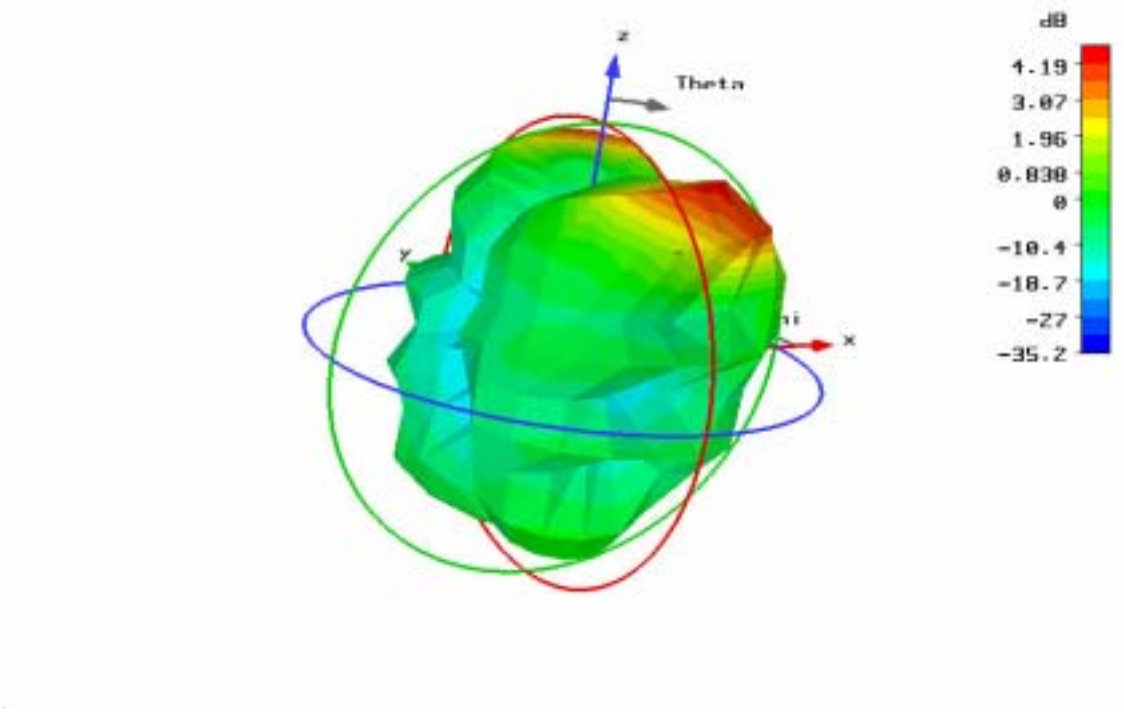

Appendix 52: 3-D cross-polar of Antenna 3

3.2 Laptop Design 2

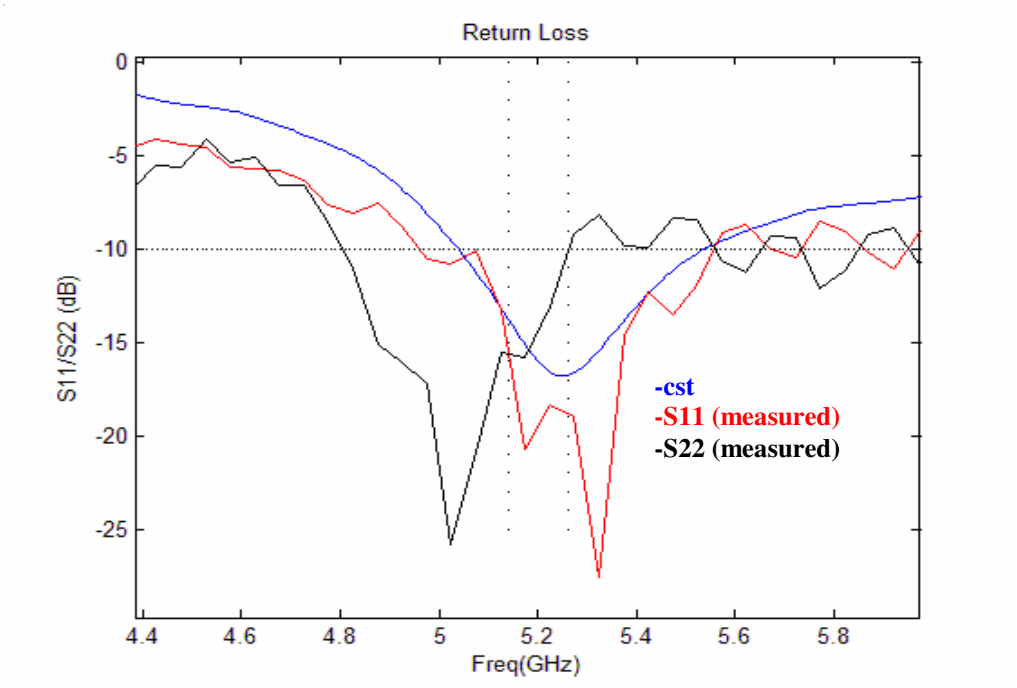

Appendix 53: Return loss of Antenna 1 and Antenna 2

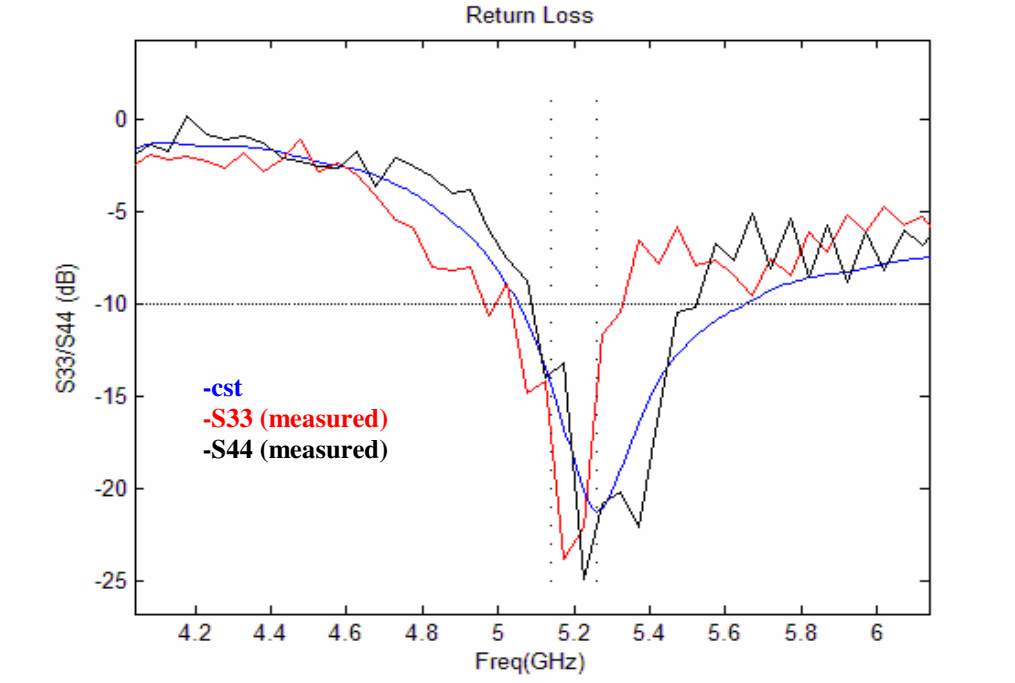

Appendix 54: Return loss of Antenna 3 and Antenna 4

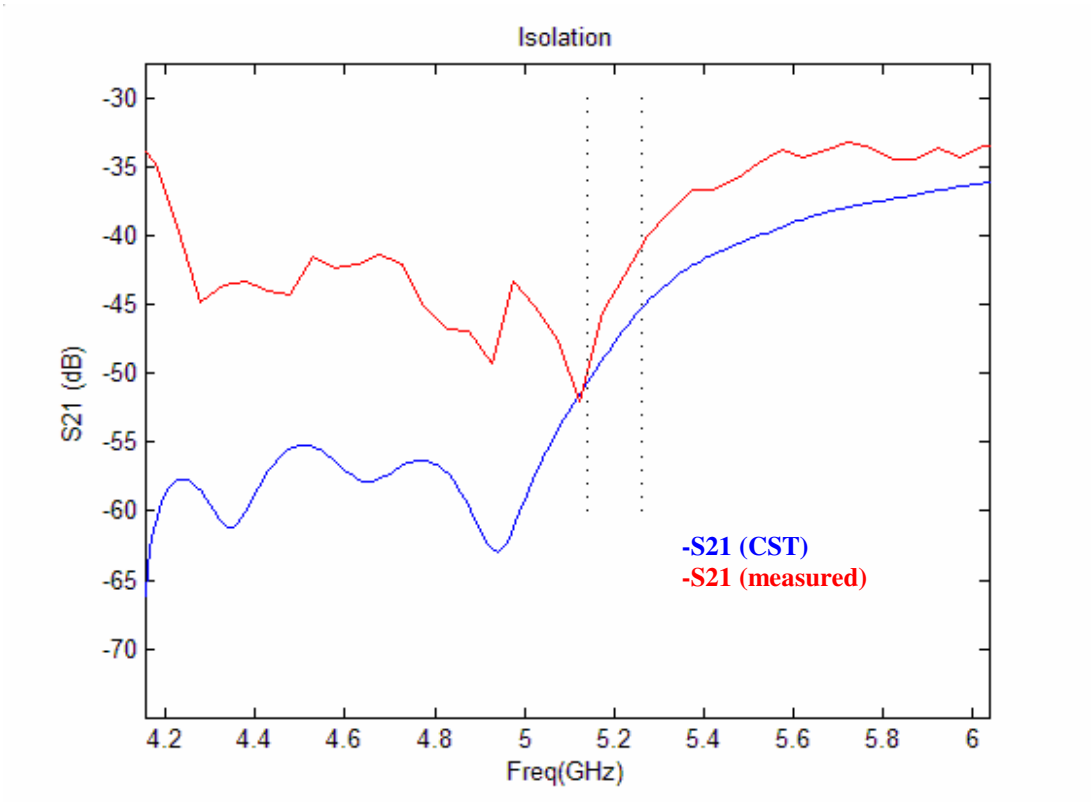

Appendix 55: Isolation between Antenna 1 and Antenna 2

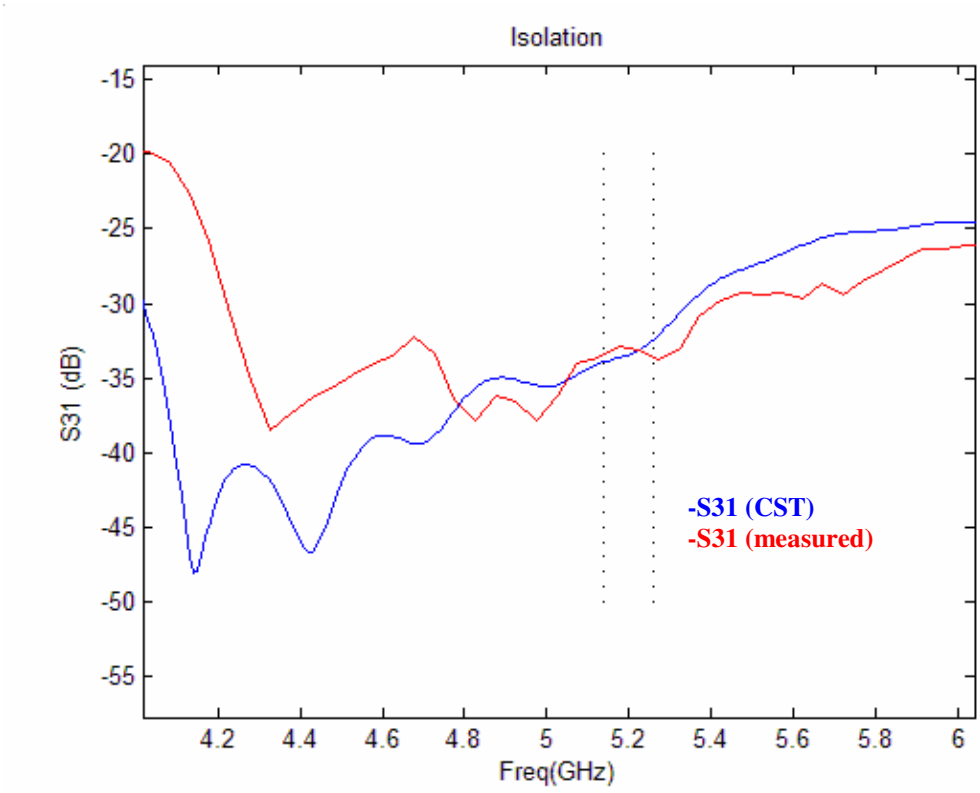

Appendix 56: Isolation between Antenna 1 and Antenna 3

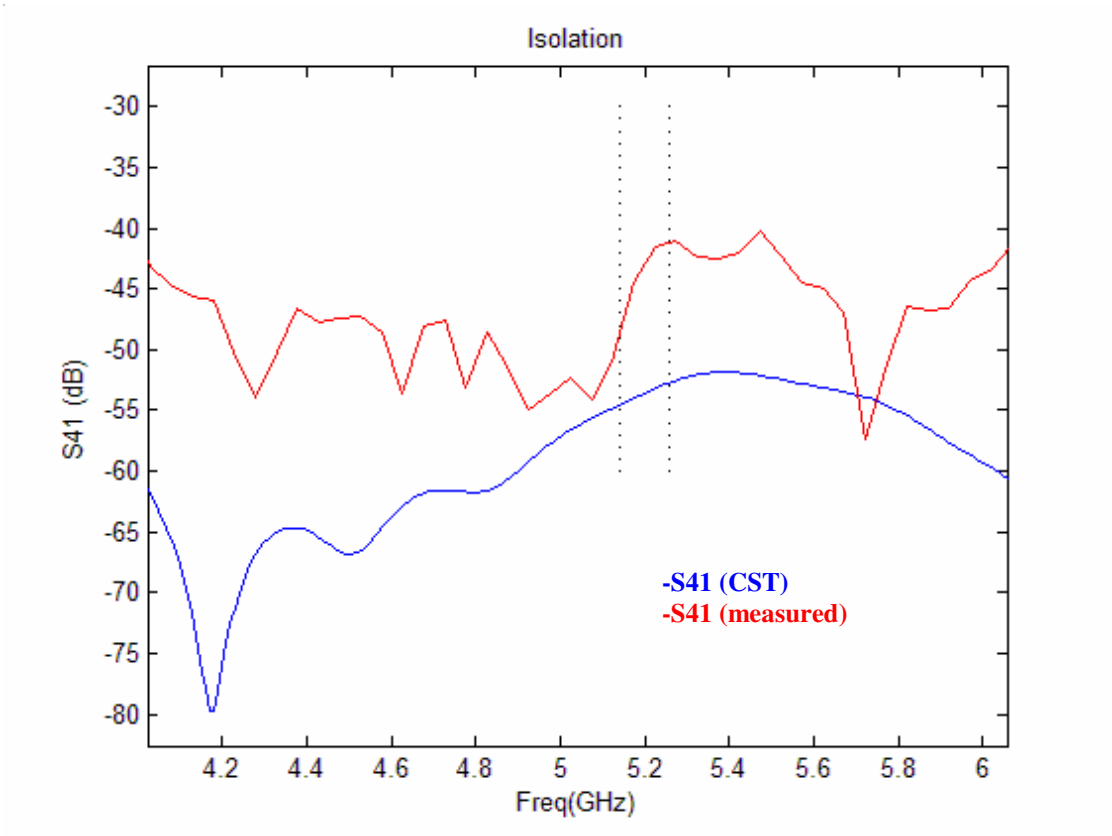

Appendix 57: Isolation between Antenna 1 and Antenna 4

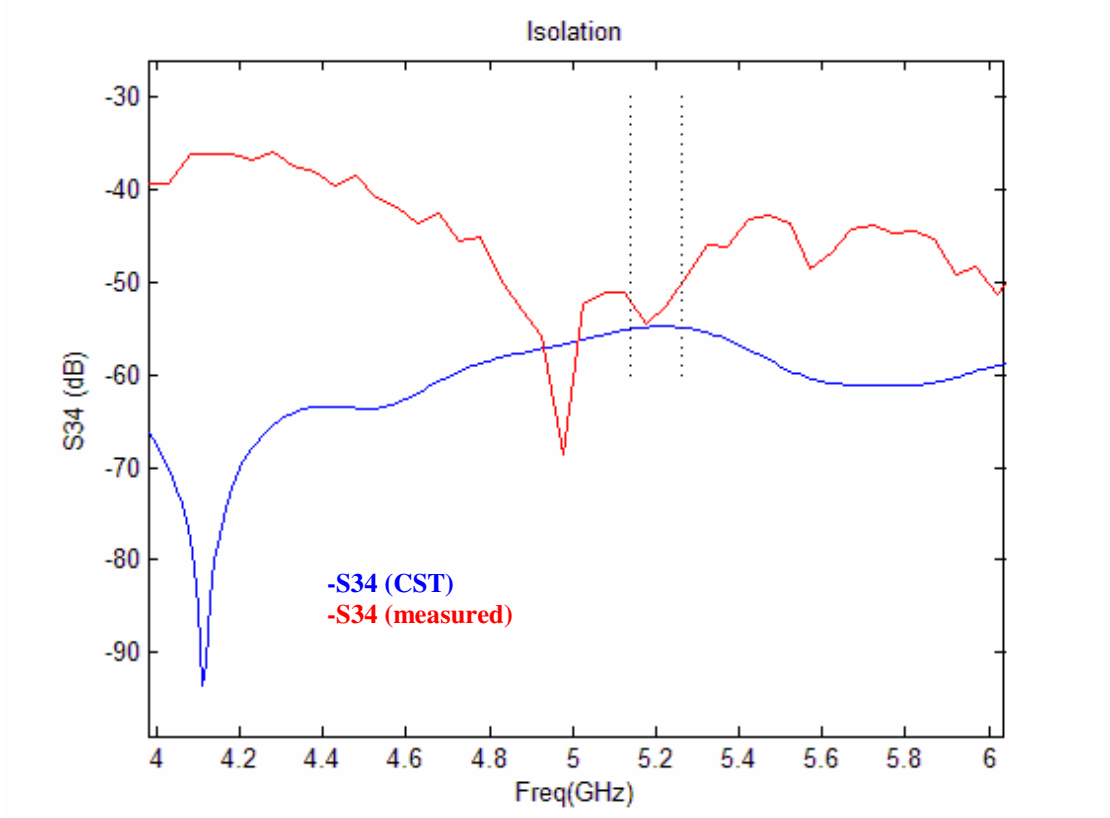

Appendix 58: Isolation between Antenna 3 and Antenna 4

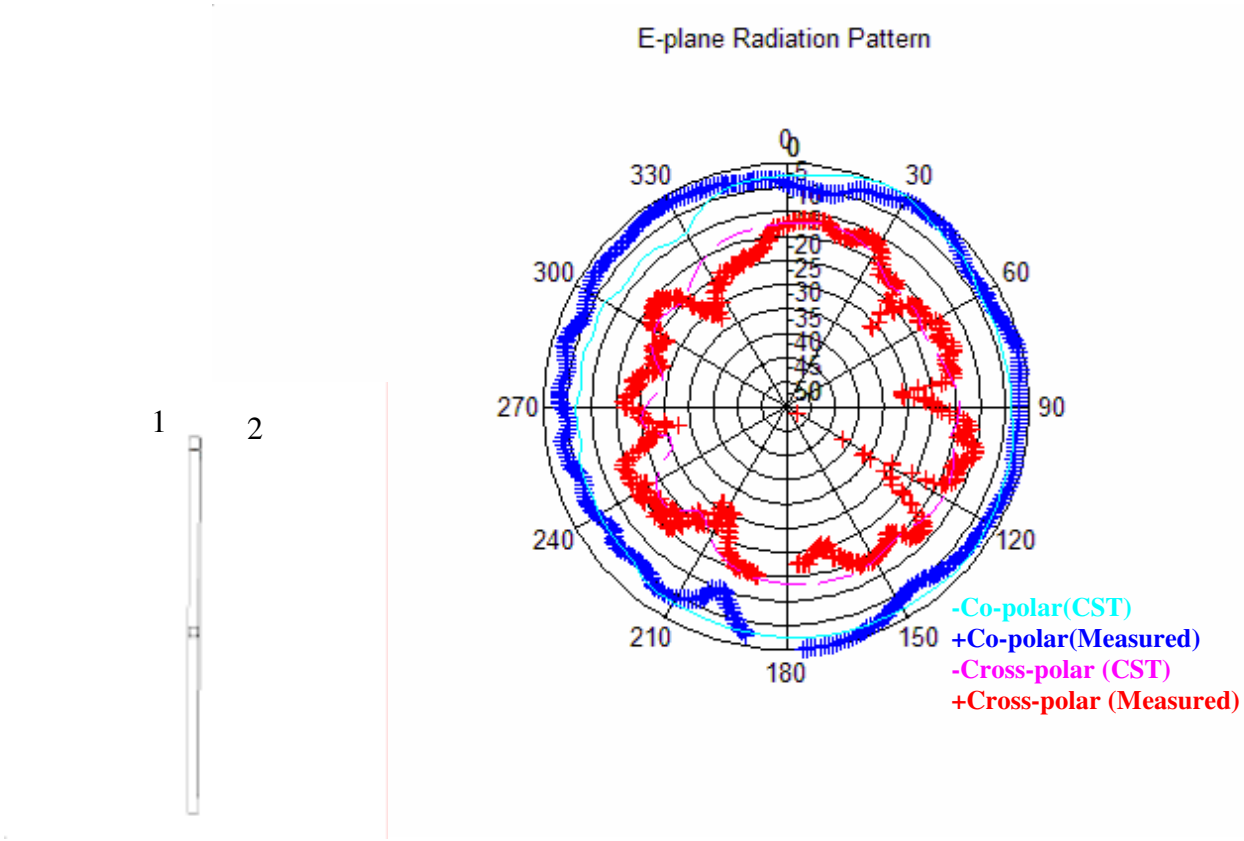

Appendix 59: E-plane co- and cross-polar of Antenna 1

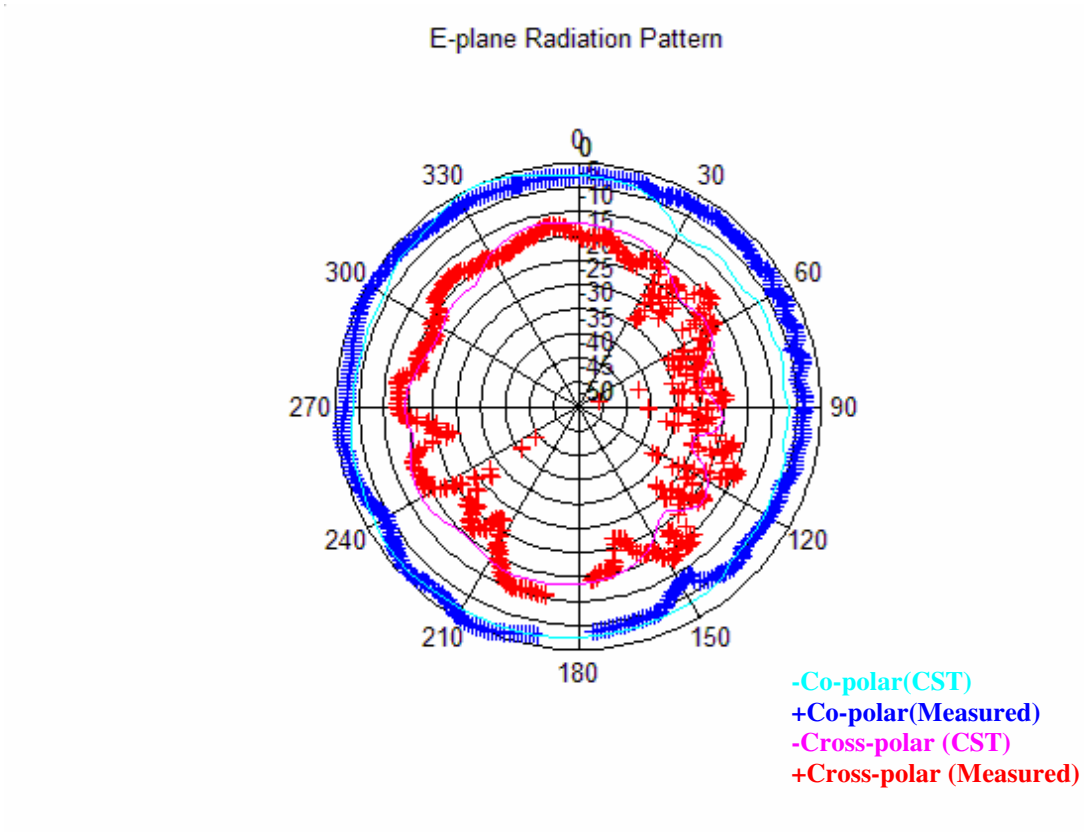

Appendix 60: E-plane co- and cross-polar of Antenna 2

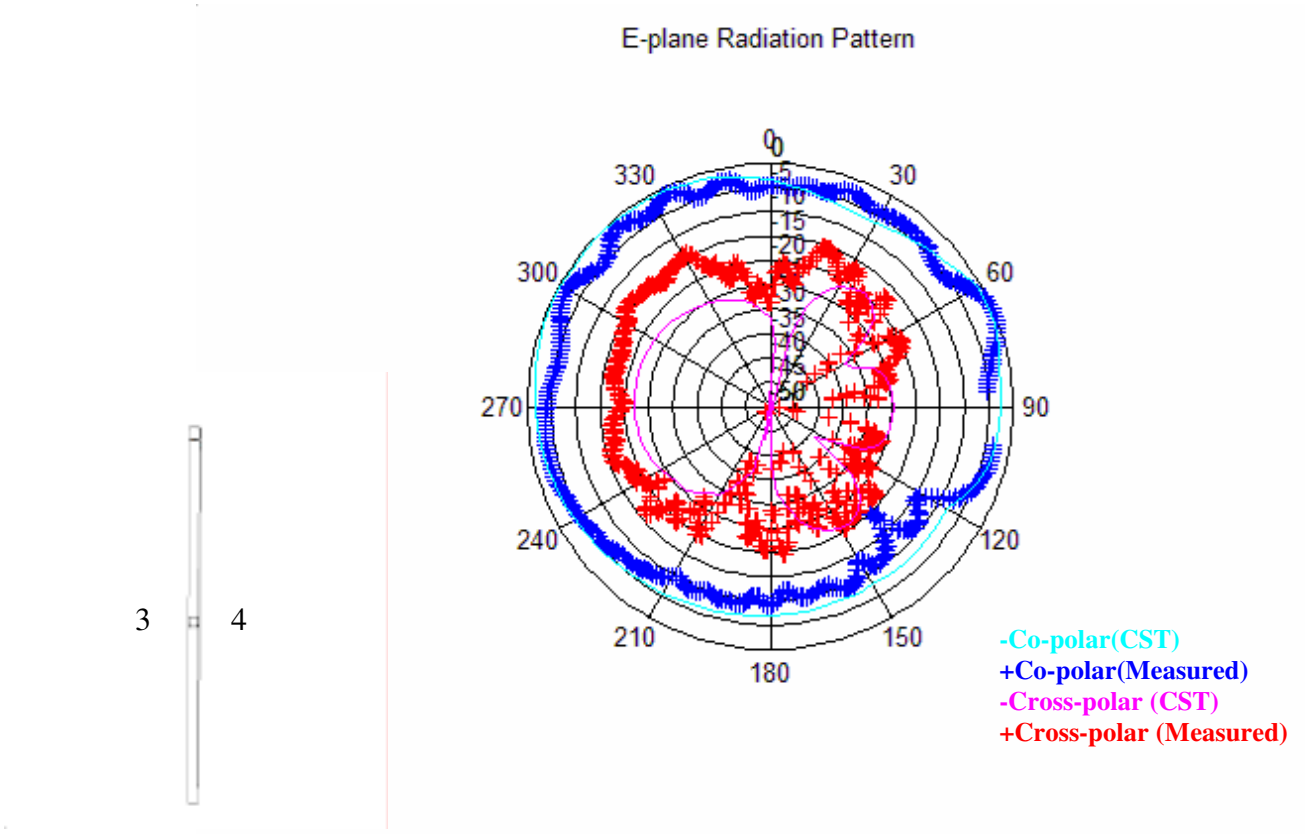

Appendix 61: E-plane co- and cross-polar of Antenna 3

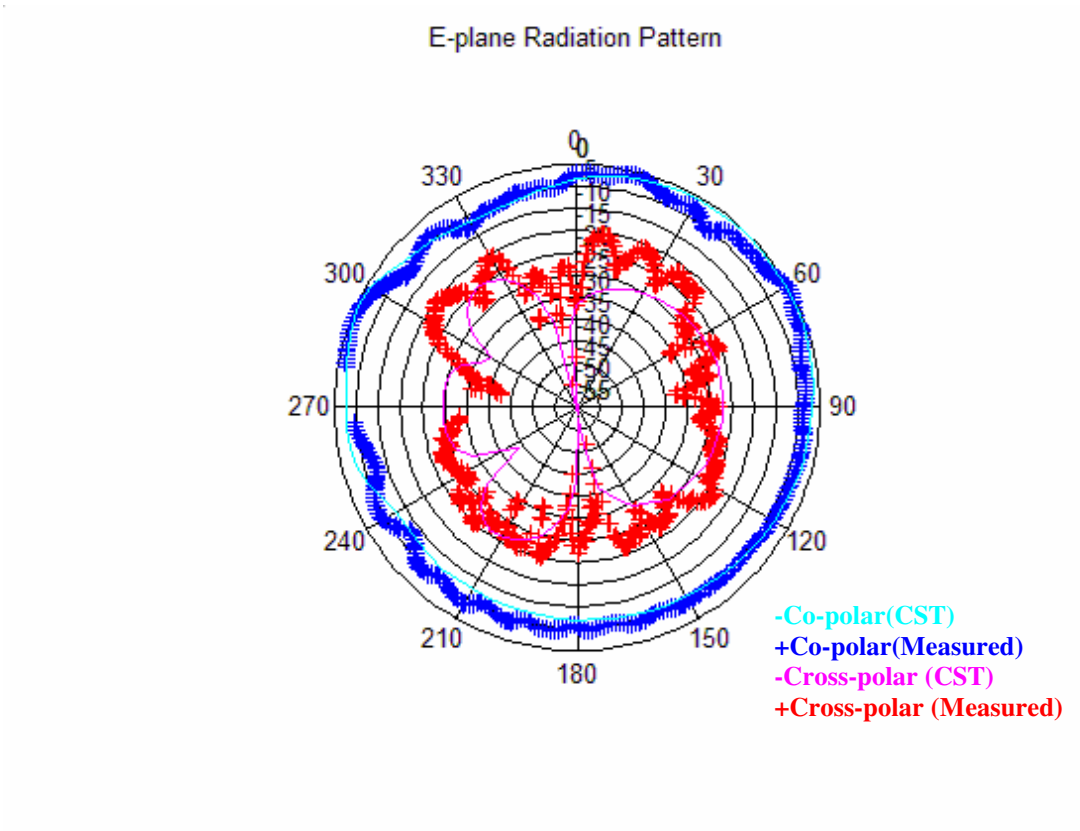

Appendix 62: E-plane co- and cross-polar of Antenna 4

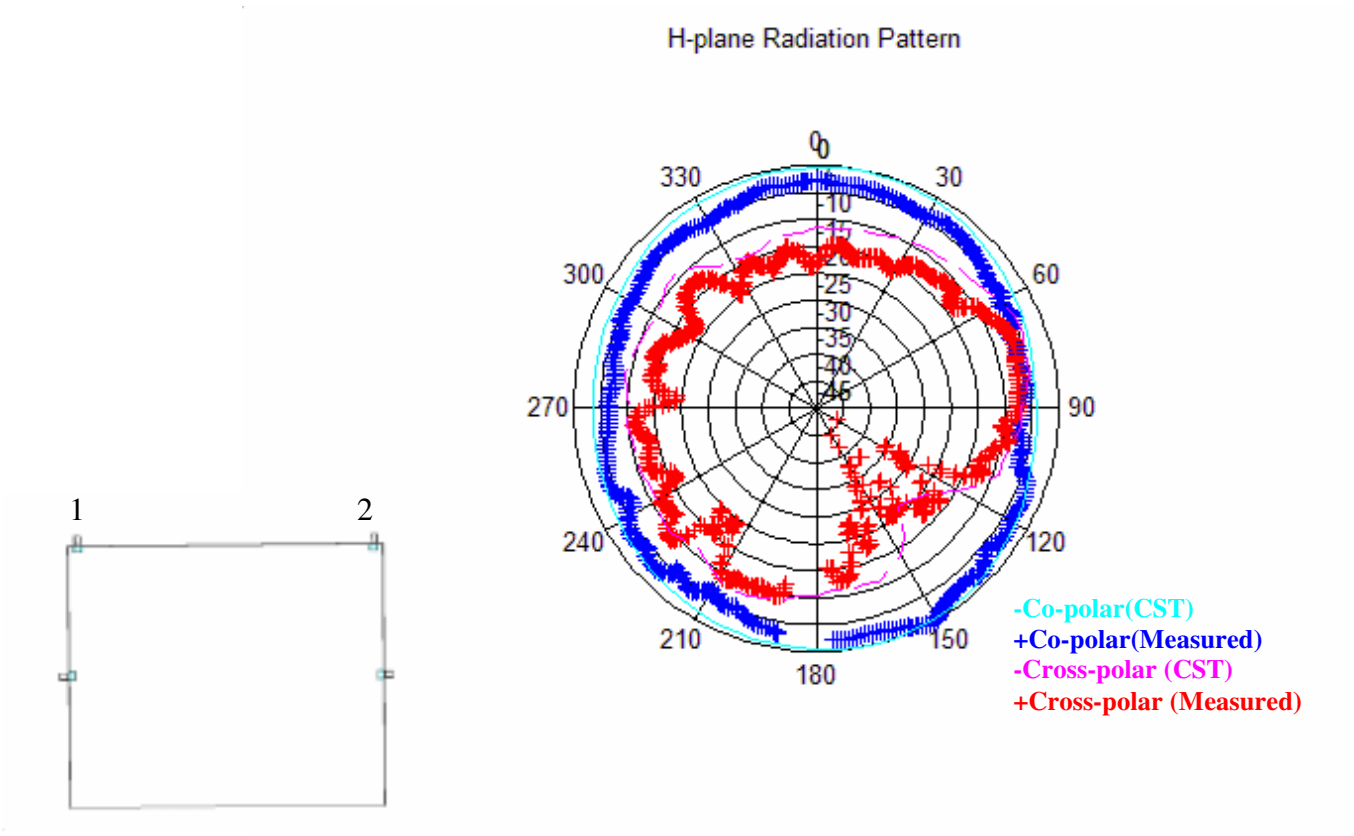

Appendix 63: H-plane co- and cross-polar of Antenna 1

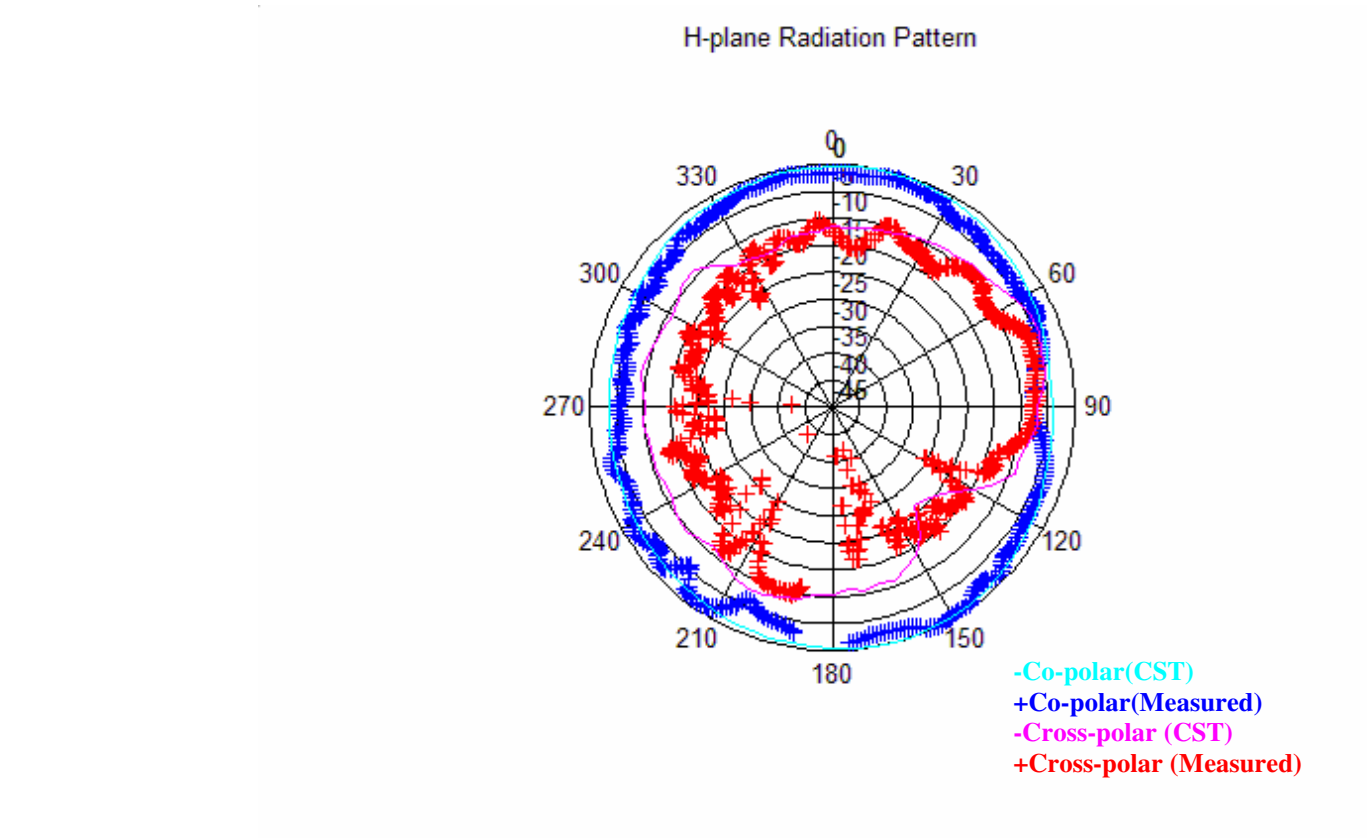

Appendix 64: H-plane co- and cross-polar of Antenna 2

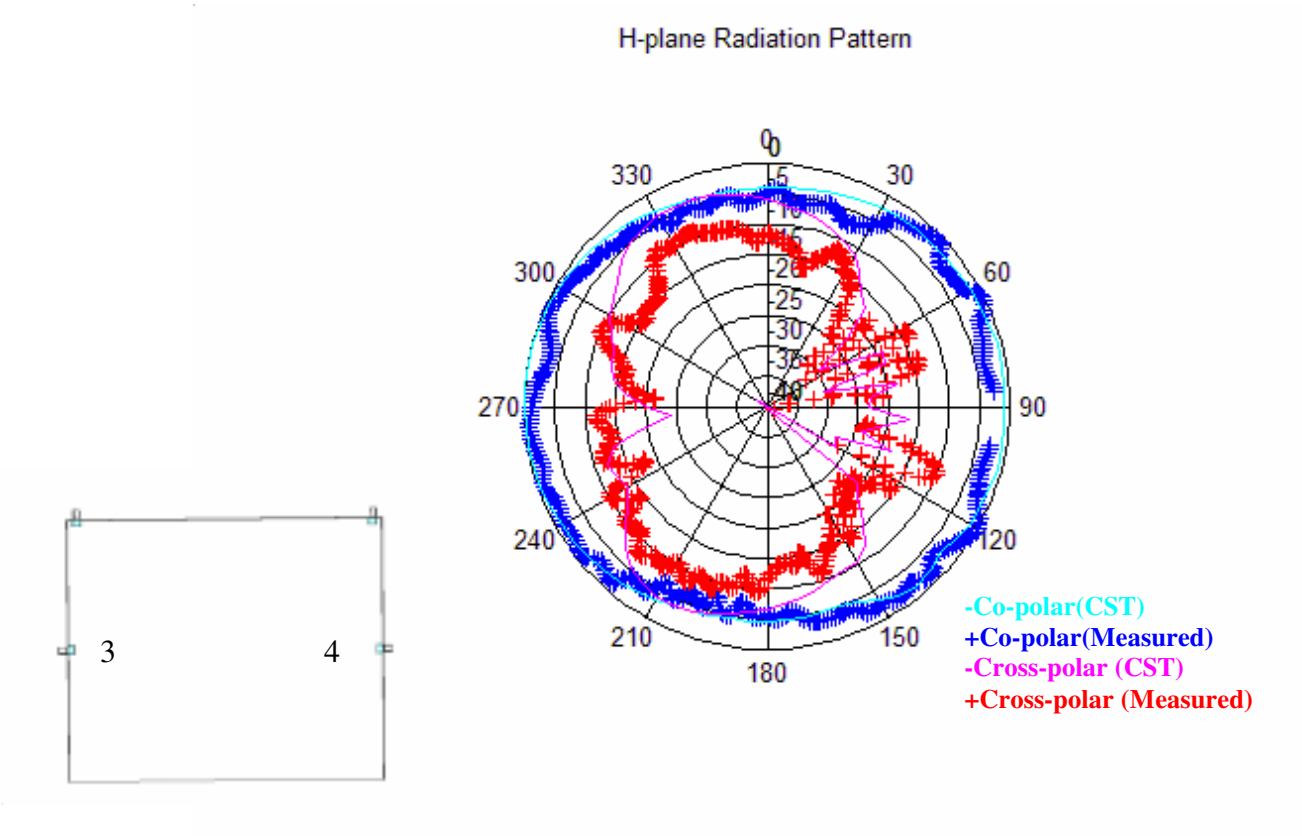

Appendix 65: H-plane co- and cross-polar of Antenna 3

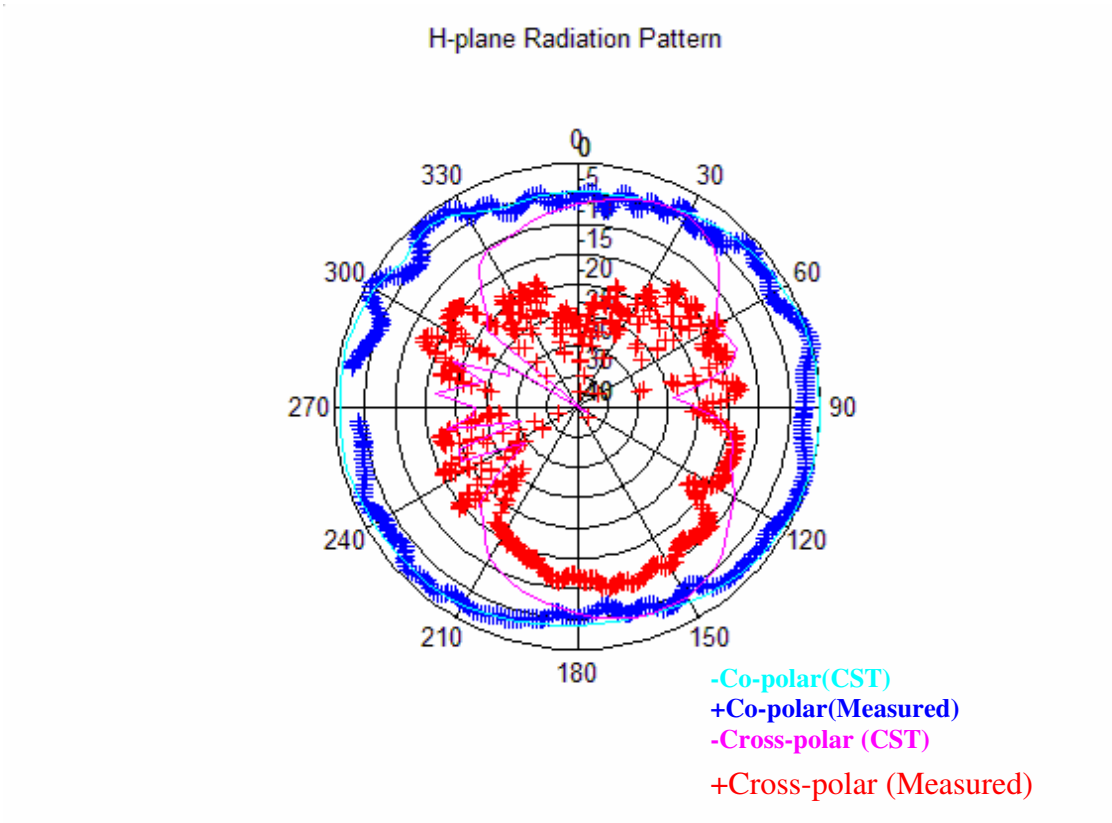

Appendix 66: H-plane co- and cross-polar of Antenna 4

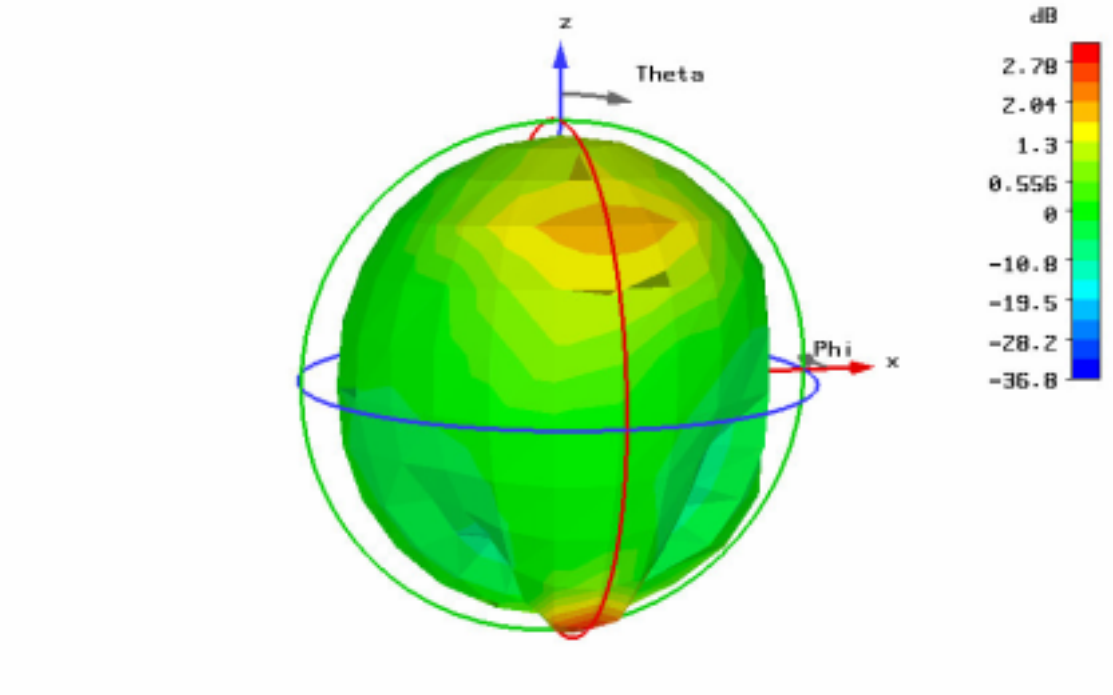

Appendix 67: 3-D co-polar of Antenna 1

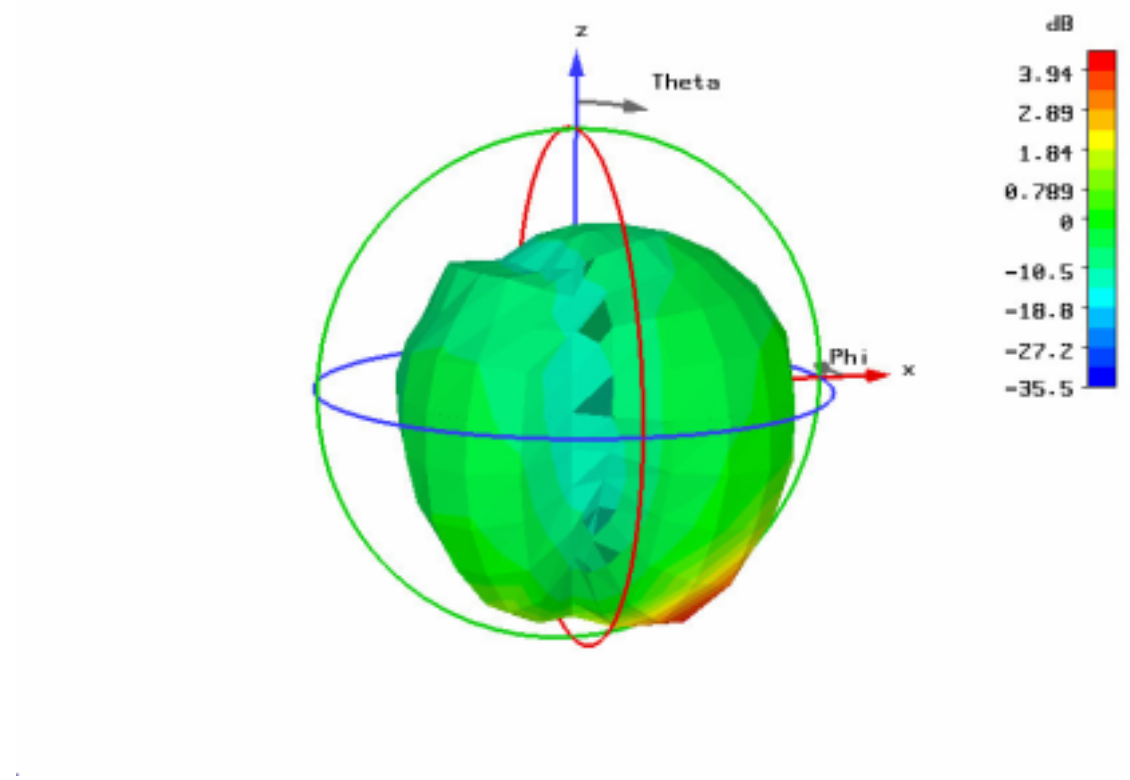

Appendix 68: 3-D cross-polar of Antenna 1

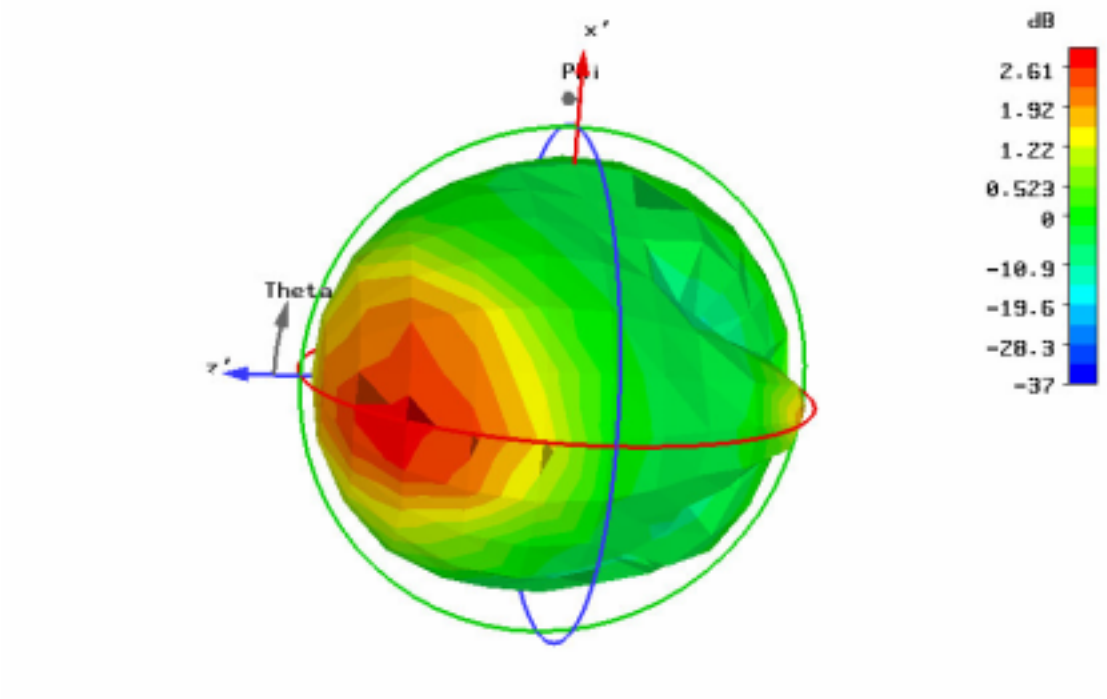

Appendix 69: 3-D co-polar of Antenna 3

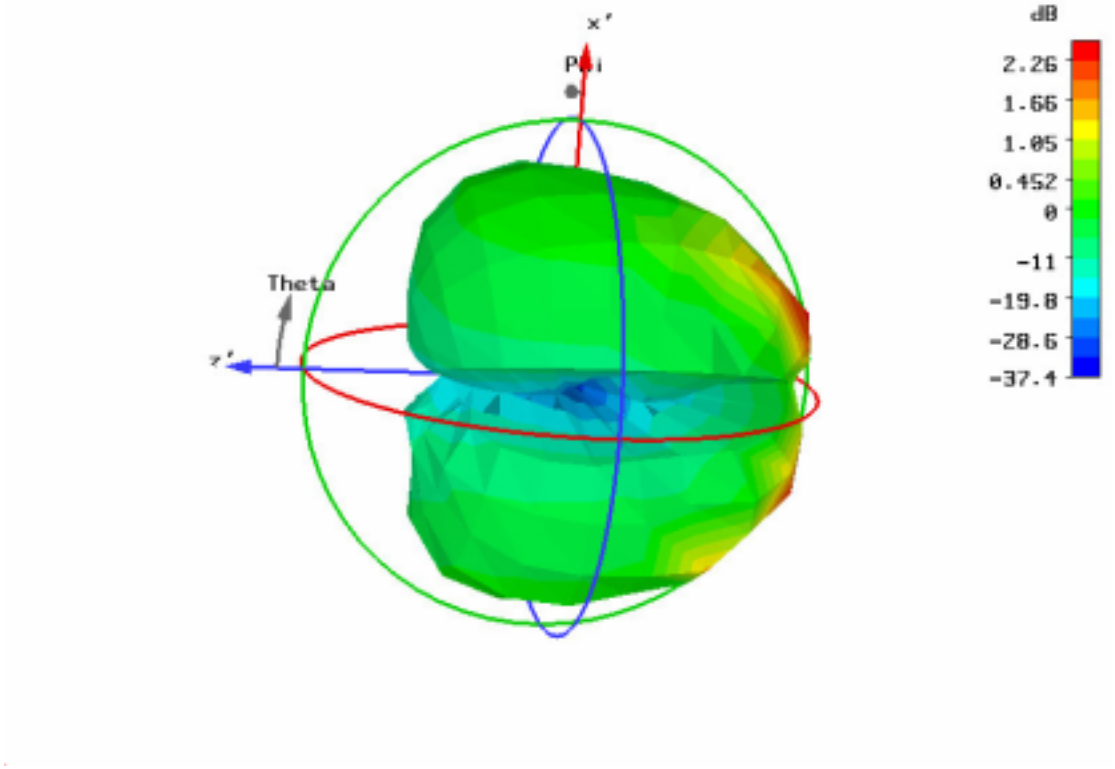

Appendix 70: 3-D cross-polar of Antenna 3

3.3 PDA Design

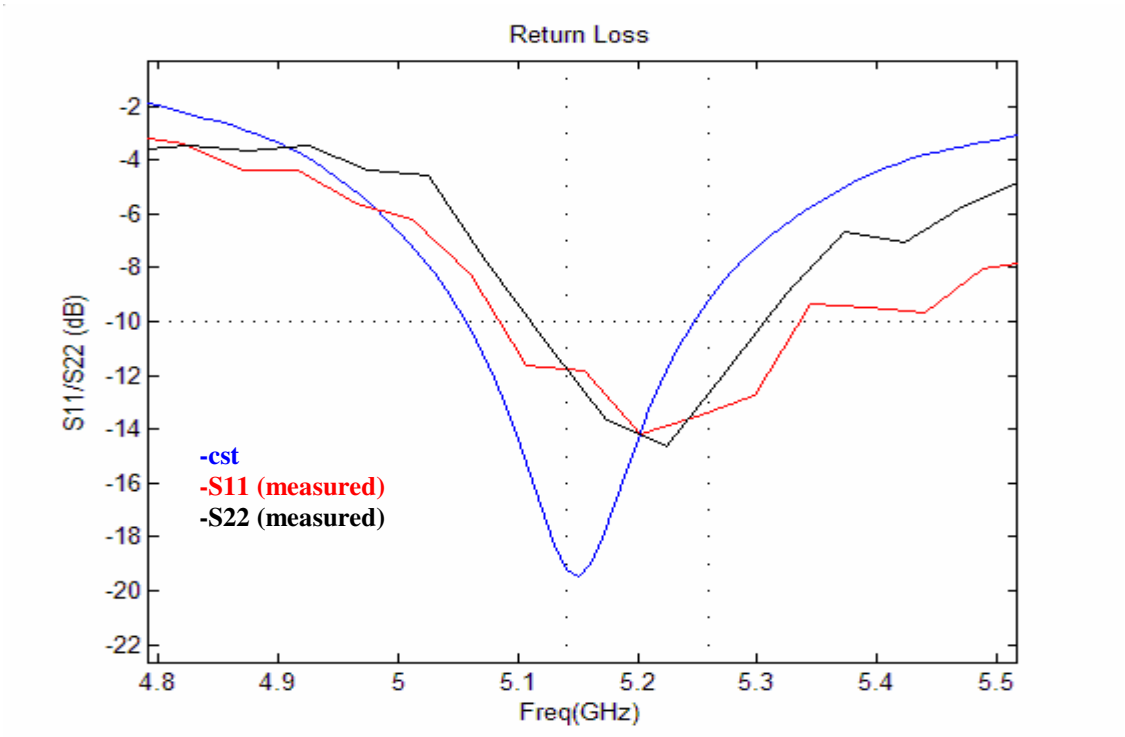

Appendix 71: Return loss of Antenna 1 and Antenna 2

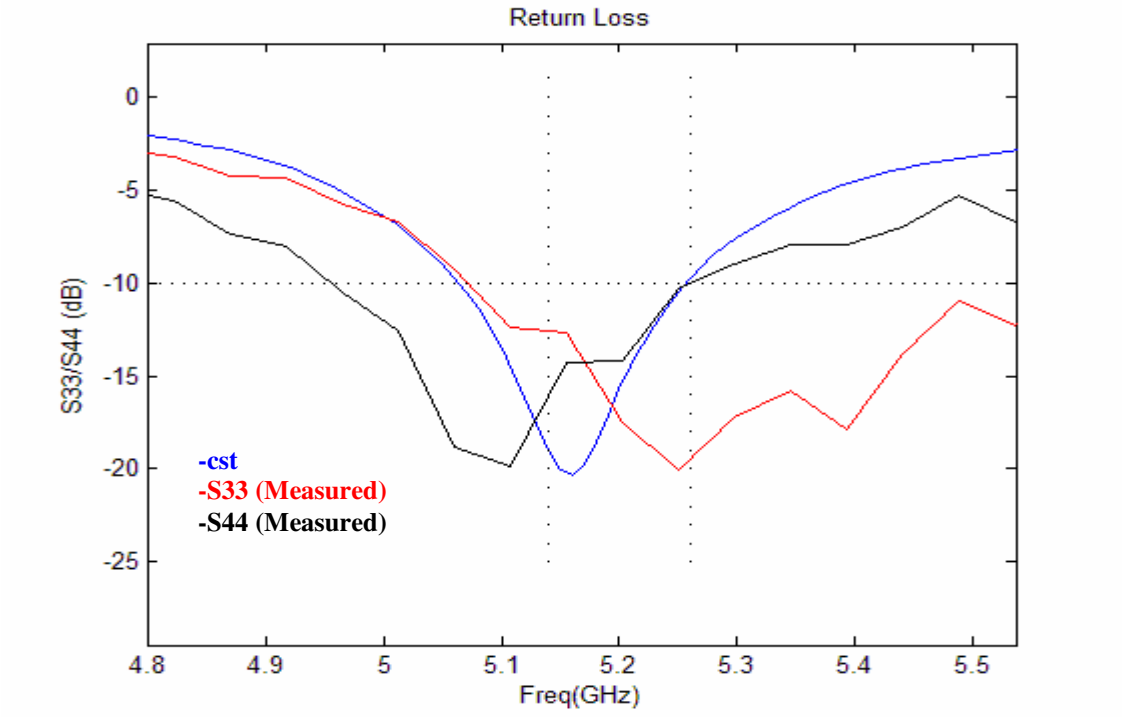

Appendix 72: Return loss of Antenna 3 and Antenna 4

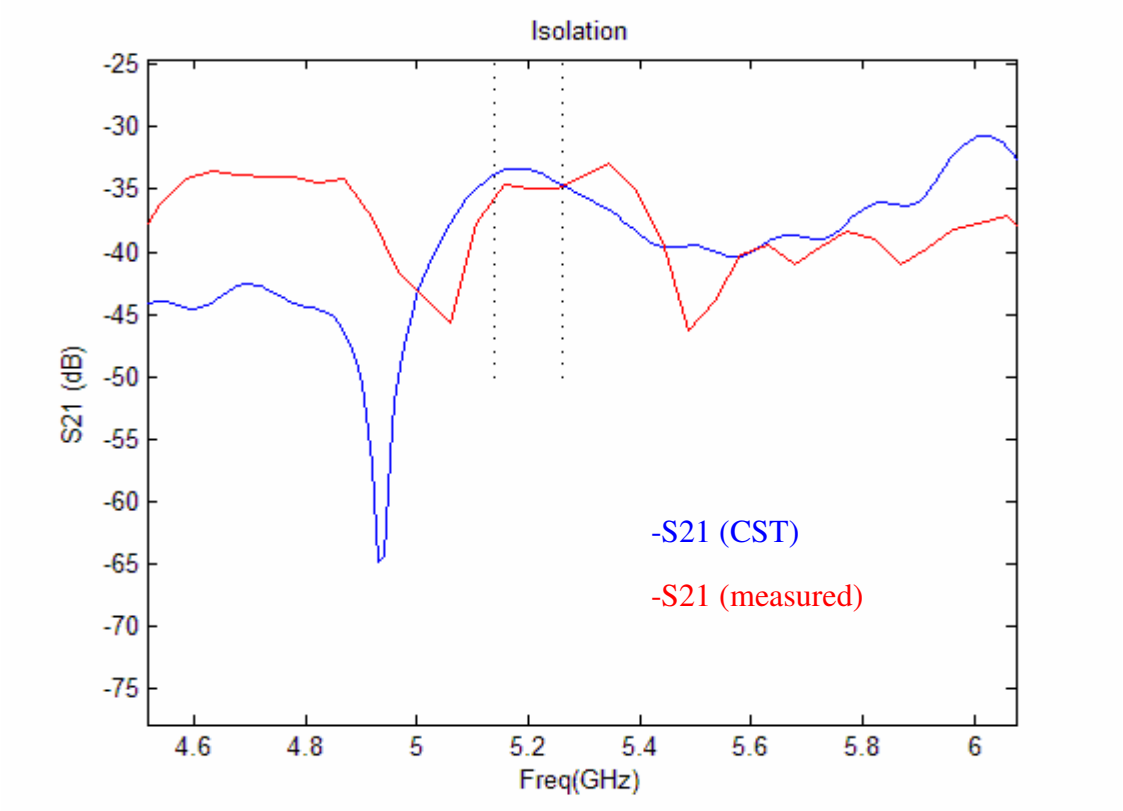

Appendix 73: Isolation between Antenna 1 and Antenna 2

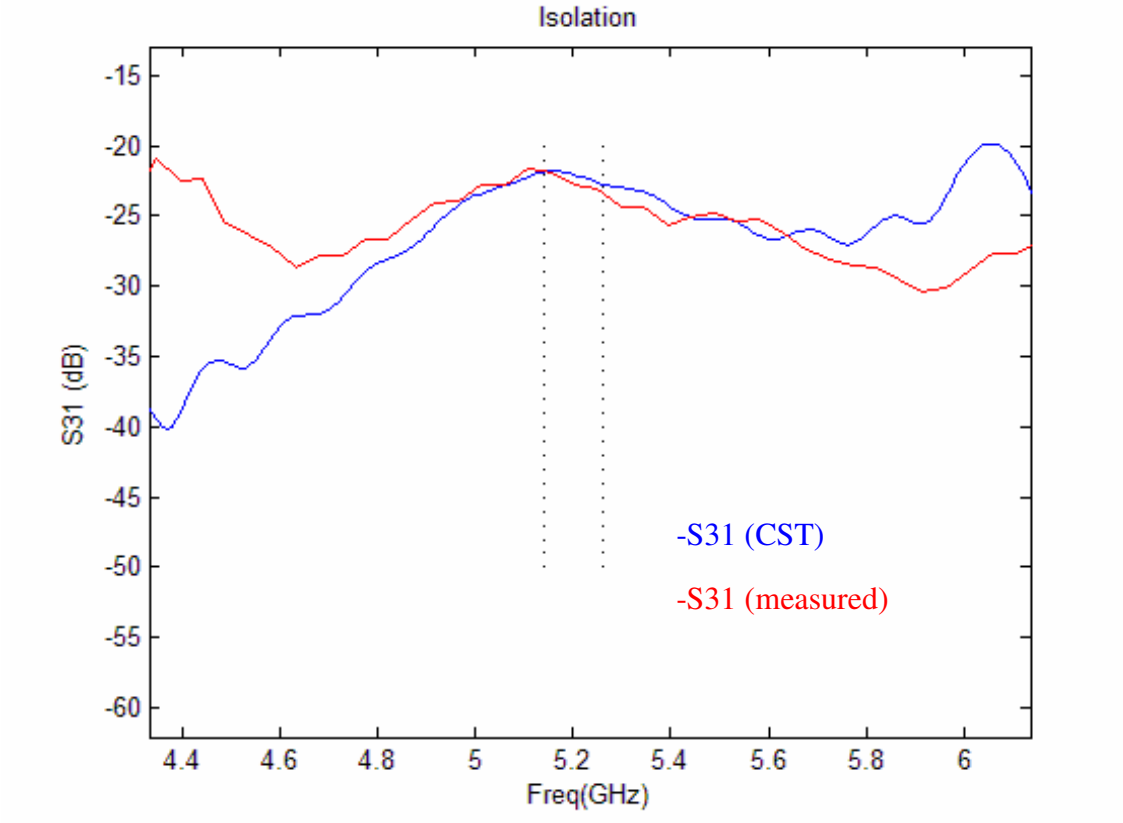

Appendix 74: Isolation between Antenna 1 and Antenna 3

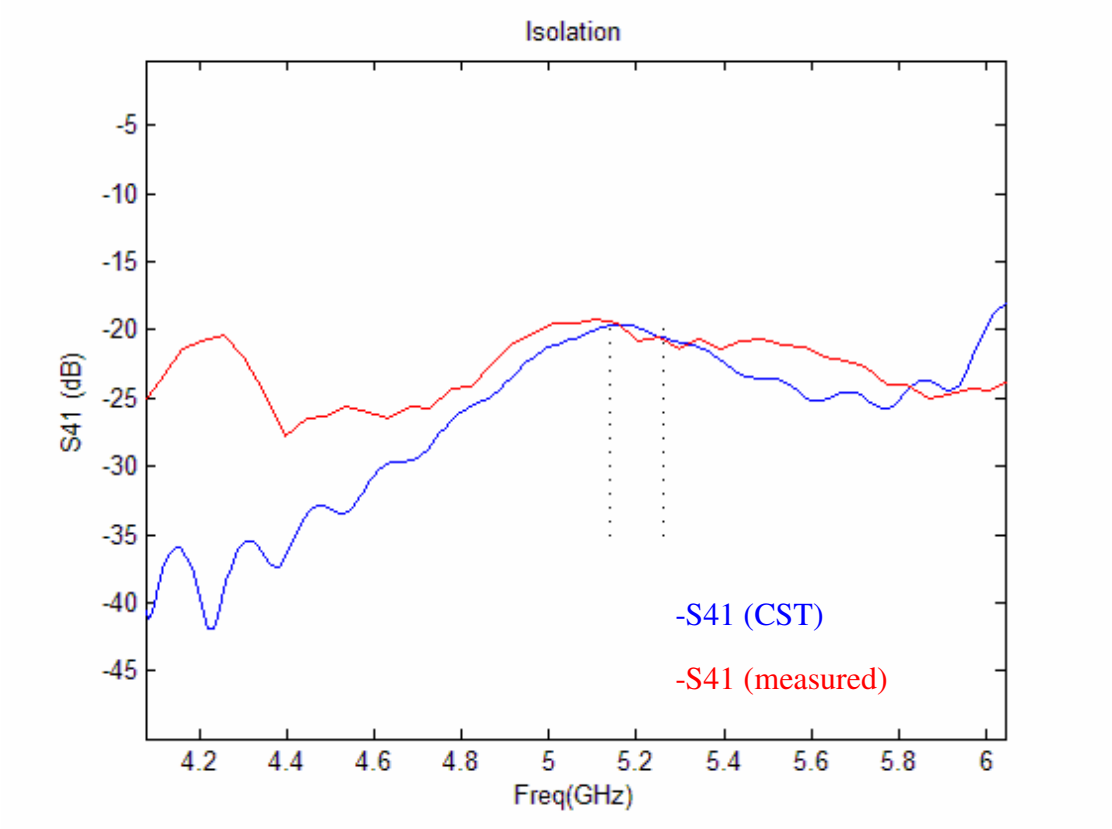

Appendix 75: Isolation between Antenna 1 and Antenna 4

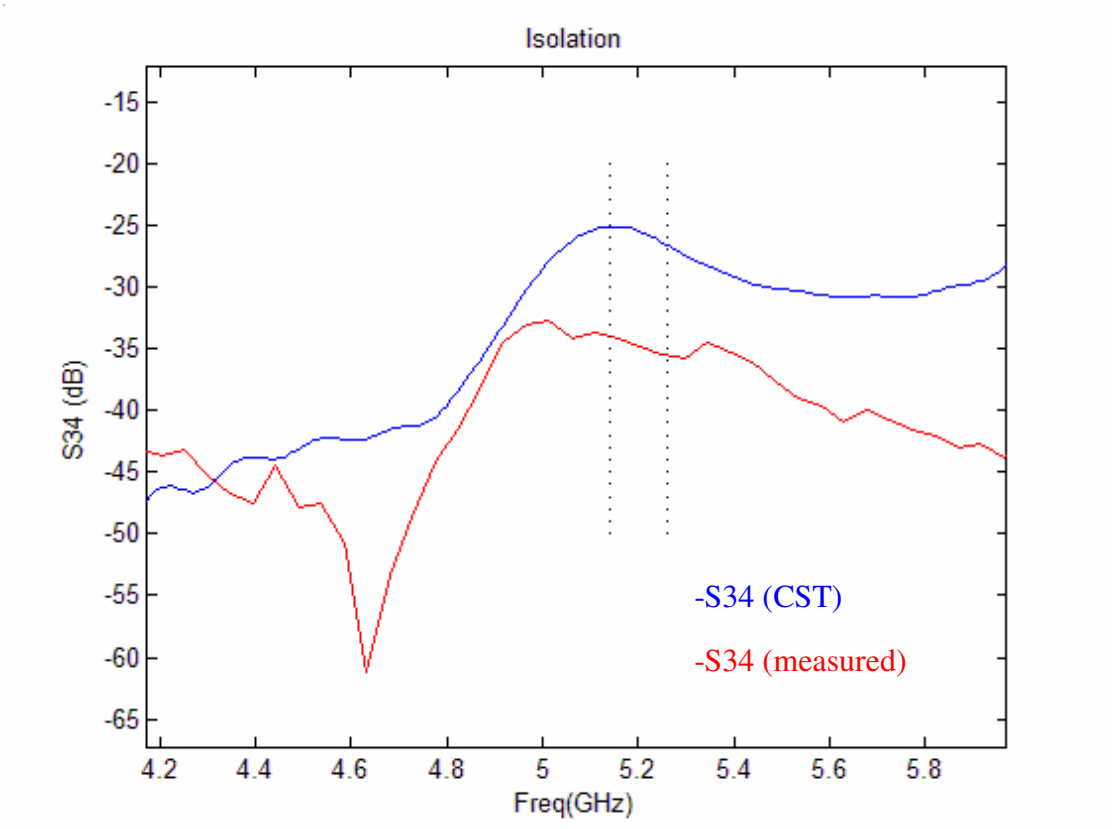

Appendix 76 :Isolation between Antenna 3 and Antenna 4

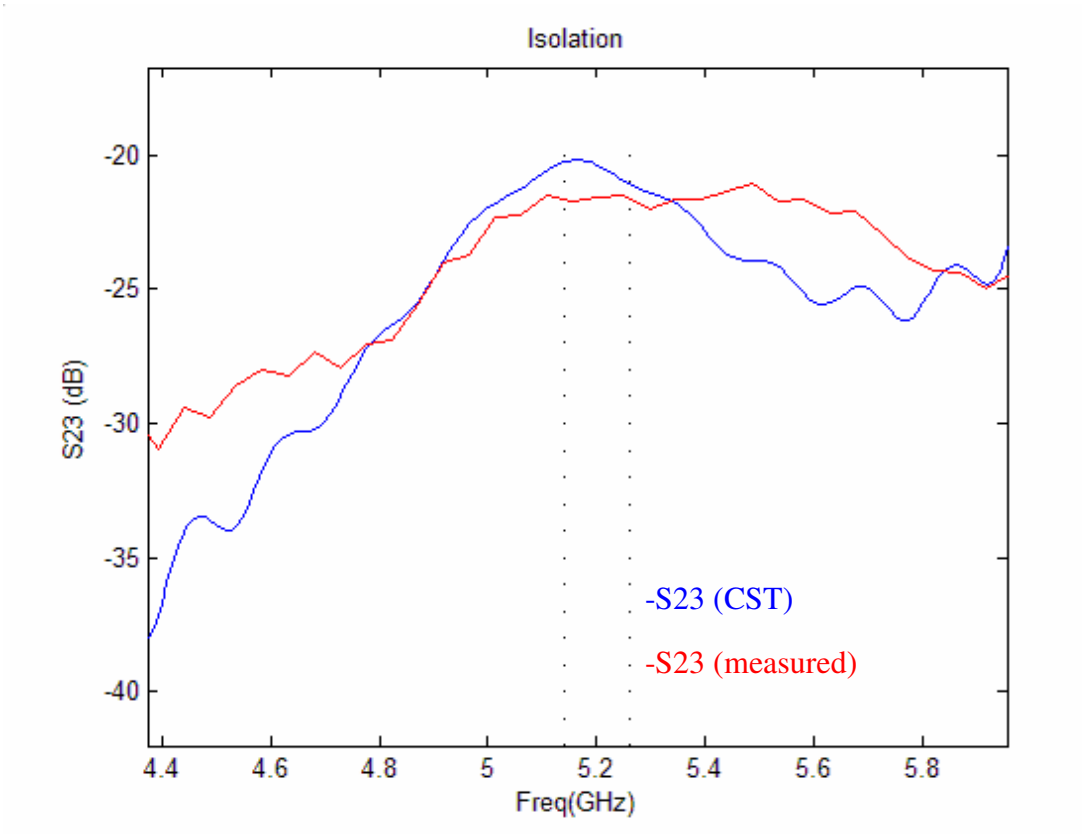

Appendix 77: Isolation between Antenna 2 and Antenna 3

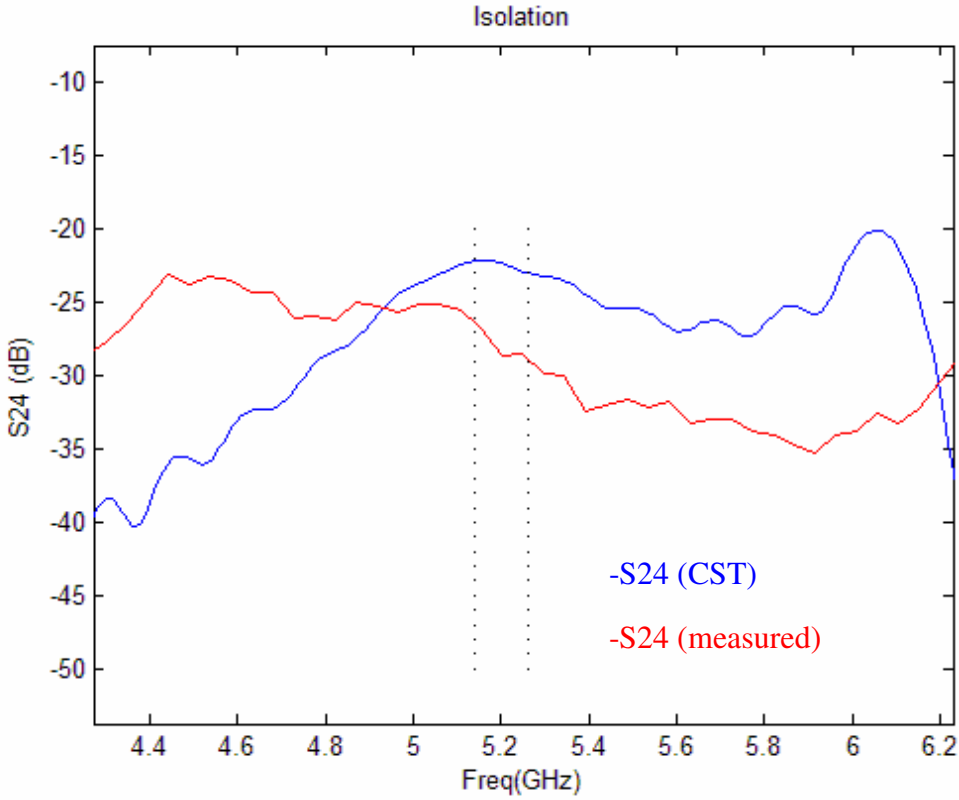

Appendix 78: Isolation between Antenna 2 and Antenna 4

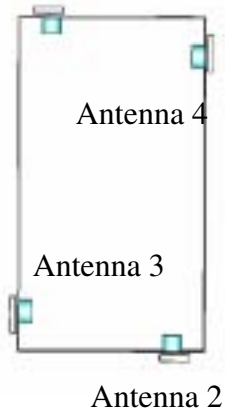

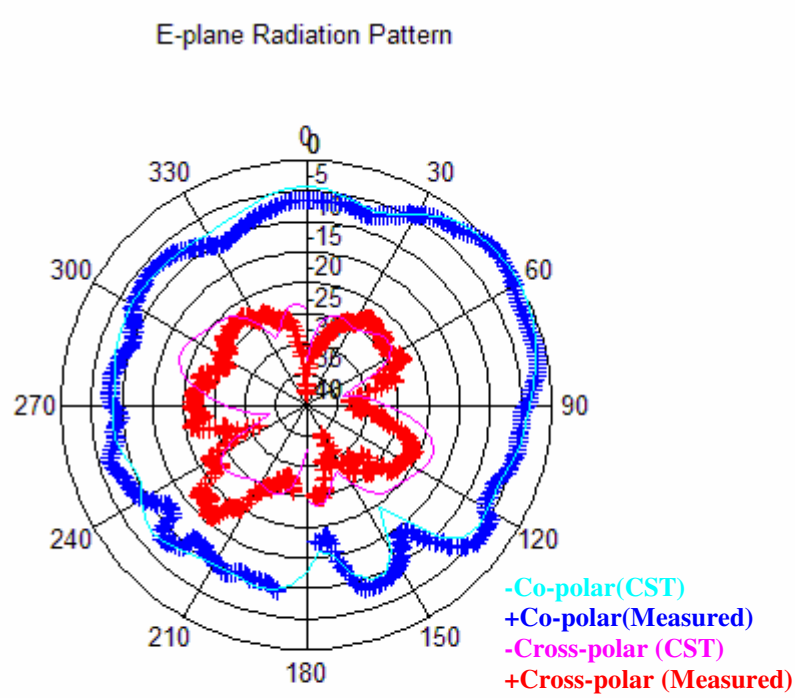

Appendix 79: Co- and cross-polar of Antenna 1

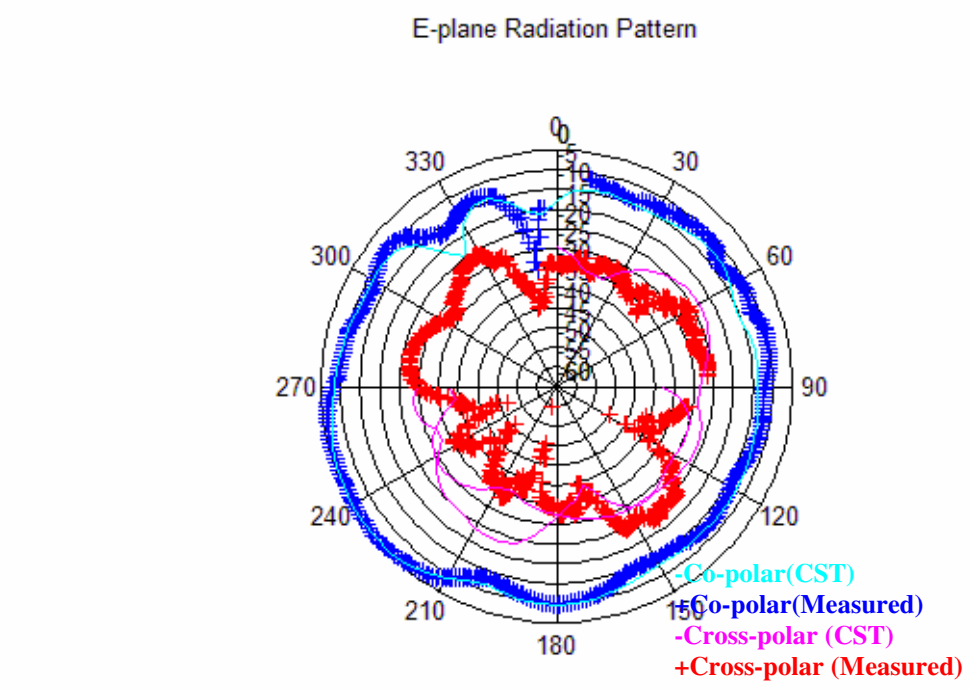

Appendix 80: Co- and cross-polar of Antenna 2

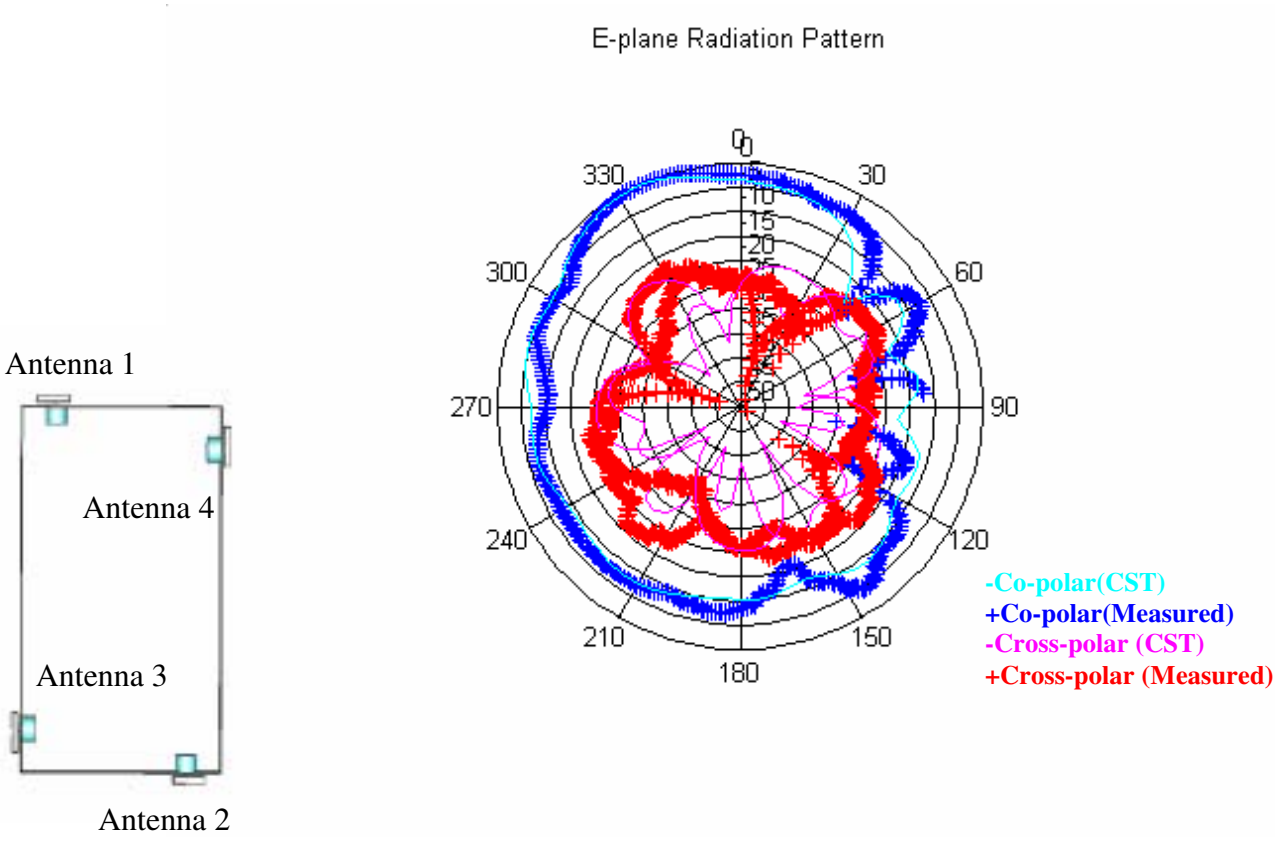

Appendix 81: Co- and cross-polar of Antenna 3

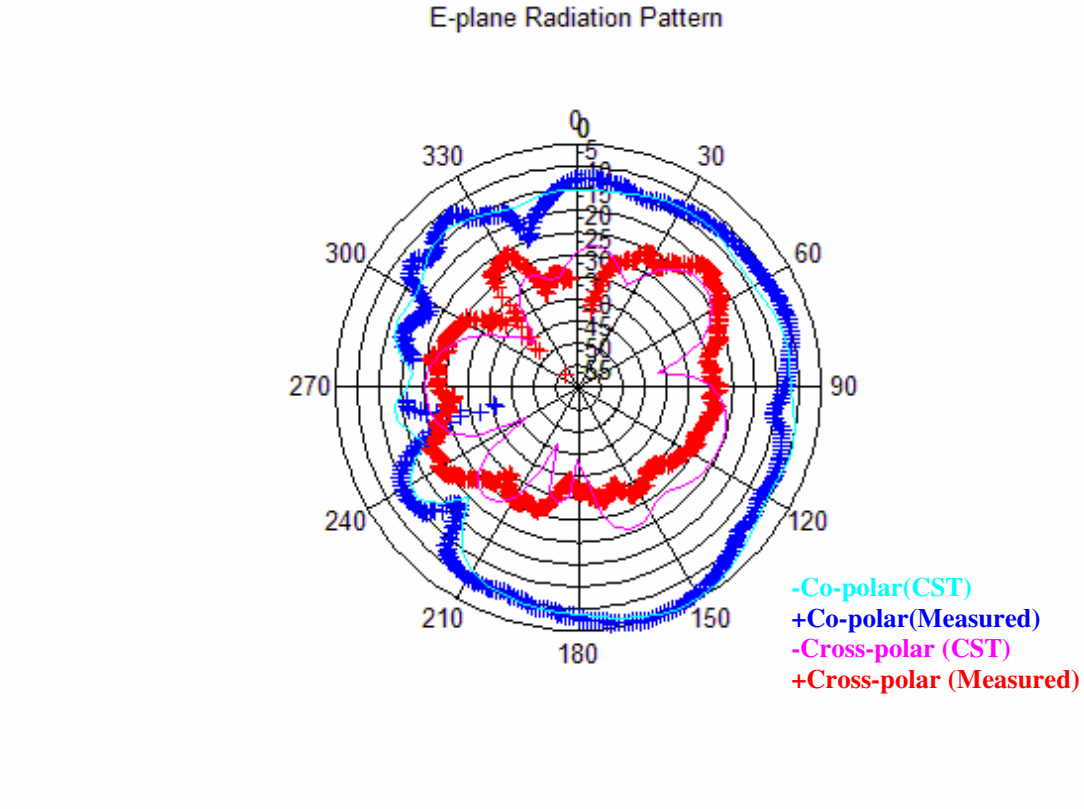

Appendix 82: Co- and cross-polar of Antenna 4

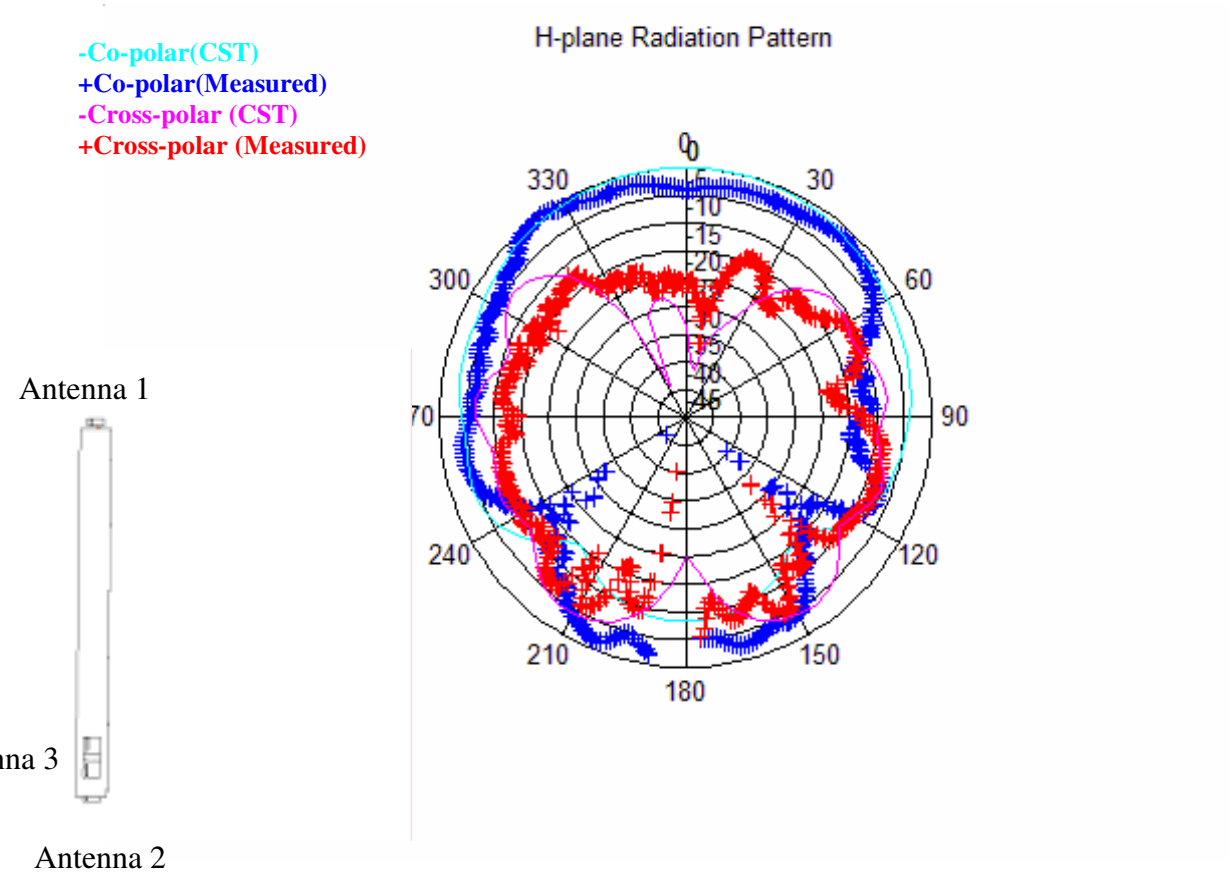

Appendix 83: Co- and cross-polar of Antenna 1

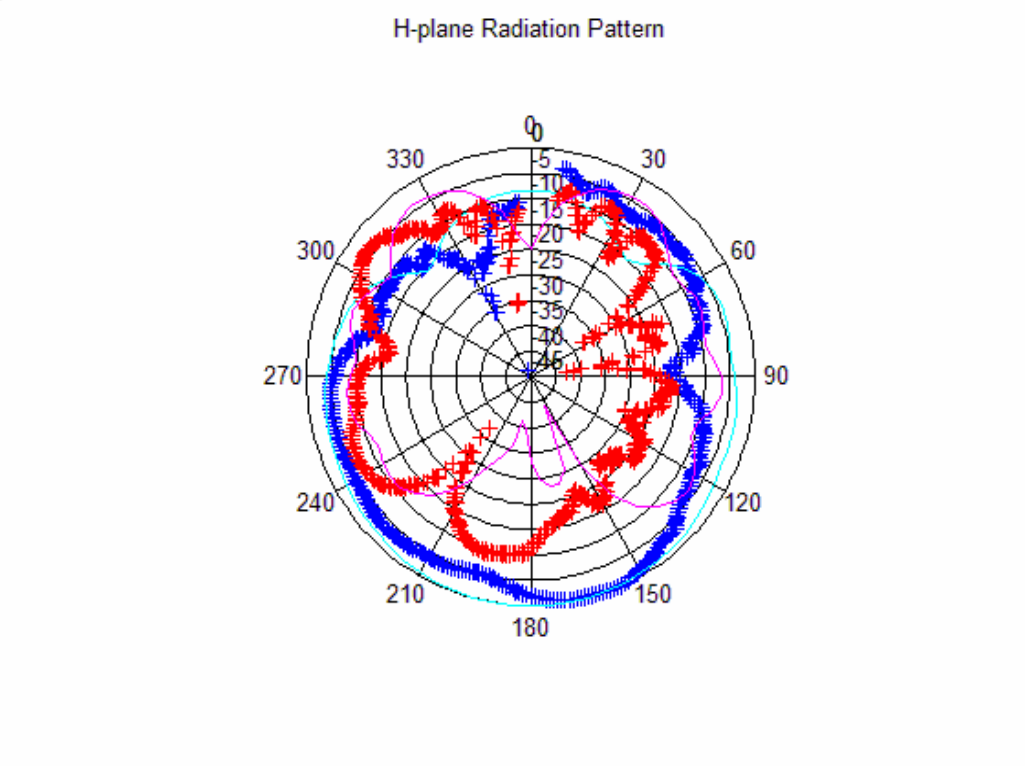

Appendix 84: Co- and cross-polar of Antenna 2

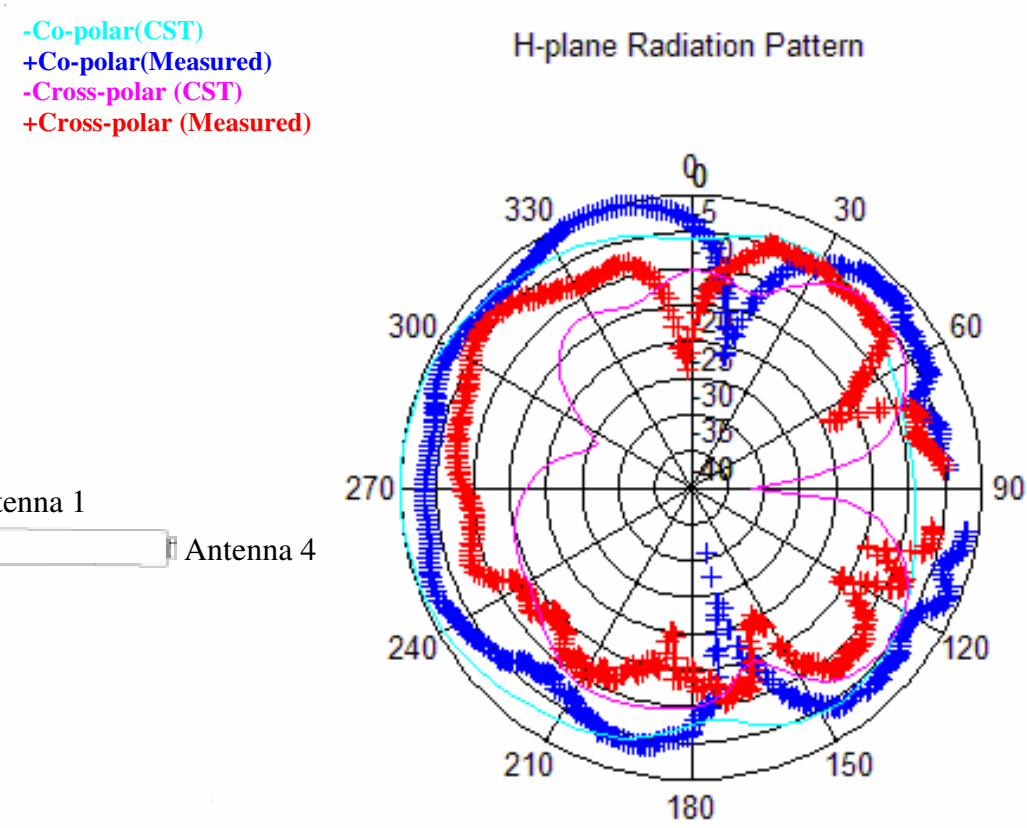

Antenna 1

Antenna 3 Antenna 4

Appendix 85: Co- and cross-polar of Antenna 3

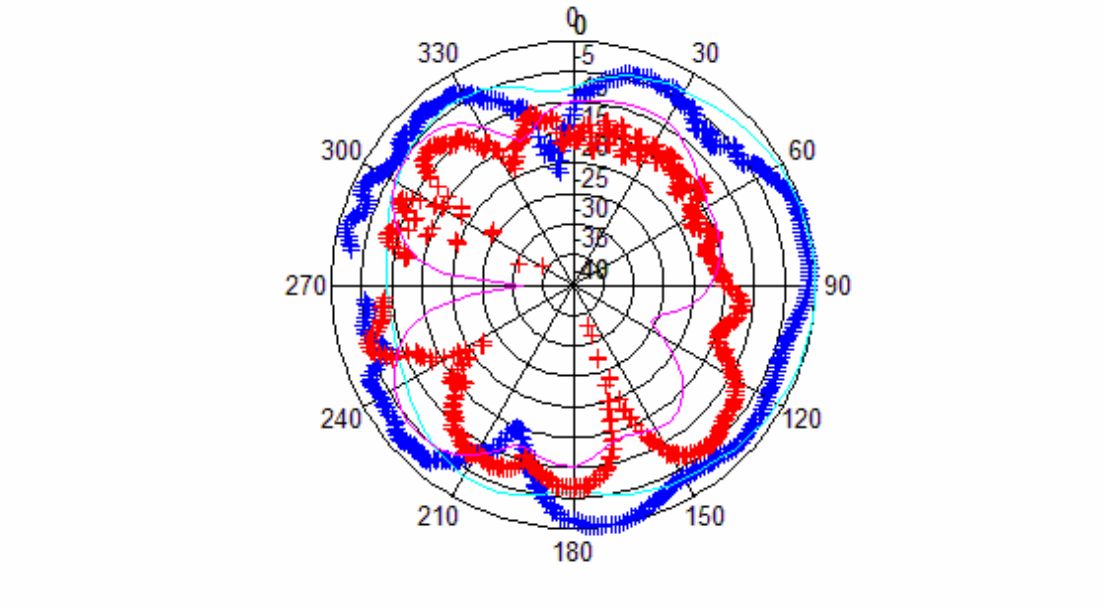

Appendix 86: Co- and cross-polar of Antenna 4

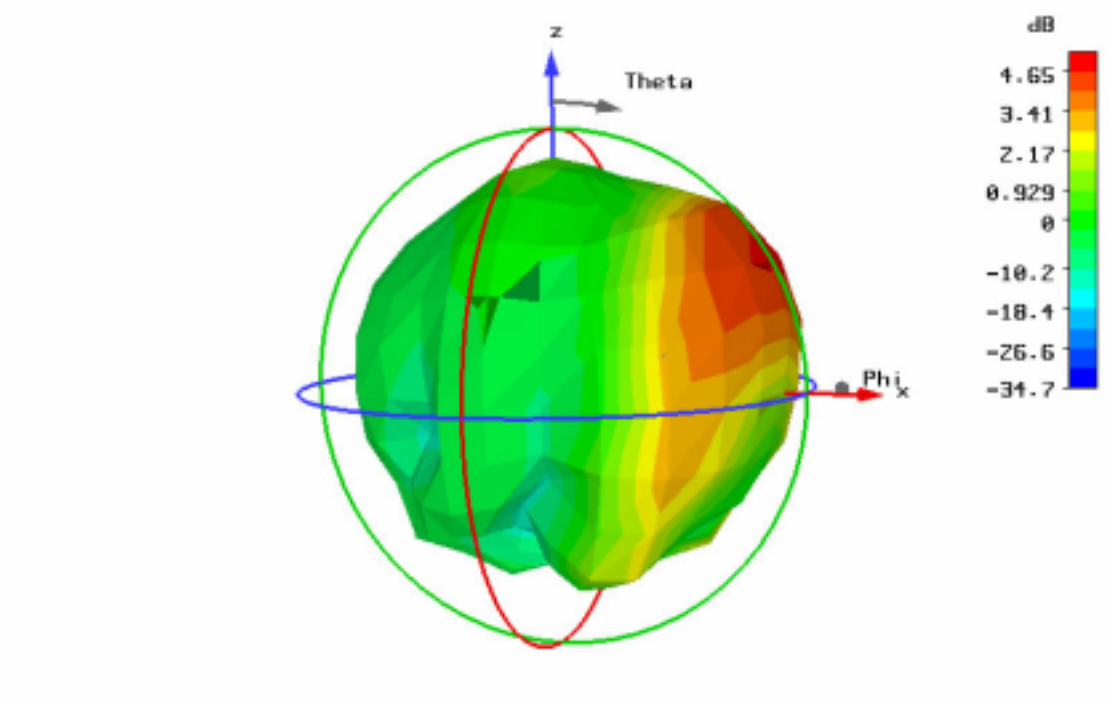

Appendix 87: 3-D co-polar of Antenna 1

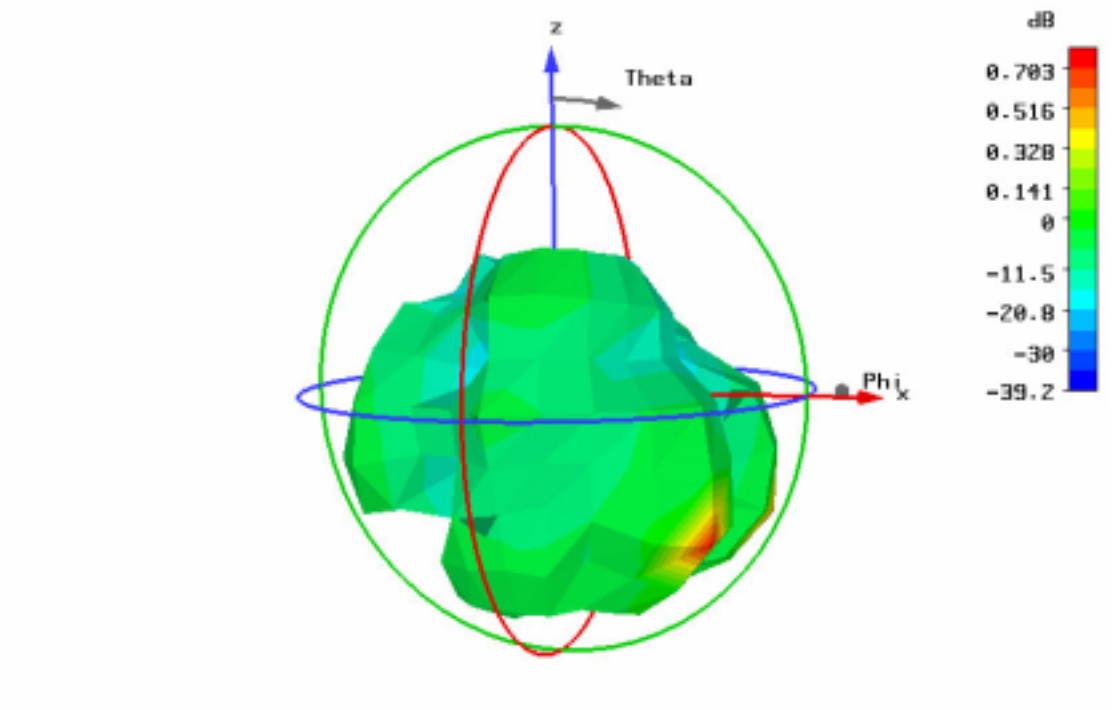

Appendix 88: 3-D cross-polar of Antenna 1

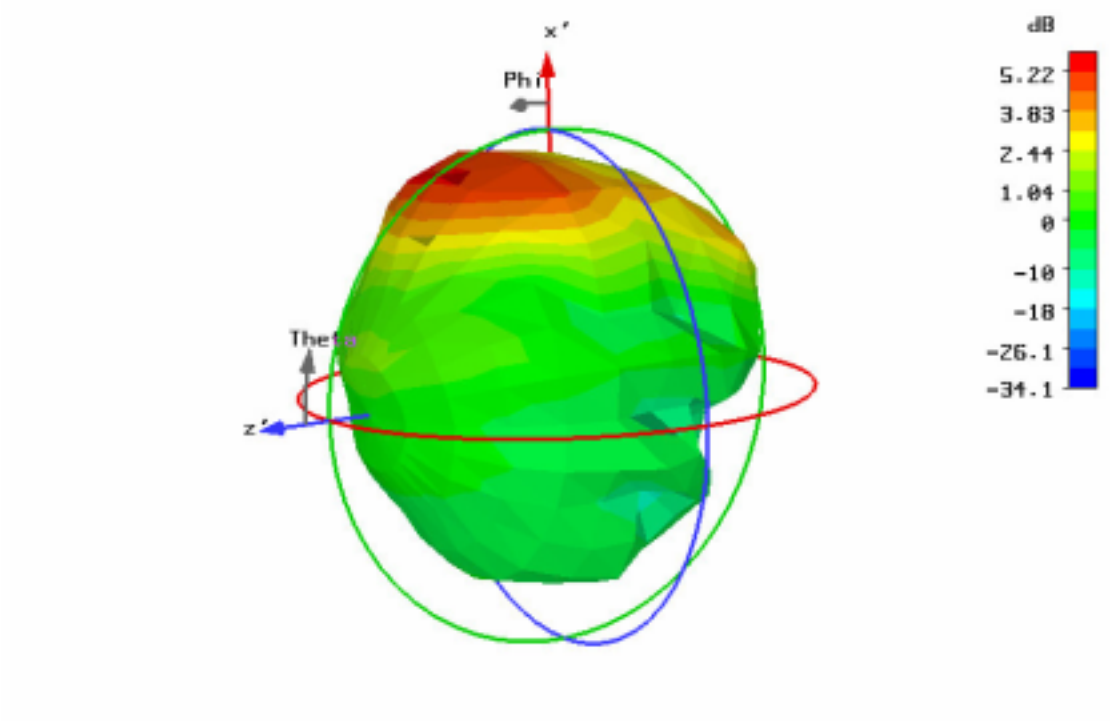

Appendix 89: 3-D co-polar of Antenna 3

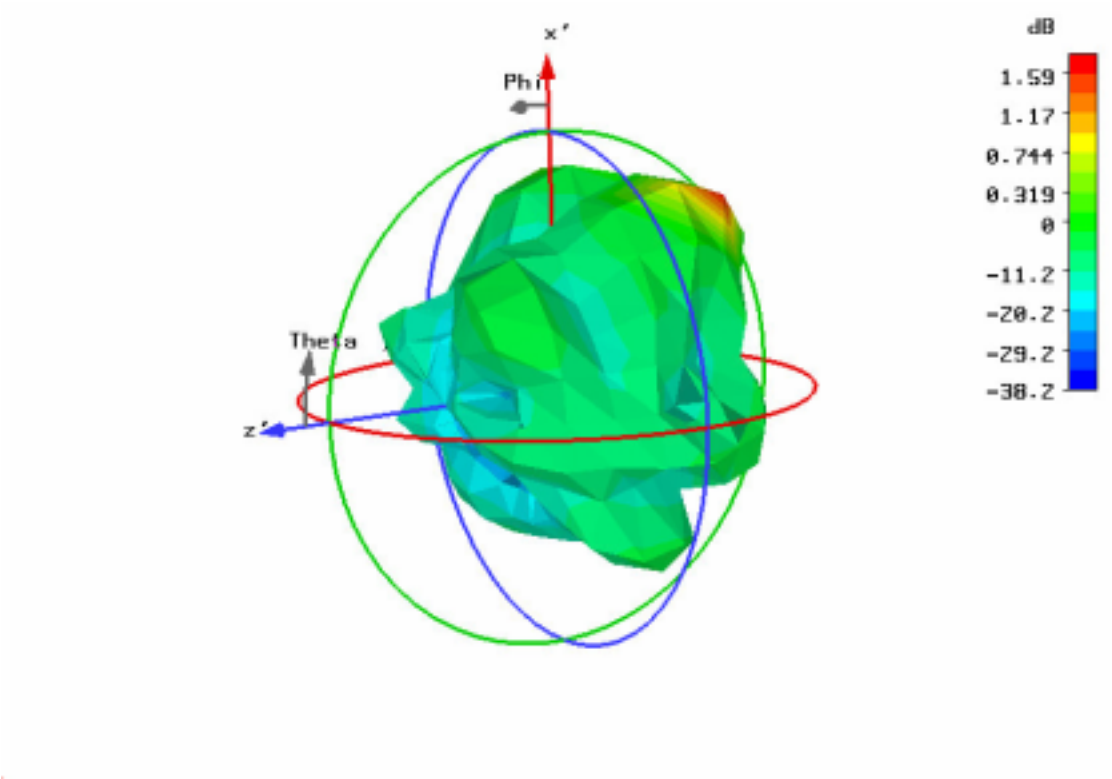

Appendix 90: 3-D cross-polar of Antenna 3

3.4 Handset Design

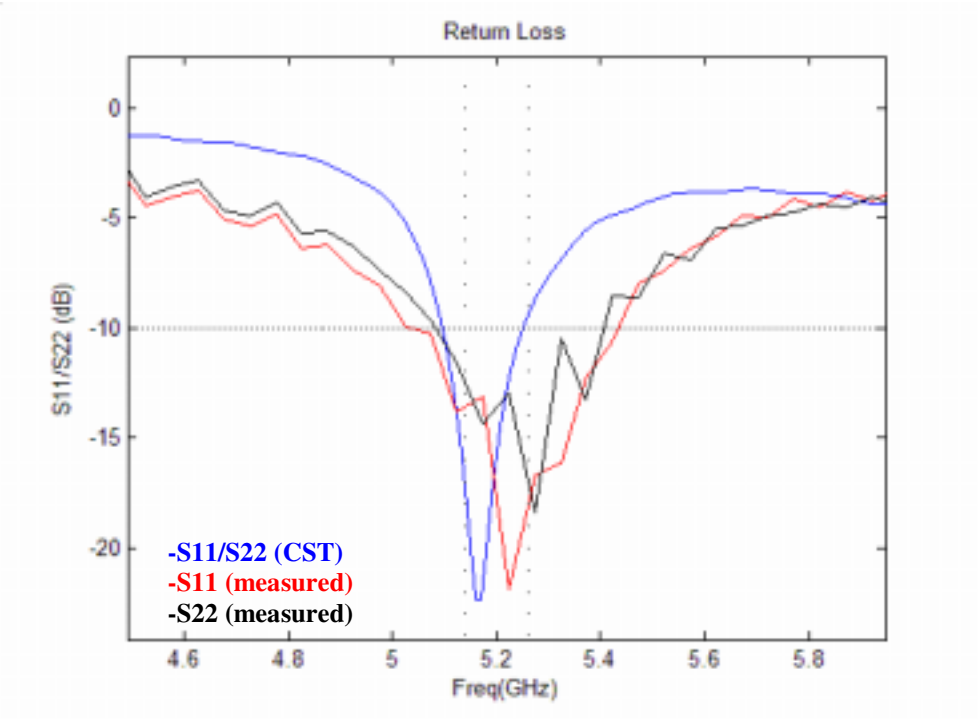

Appendix 91: Return loss of Antenna 1 and Antenna 2

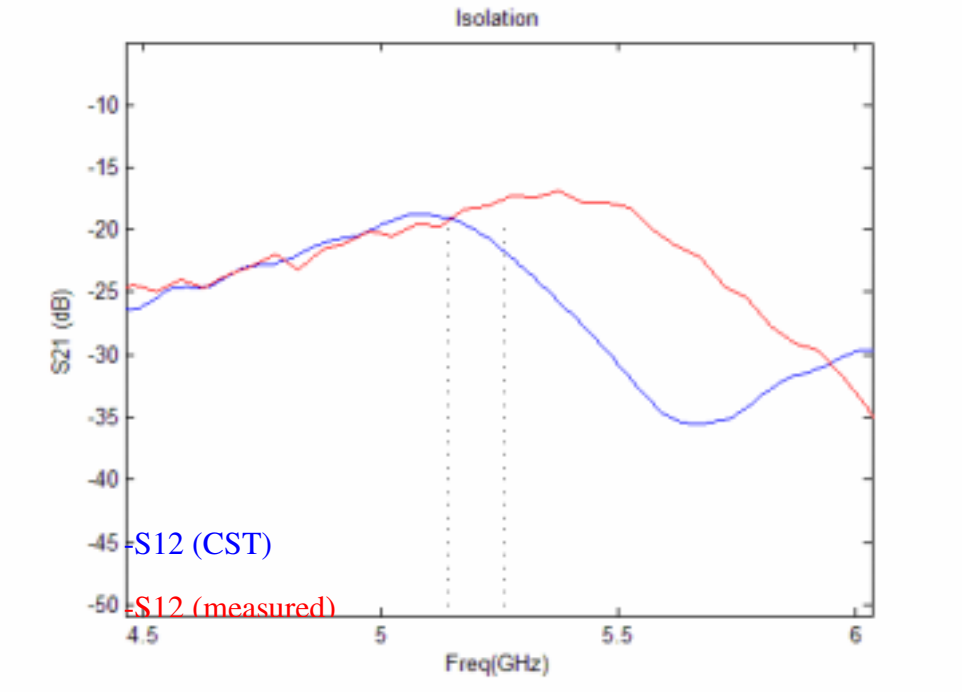

Appendix 92: Isolation between Antenna 1 and Antenna 2

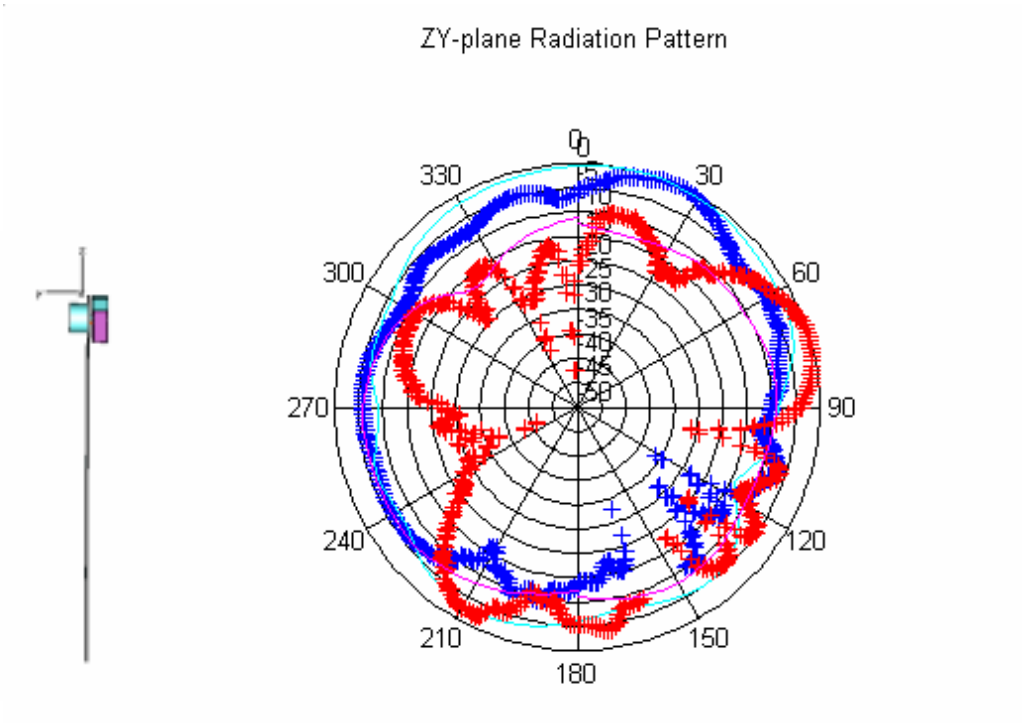

Appendix 93: Co- and cross-polar pattern of Antenna 1 in the zy-plane

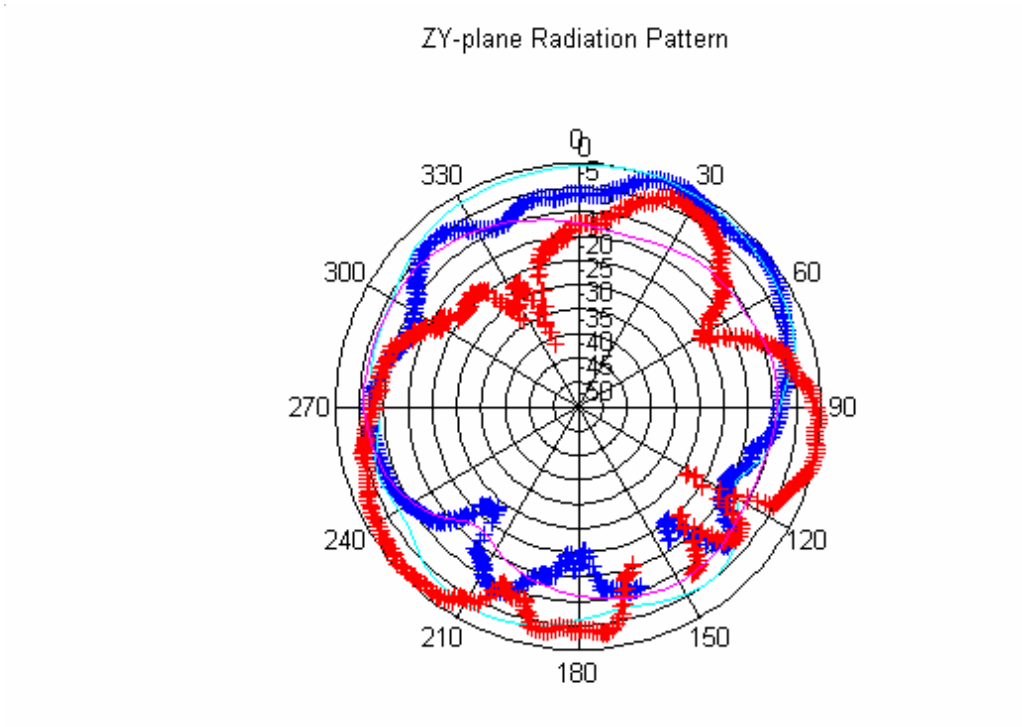

Appendix 94: Co- and cross-polar pattern of Antenna 2 in the zy-plane

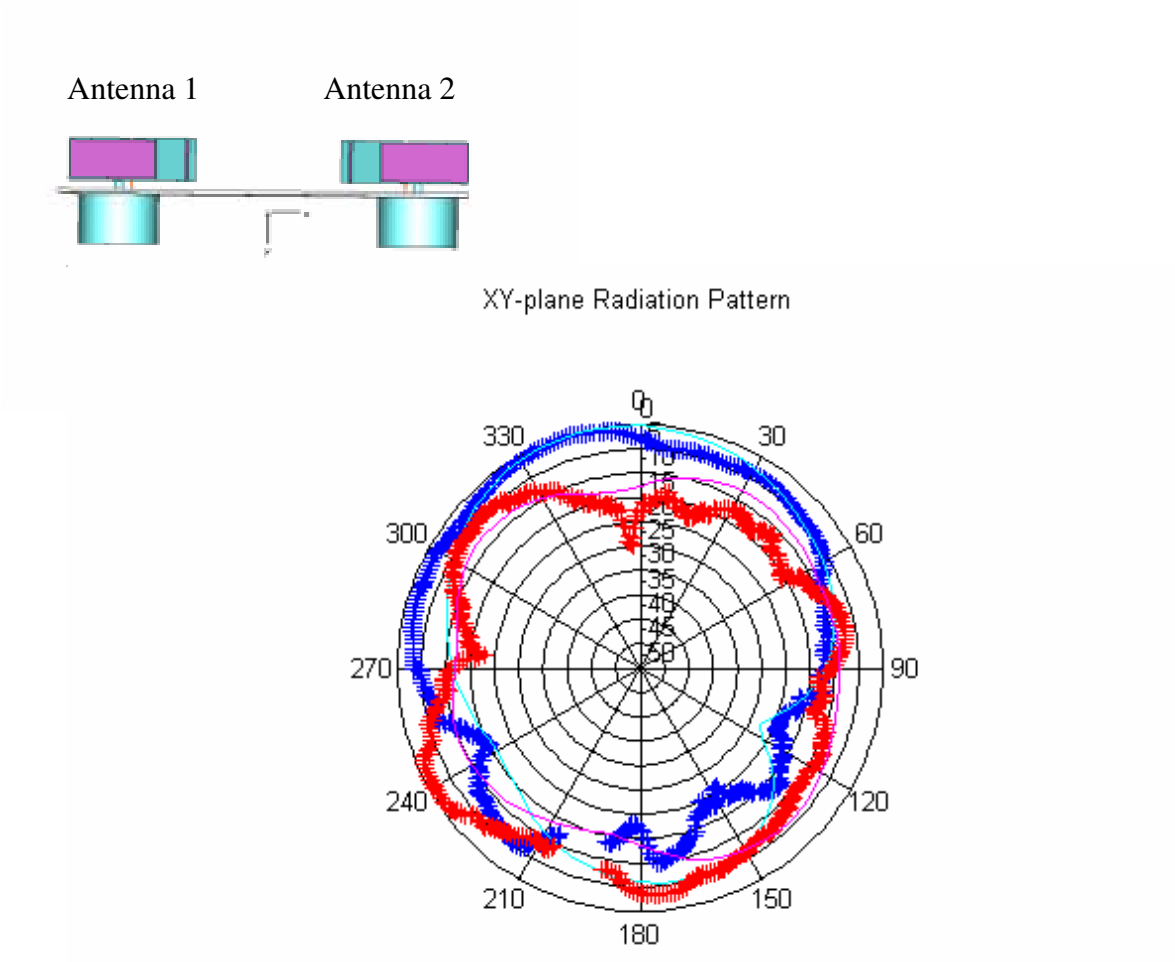

Appendix 95: Co- and cross-polar pattern of Antenna 1 in the xy-plane

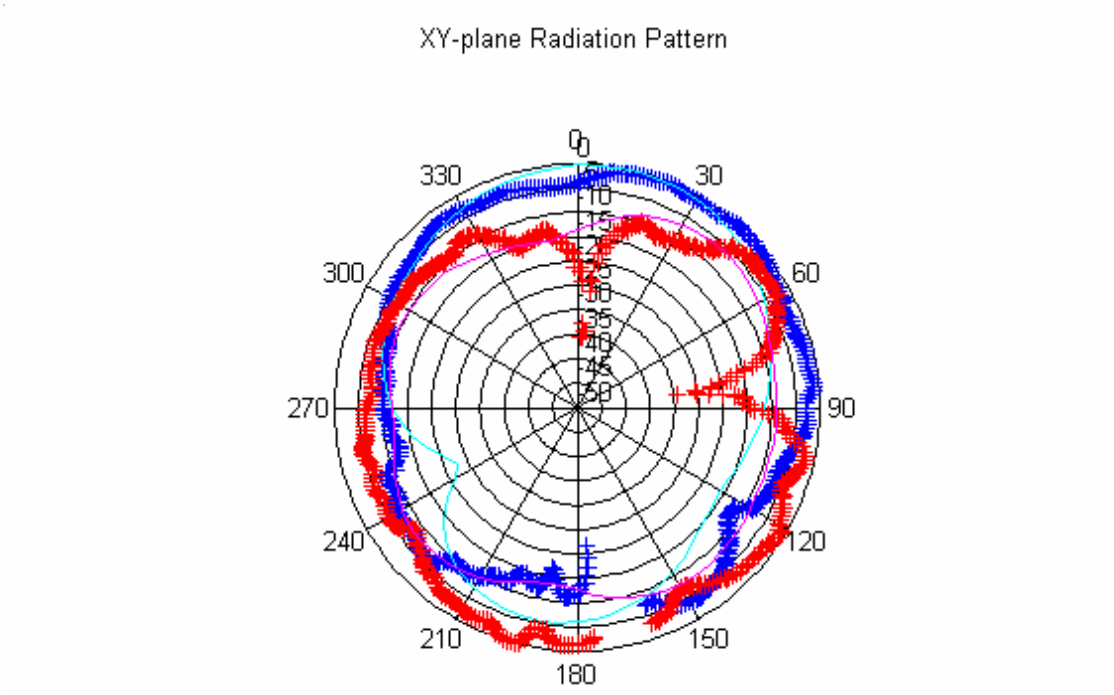

Appendix 96: Co- and cross-polar pattern of Antenna 2 in the xy-plane

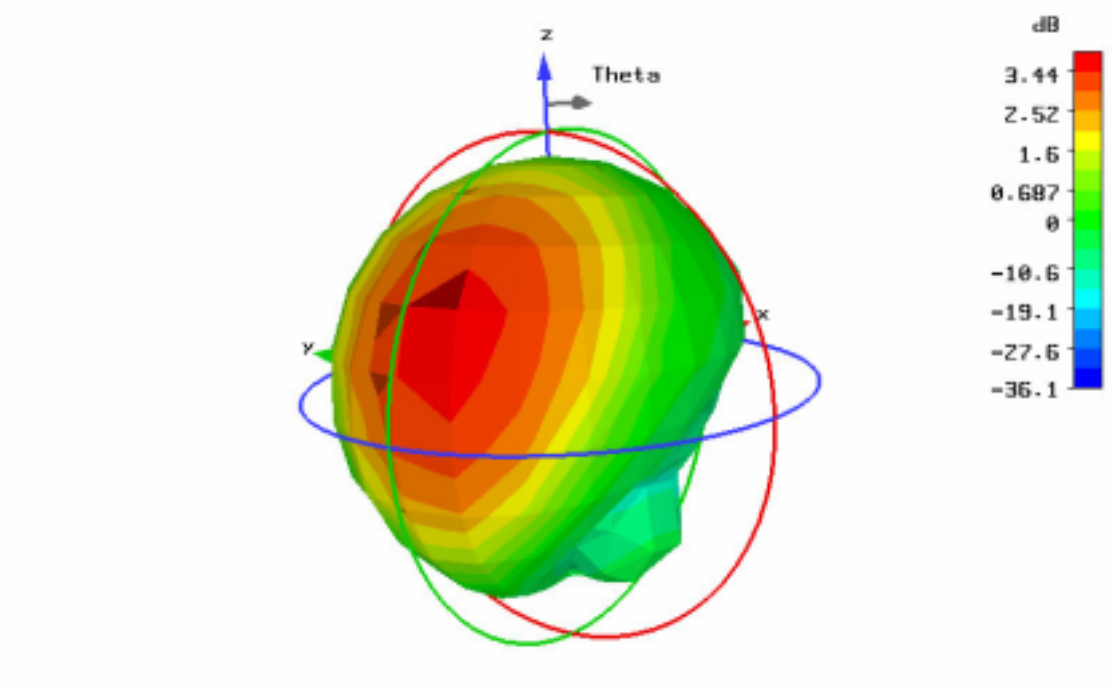

Appendix 97: 3-D co-polar pattern of Antenna 1

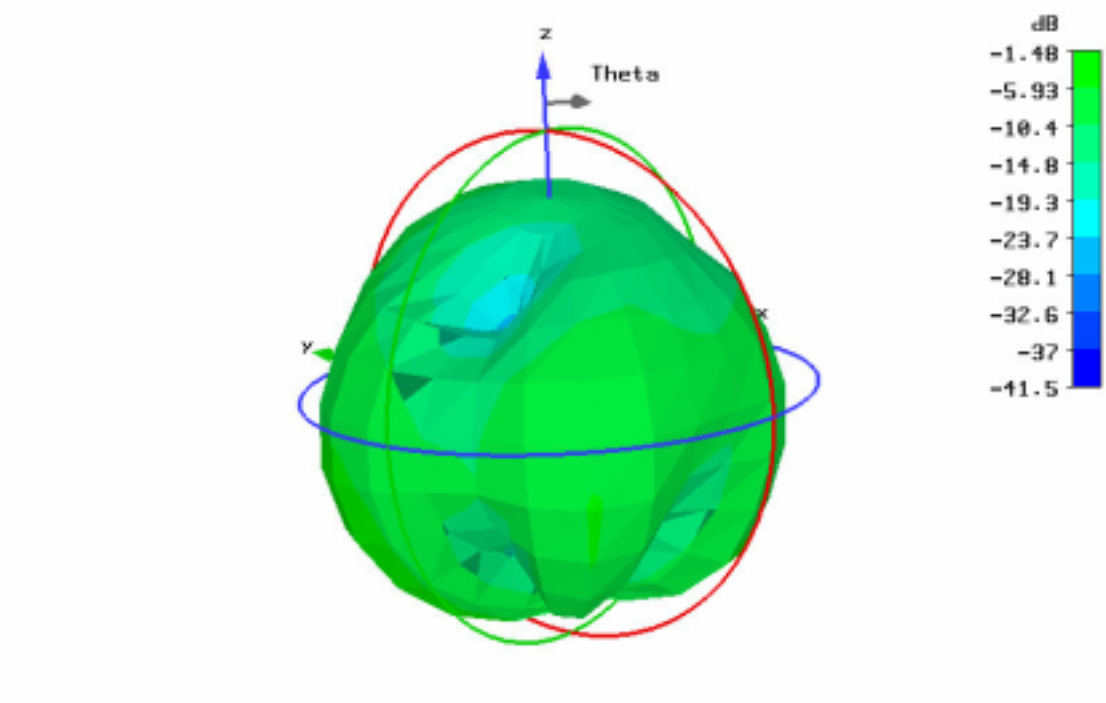

Appendix 98: 3-D cross-polar pattern of Antenna 1

3.5 Electromagnetic Band-Gap

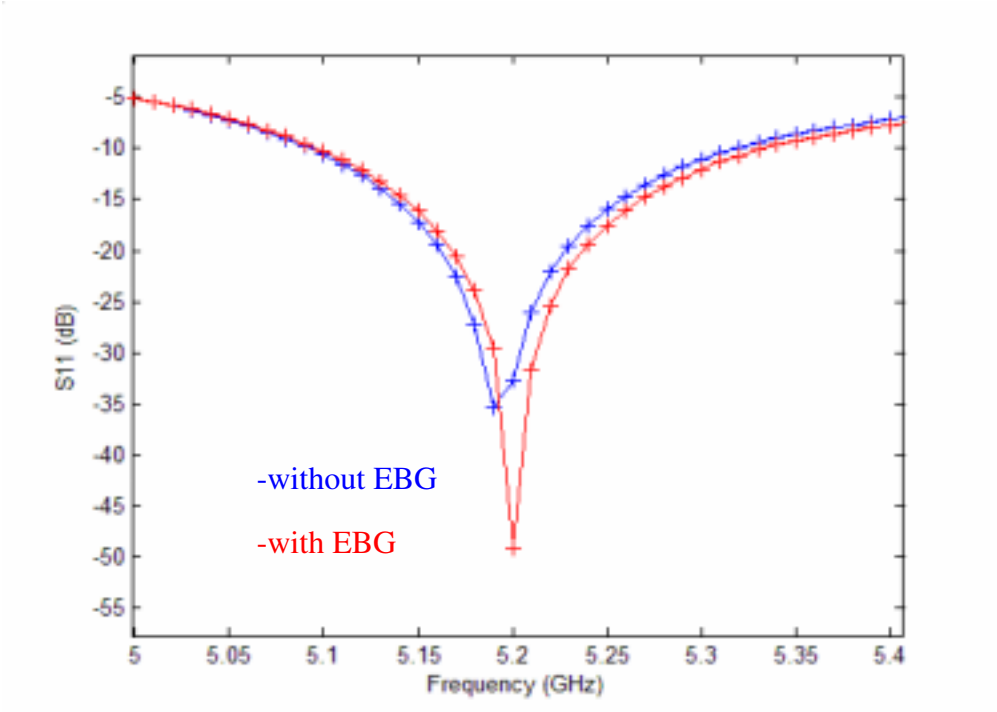

Appendix 99 :S11

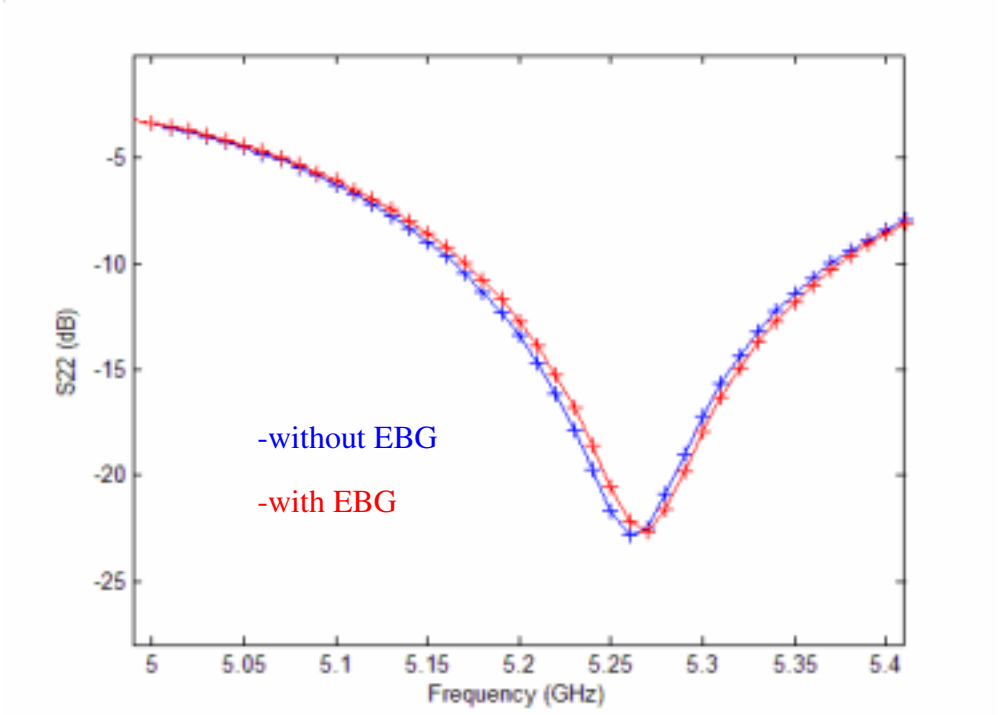

Appendix 100: S22

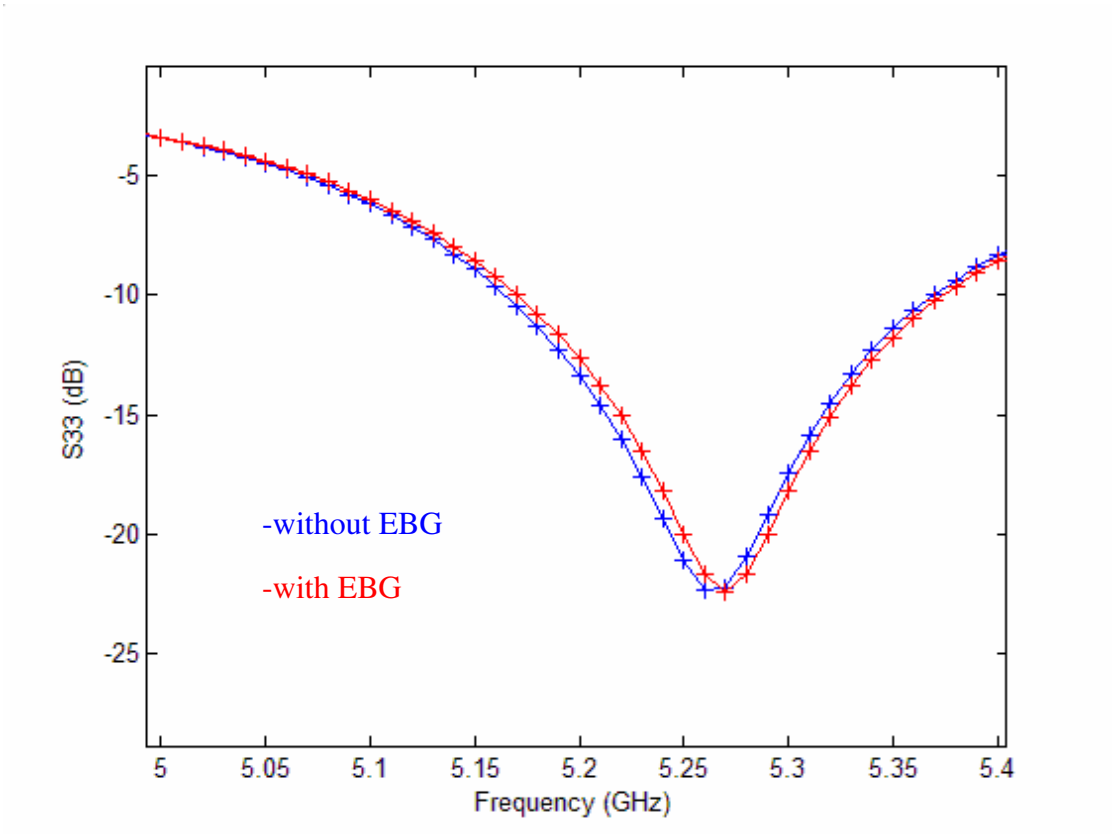

Appendix 101: S33

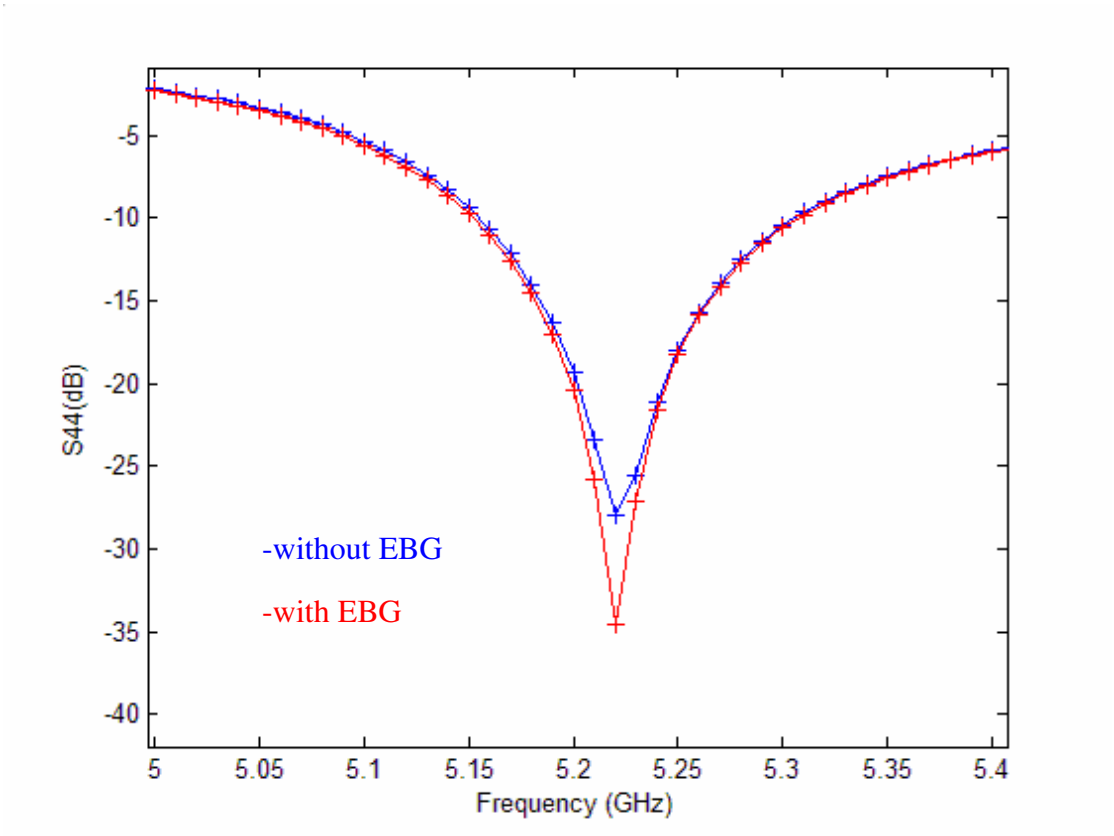

Appendix 102: S44

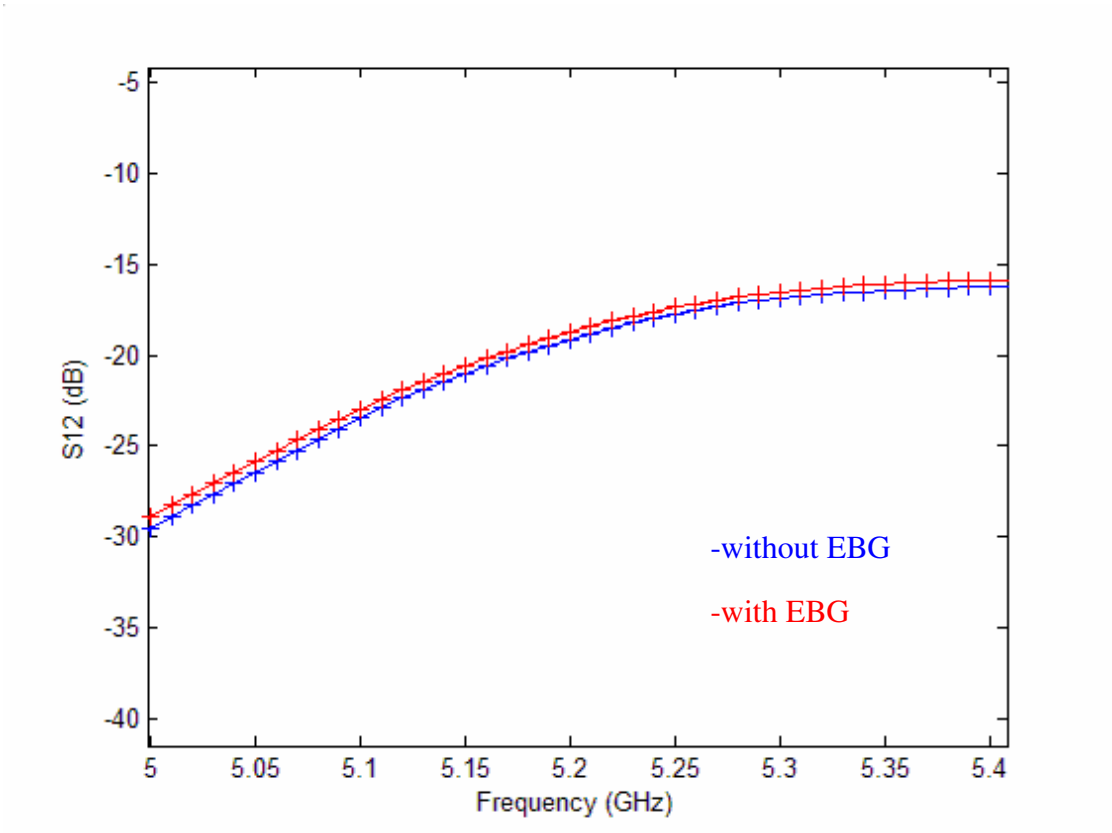

Appendix 103: S12

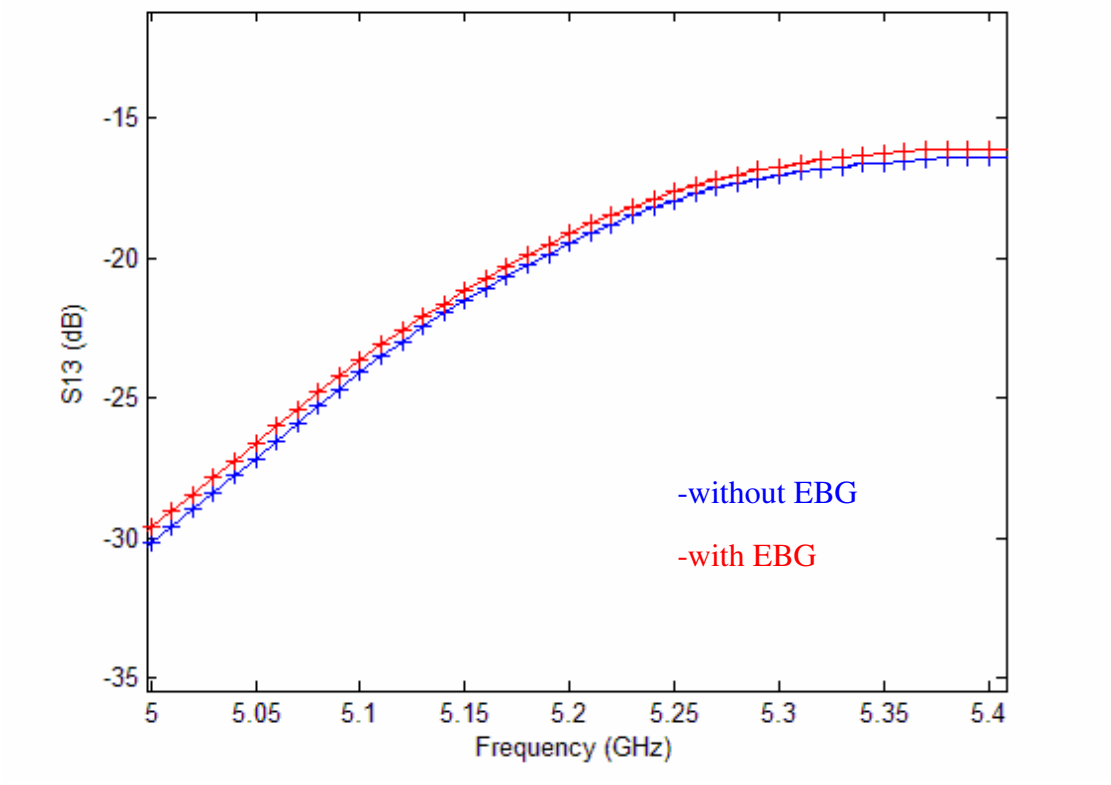

Appendix 104: S13

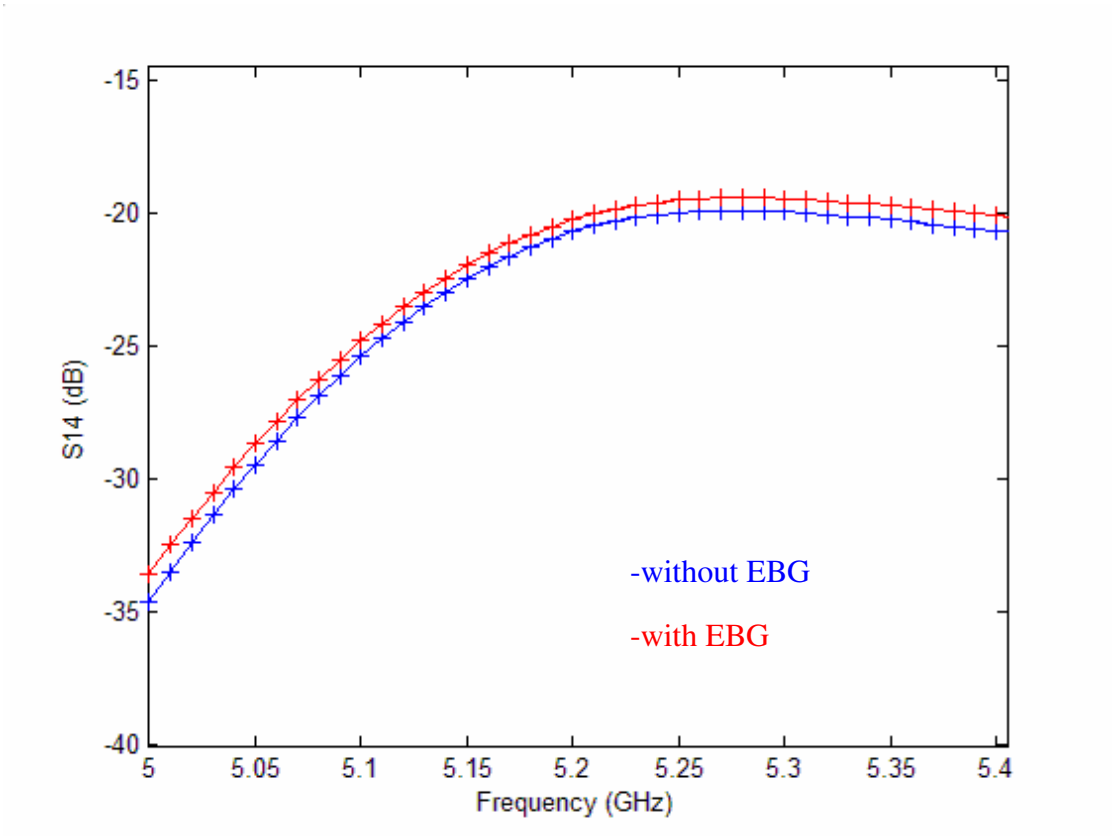

Appendix 105: S14

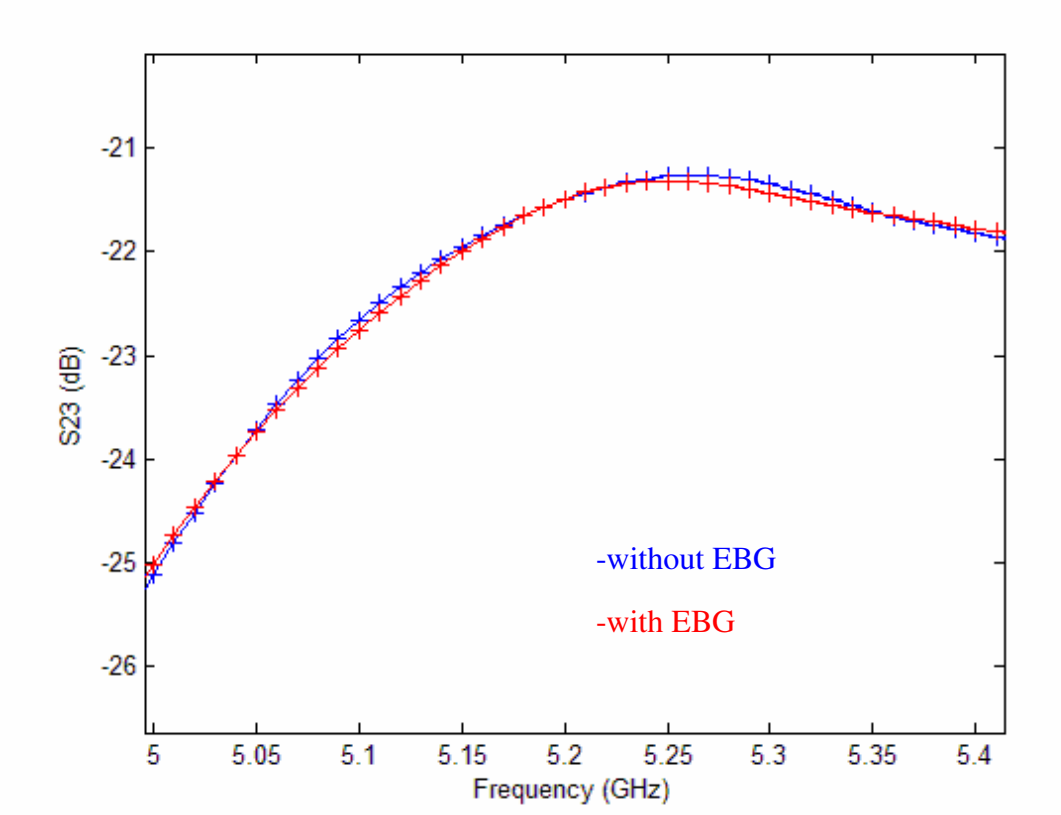

Appendix 106: S23

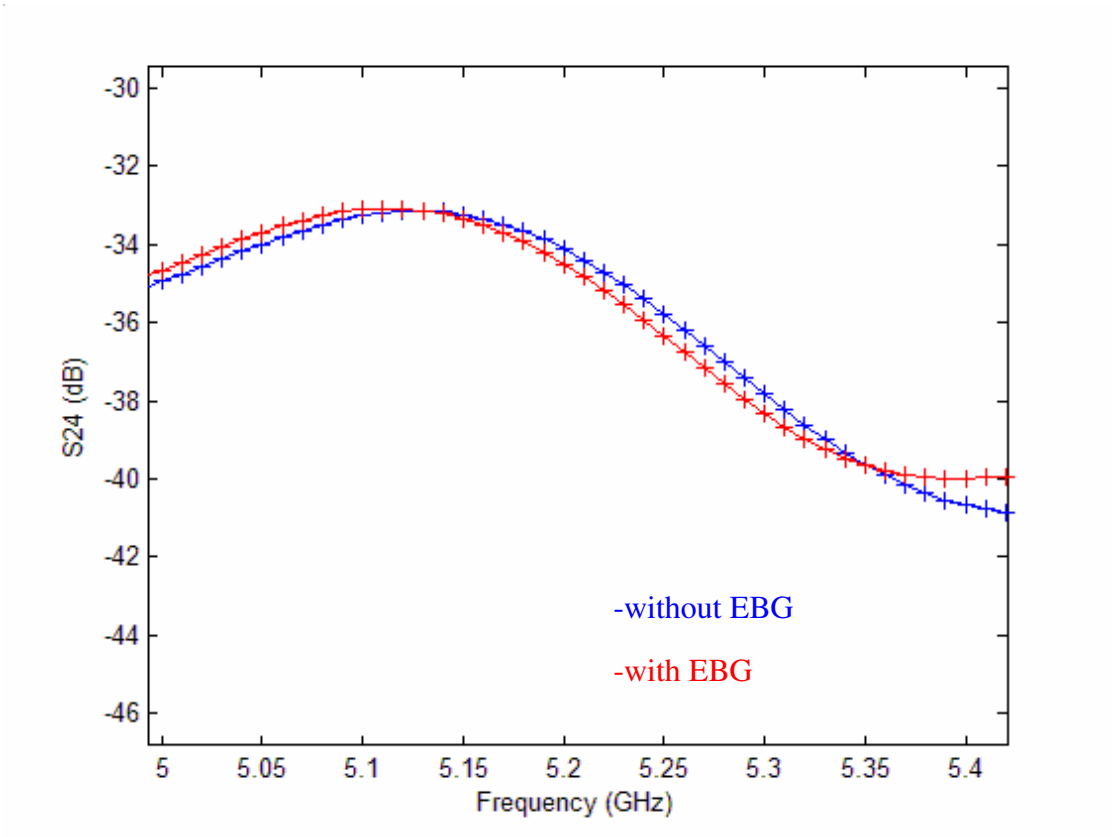

Appendix 107: S24

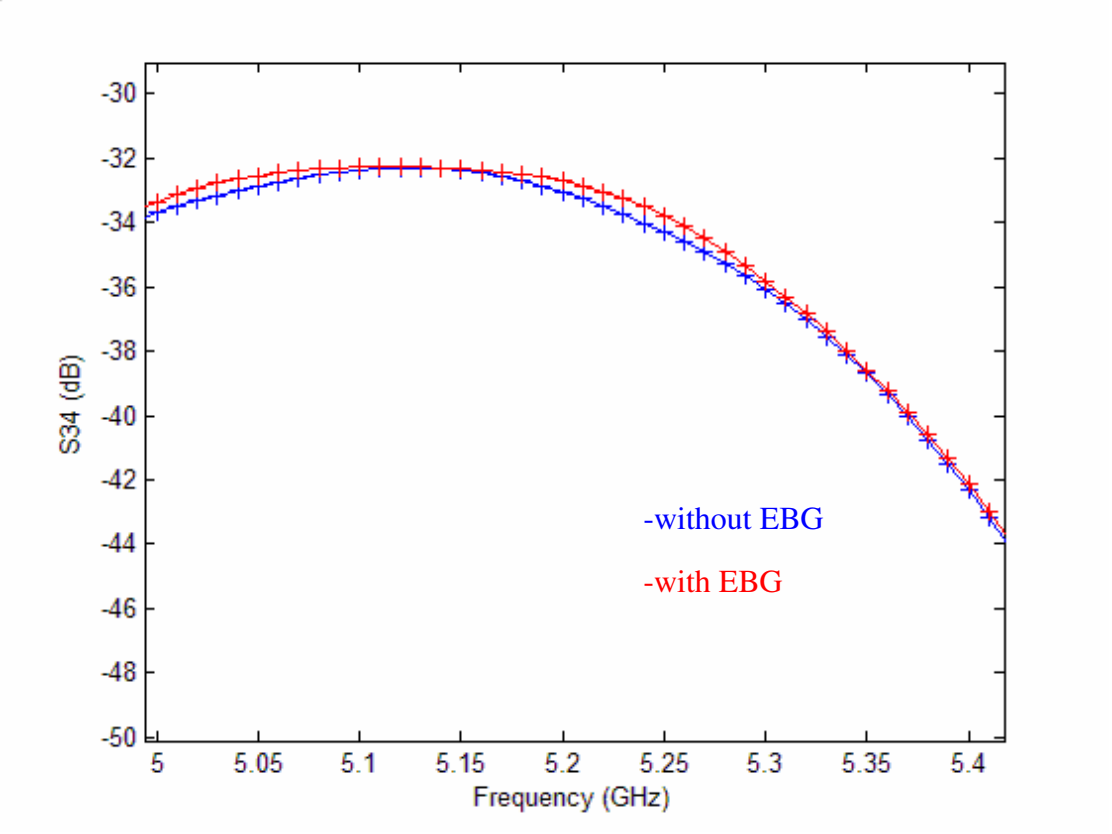

Appendix 108: S34